

Grey Galaxies in AdS_5

Kabir Bajaj,^a Vipul Kumar,^{b,2} Shiraz Minwalla,^{b,3} Jyotirmoy Mukherjee,^{b,4} Asikur Rahaman.^{b,5}

^a*Department of Physics, Indian Institute of Technology Bombay, Powai, Mumbai 400076, India*

^b*Department of Theoretical Physics, Tata Institute of Fundamental Research, Homi Bhabha Rd, Mumbai 400005, India*

ABSTRACT: It has recently been conjectured [1] that the end point of the rotational super-radiant instability of black holes in AdS_4 is a Grey Galaxy: an $\omega = 1$ black hole sitting at the centre of AdS_4 , surrounded by a large disk of rapidly rotating gravitons and other bulk fields. In this paper we study Grey Galaxies in AdS_5 . In this case, the rotational group is of rank 2, and so has two distinct angular velocities ω_1 and ω_2 . We demonstrate that AdS_5 hosts two qualitatively distinct Grey Galaxy phases: the first with either $\omega_1 \approx 1$ or $\omega_2 \approx 1$, and the second with both angular velocities ≈ 1 . We use these results to present a conjecture for a part of the phase diagram of $\mathcal{N} = 4$ Yang-Mills (as a function of energy and the two angular momenta) that displays several phase transitions between regular black holes and various Grey Galaxy phases. We present an explicit gravitational construction of the phases in which ω_1 and ω_2 are both parametrically close to unity, and demonstrate that the corresponding boundary stress tensor is the sum of two pieces. The first is the stress tensor of the central black hole. The second - the contribution of the bulk gas - takes the form of the stress tensor of an equilibrated boundary conformal fluid, rotating at the given angular speeds ω_i . We also briefly comment on the structure of Grey Galaxies in AdS_D for $D > 5$.

¹kabir.bajaj@iitb.ac.in

²vipul.kumar@tifr.res.in

³minwalla.theory@tifr.res.in

⁴jyotirmoy.mukherjee.119@tifr.res.in

⁵asikur.rahaman@tifr.res.in

Contents

1	Introduction	2
1.1	Grey Galaxies of higher rank	2
1.2	Microcanonical Phase diagram in AdS_5	3
1.3	Rank 2 Grey Galaxies in AdS_5	4
1.4	A Bulk Solution for a rank 4 Grey Galaxy	4
1.5	Fluid Interpretation of the Boundary Stress Tensor	6
1.6	' AdS_D Gregory Laflamme' and Black Rings?	7
1.7	Structure of this Paper	7
2	Kerr - AdS_5 Black Holes	8
2.1	The Metric	8
2.1.1	The special case $a = b$	10
2.2	Large r behaviors	10
2.3	Thermodynamics of the Black Hole	11
2.4	Thermodynamics at Extremality	12
2.5	Superradiant Instability	12
2.6	Charges at boundary of superradiance	13
2.6.1	Thermodynamical Formulae	14
2.6.2	Specific Heats	14
2.6.3	An inequality for E as a function of J	15
2.7	Boundary Stress Tensor for Black Hole	15
2.7.1	Components of the boundary stress tensor	15
2.7.2	Fluid nature of the boundary stress tensor	15
2.8	Energy Density as a function of θ	16
3	The Phase diagram	17
4	Gas thermodynamics in the canonical ensemble	21
4.1	Partition function for a single scalar in AdS_5	21
4.2	Partition function for the $10d$ dilaton	23
4.3	The partition function for II SUGRA on $AdS_5 \times S^5$	24
5	Bulk Gas Stress tensor	24
5.1	The problem addressed	24
5.2	Computation in 10d Euclidean Space	25
5.2.1	Setting up the computation	25
5.2.2	The large r scaling limit	27
5.2.3	Simplification from Chirality	28
5.2.4	Final Result at leading order	29

5.3	Matching the total energy with the thermodynamical prediction	31
6	Back-reactions on the metric	32
6.1	AdS_5 metric in terms of right invariant one forms	32
6.2	Bulk Stress tensor in terms of right invariant oneforms	33
6.3	Computation of the backreaction	33
6.4	Boundary Stress Tensor	36
7	Conjectured Boundary Stress Tensor for general bulk matter	37
8	Conclusion and Discussion	38
A	Black Rings and Gregory Laflamme Instabilities	41
A.1	Gregory Laflamme Type instabilities	42
A.1.1	GL instabilities in flat space	42
A.1.2	Gregory Laflamme instabilities in AdS space	43
A.2	Black Rings	44
B	Mass and the radius of the extremal Kerr-AdS_5 black holes	45
C	Partition function of a single scalar in AdS_5	47
D	The Gas partition function in $AdS_5 \times S^5$	48
D.1	Review of conformal characters	48
D.2	$SU(4)$ character formula	49
D.3	Full Single Particle Partition Function	51
D.4	Matching with the superconformal index	53
D.5	Turning $SU(4)$ chemical potentials off	53
D.5.1	Partition function at $\omega_1 \rightarrow 1, \omega_2 \rightarrow 1$	54
E	The Dilaton Propagator in $AdS_5 \times S^5$	54
F	Sum over KK modes	57
F.1	Decomposition of the 10d propagator	57
F.2	Explicit check of equality of 10d and 5d stress tensors	58
G	Stress tensor of conformally coupled free scalar on $S^1 \times S^3$	60
G.1	Two Point function on $S^3 \times$ time	61
G.2	Greens function on (twisted) $S^3 \times S^1$	62
G.3	Derivative structures required to compute the stress tensor in the $\omega_i \rightarrow 1$ limit	63
G.4	The stress tensor	64
H	Spin-1 contribution to the bulk stress tensor	65
H.1	Stress tensor in thermal AdS_5	66

1 Introduction

It has been known for over twenty years that spinning black holes with angular velocities greater than unity are unstable in AdS space [2–10]. The endpoint of this instability has recently been conjectured [1] to be a Grey Galaxy: an $\omega = 1$ AdS black hole surrounded by a gas of fast rotating gravitons and other bulk fields, with a total energy of order $1/G_N$ (G_N is Newton’s constant). The authors of [1] focused on the study of AdS_4 and demonstrated that the graviton gas arranges itself into a large flat disk with a radius of order $1/G_N^{\frac{1}{4}}$ and a proper thickness of order unity. They also demonstrated that the gas contribution to the boundary stress tensor takes a striking form; it is a delta function, localized on the equator of the boundary S^2 .¹

Spinning AdS_D black holes with $\omega > 1$ are also unstable for $D > 4$. The thermodynamical arguments of [1] suggest that Grey Galaxies also constitute the end point of this instability - and dominate the microcanonical ensemble at large angular momentum. Grey Galaxies in $D > 4$, thus, likely compute the entropy (as a function of energy and angular momentum, at large angular momentum) in much studied theories like $\mathcal{N} = 4$ Yang-Mills and the $(0, 2)$ theory, and so are of great interest.

1.1 Grey Galaxies of higher rank

When $D \geq 5$ the rotational group $SO(D - 1)$ has² rank greater than unity. Consequently, black holes in such dimensions are characterized by multiple angular momenta J_i and multiple angular velocities ω_i . Grey Galaxies are made up of a black hole with $|\omega_i| \approx 1$ ³ for at least one value of i .⁴ In $D \geq 5$ these solutions appear in several distinct families, parameterized by the number of i for which $|\omega_i| \approx 1$. The chiral gas of gravitons in a Grey Galaxy carries angular momentum only in those two planes that have $|\omega_i| \approx 1$; consequently, the rank r of the $SO(D - 1)$ angular momentum matrix of the gas is generically twice this number. Through this paper, we label distinct Grey Galaxy phases with the rank r of the angular momentum of their gas component.

AdS_D Grey Galaxies of rank 2 turn out to be qualitatively very similar to their 4-dimensional cousins. The bulk gas in these solutions is sharply localized around a two-dimensional disk of radius of order $1/G_N^{\frac{1}{4}}$. And its contribution to the boundary stress tensor is sharply localized around an equator of S^{D-2} .

In contrast, both the bulk gas and its boundary stress tensor are less sharply localized in Grey Galaxies of rank $r > 2$. Instead, the bulk gas is concentrated around an r dimensional surface⁵ while its boundary stress tensor is concentrated round an $r - 1$ dimensional submanifold of S^{D-2} . This difference is most pronounced when D is odd and r takes its

¹In contrast, the boundary stress tensor from the black hole part of the Grey Galaxy is smoothly distributed over the boundary S^2 .

² $SO(D - 1)$ is the maximal compact subgroup of the conformal group $SO(D - 1, 2)$.

³Here the symbol \approx means ‘parametrically near to’.

⁴All other $|\omega_j|$ are necessarily less than unity.

⁵The ‘radius’ of this region turns out to be of order $(1/G_N)^{\frac{1}{r+2}}$.

maximal value $D - 1$; in this case, the gas is smoothly distributed over the full spatial bulk, and its boundary stress tensor is smoothly distributed over the full boundary sphere.

Grey Galaxy solutions of rank r enjoy invariance under $U(1)^{\frac{r}{2}}$ rotations in each of their $\frac{r}{2}$ two planes. Thus while their boundary stress tensor is spread over a $r - 1$ dimensional submanifold, it is a nontrivial function of only $(r - 1) - (\frac{r}{2}) = \frac{r}{2} - 1$ coordinates on this surface. When $r = 2$, $\frac{r}{2} - 1 = 0$, so the boundary stress tensor is distributed uniformly around a one-dimensional equator (as in [1]). When $r > 2$, however, $\frac{r}{2} - 1 > 0$, and the distribution of the boundary stress tensor along these $\frac{r}{2} - 1 > 0$ coordinates is not determined by symmetry considerations. A prediction for the precise form of the spatial distribution of the boundary stress tensor of Grey Galaxies with rank $r > 2$ is one of the key goals of the current paper.

1.2 Microcanonical Phase diagram in AdS_5

The simplest AdS_D space with $D > 4$ is AdS_5 . In this case, Grey Galaxies are either of

- rank 2 (when the central black hole has either $\omega_1 \approx 1$ with $\omega_2 < 1$ or $\omega_2 \approx 1$ with $\omega_1 < 1$ ⁶).
- rank 4 (when the central black hole has $(\omega_1, \omega_2) \approx 1$.⁷)

It seems likely ⁸ that the thermodynamically dominant bulk phase - at any value of E , J_1 and J_2 - is always either a vacuum black hole (see subsection 2 for a review) or one of the Grey Galaxies described above. Making this assumption, in section 3 we construct a fully quantitative⁹ phase diagram of $\mathcal{N} = 4$ Yang-Mills theory as a function of energy and angular momenta in the microcanonical ensemble. Our phase diagram exhibits several phase transitions. At high enough energies (at every value of angular momenta) we find in section 3 that the dominant phase is always the usual Kerr black hole. If we lower energies at fixed J_i with $J_i > J_j$, the system undergoes a phase transition to a rank 2 with $\omega_i \approx 1$ at a critical energy. At a lower critical energy, the system then makes a second phase transition to the rank 4 Grey Galaxy case and stays in this phase all the way down to the unitarity bound. In the special case $J_1 = J_2$, the system undergoes only one phase transition, directly from the vacuum black hole to the rank 4 Grey Galaxy phase, and stays in this phase down to the unitarity bound.¹⁰

The analysis of section 3 also applies to $AdS_5 \times S^5$ (the bulk dual to $\mathcal{N} = 4$ Yang-Mills theory at large N and strong coupling) except for one complication ¹¹. Small 5d black holes in $AdS_5 \times S^5$ are unstable to a Gregory Laflamme clumping in the S^5 direction [12].

⁶In this case the gas carries a macroscopic amount of angular momentum only in the plane in which $\omega \approx 1$.

⁷In this case the gas carries macroscopic angular momentum in both planes

⁸See 1.6 for some discussion of this assumption.

⁹Our phase diagram is quantitative, in the sense that we have precise equations for each of the phase boundaries, and an equation for the entropy as a function of energy and angular momenta in each phase.

¹⁰In qualitative terms the phase diagram is similar (but simpler than) the DDBH phase diagram for $\mathcal{N} = 4$ Yang-Mills theory as a function of energy and the three $SO(6)$ charges, see [11].

¹¹We thank E. Lee for a very useful discussion on this point.

The analysis of this paper is blind to the S^5 , and so to these new phases. Once this effect is taken into account, we expect the ‘high energy’ (compared to a critical value, of order unity in units of N^2) part of the $\mathcal{N} = 4$ Yang Mills phase diagram to follow the analysis of this paper. At lower energies the dominant solutions will be given by 10 dimensional black holes.¹² We leave a careful demarcation of these two different families of phases (and a detailed study of the clumped phases) to future work.

1.3 Rank 2 Grey Galaxies in AdS_5

The metric at the boundary of AdS_5 is Weyl equivalent to $S^3 \times \text{time}$. It is useful to picture the S^3 as embedded in an \mathbb{R}^4 with coordinates x_i ($i = 1 \dots 4$). Rank 2 Grey Galaxies carry an angular momentum in a single plane - let’s say the x_1x_2 plane of this \mathbb{R}^4 . As in AdS_4 (see [1]) the bulk centrifugal force flattens rank 2 Grey Galaxies into disks that are tightly localized around the plane $x_3 = x_4 = 0$. The boundary stress tensor of this Grey Galaxy is (parametrically sharply) localized about the equator on which this plane intersects the boundary S^3 . If we let θ be a coordinate that vanishes on the equator, then the boundary stress tensor of the gas component of a Grey Galaxy takes the form $A\delta(\theta)(dt - d\phi)^2$ (note the similarity with Eq 5.33 of [1]) where A is a constant¹³ whose value can be read off from gas thermodynamics (see section 4). As anticipated at the end of subsection 1.1, it follows that the boundary stress tensor of rank 2 Grey Galaxies can be determined by simple thermodynamical considerations, without a detailed bulk construction of the relevant solution.

1.4 A Bulk Solution for a rank 4 Grey Galaxy

In contrast (and as already mentioned at the end of subsection 1.1), the boundary stress tensor of a rank 4 Grey Galaxy is not immediately determined directly from thermodynamical and symmetry considerations alone. In order to evaluate this boundary stress tensor, we have determined its bulk solution. In this subsection, we describe this solution within a simple model. We take our bulk to be $AdS_5 \times S^5$, and take the bulk matter to consist of a single 10d massless scalar field (let us call it the dilaton). We discuss the generalization to models with more realistic bulk matter in the next subsection.

Our construction of the bulk solution follows the method presented in [1]. We first calculate the bulk stress tensor of the bulk gas and then use Einstein equations to evaluate the backreaction of this stress tensor on the metric. We now describe each of these steps in more detail.

¹²This will certainly be the case when the black holes in the dominant phase of this paper turn out to be S^5 Gregory Laflamme unstable. The Grey Galaxy phase extends all the way down to this instability curve if the phase transition to localized black holes is of second order. If this phase transition is of first order, on the other hand, 10d black holes will dominate the ensemble even before the dominant 5d (Grey Galaxy) black holes go unstable.

¹³That A is a constant along the equator follows from the $U(1)$ invariance of the solution, as explained at the end of subsection 1.1

At radial coordinates $r \gg 1$, the black hole spacetime is indistinguishable from thermal $AdS_5 \times S^5$. As the dominant contribution to the bulk stress tensor comes at large values of the radius, we work in this simpler background spacetime. We compute the bulk stress tensor by first taking the appropriate derivatives of the thermal dilaton propagator and then taking the coincident limit.¹⁴ The thermal $AdS_5 \times S^5$ Greens function is constructed from the vacuum propagator via the method of images. Happily, this vacuum propagator turns out to be extremely simple; it is simply given by a Weyl transformation of the flat space 10d massless scalar propagator [13, 14]. The train of facts mentioned above allows for a simple computation of the dilaton contribution to the bulk gas stress tensor.¹⁵

The gravitational backreaction caused by this bulk gas can also be computed rather simply.¹⁶ The stress tensor of the bulk gas of the previous paragraph turns out to live dominantly at an AdS_5 radial coordinate of order $r = N^{\frac{1}{3}}$. The ‘scale transformation’ coordinate change

$$r \rightarrow r' N^{1/3}, \quad x^\mu \rightarrow \frac{x'^\mu}{N^{1/3}} \quad (1.1)$$

brings the gas to r' of order unity, but has it varying (in the coordinates x'^μ) over parametrically large scales of order $N^{\frac{1}{3}}$ ¹⁷. To leading order in the large N limit, therefore, the spatial variation can simply be ignored.¹⁸ one computes the gravitational backreaction ‘point by point’ (in x^μ), and finds the final solution by sewing together these point-wise solutions.¹⁹

Once we have the bulk solution, the determination of its boundary stress tensor is a simple exercise. We find

$$T_{\mu\nu} = \frac{2h_\phi(\beta)}{\beta\pi^2} \gamma^A(\theta) (4u_\mu u_\nu + g_{\mu\nu}) \quad (1.2)$$

where $g_{\mu\nu}$ is the boundary metric, u^μ is a ‘velocity’ vector field on this space, and $\gamma(\theta)$ is the usual special relativistic ‘gamma factor’ for this velocity field

$$ds^2 = g_{\mu\nu} dx^\mu dx^\nu = -dt^2 + d\theta^2 + \sin^2 \theta d\phi_1^2 + \cos^2 \theta d\phi_2^2 \quad (1.3)$$

$$u^\mu \partial_\mu = \gamma (\partial_t - \omega_1 \partial_{\phi_1} - \omega_2 \partial_{\phi_2}) \quad (1.4)$$

¹⁴See Section 4.3 of [1]. As explained in [1] it is sufficient to work at quadratic when studying Grey Galaxies, as terms in the stress tensor that are of higher homogeneity than quadratic are subleading in inverse powers of $1/N$.

¹⁵Though the final result for this bulk stress tensor is the sum over the stress tensor, the five-dimensional Kaluza Klein modes of the dilaton, the full answer obtained from the sum turns out to be much simpler than any individual component.

¹⁶The computation presented here is, in fact, significantly simpler than the computation presented in [1], see below.

¹⁷This follows because the gas varies over distances of order unity in the original x^μ coordinates.

¹⁸In the rank 2 case, in contrast, the bulk gas varies very rapidly in the original x^μ coordinates, in such a manner that it varies on scale unity in the x'^μ coordinates. In this case, the back reaction cannot be computed ‘point by point’, but must be computed in a more complicated manner, see [1].

¹⁹This is highly reminiscent of the derivation of the Fluid Gravity correspondence presented in [15–18]. The analogy is quite close: in fact the equation that appears in the computation of this paper is almost identical to the differential equation in the ‘tensor sector’ of [19].

$$\gamma(\theta) = \frac{1}{\sqrt{1 - \omega_1^2 \sin^2 \theta - \omega_2^2 \cos^2 \theta}} \quad (1.5)$$

²⁰ The function $h_\phi(\beta)$ in (1.2) is thermodynamical in origin. This function may be read off from the expression of the partition function of the dilaton gas in $AdS_5 \times S_5$. When $\omega_1 \approx 1$ and $\omega_2 \approx 1$, this partition function turns out to take the form

$$Z_{\text{gas}}(\beta, \omega_i) = \frac{4h_\phi(\beta)}{(1 - \omega_1^2)(1 - \omega_2^2)} \quad (1.6)$$

so $h_\phi(\beta)$ may be read off from (1.6).

While the stress tensor (1.2) has no explicit dependence on N , ²¹ it nonetheless evaluates to a value of order N^2 when ω_1 and ω_2 differ from unity only at order $1/N^{\frac{2}{3}}$, ²² as is the case for Grey Galaxies of rank 4.

1.5 Fluid Interpretation of the Boundary Stress Tensor

Equation (1.2) has a striking physical interpretation: it is the equilibrium stress tensor of a ‘conformal fluid’ rotating on S^5 with fluid velocity u^μ [15]. The reader may find the emergence of a hydrodynamical stress tensor at every β surprising, as one usually expects hydrodynamics to be quantitatively accurate only at high temperatures in units of the radius of the sphere. In Appendix G, we investigate this point by directly evaluating the stress tensor of a free conformal scalar on $S^3 \times S^1$ at nonzero angular velocities. We verify that while the stress tensor does indeed take the completely hydrodynamical form (1.2) at high temperatures, it also takes the form (1.2) in the limit $\omega_i \rightarrow 1$. ²³ We offer a physical explanation for why this works (in terms of Lorentz contractions, or, equivalently, redshift factors).

While we have honestly derived (1.2) only in the context of a simple model of bulk matter (consisting only of a single dilaton), the physical interpretation above suggests that the structural properties of our result are, in fact, universal. We are led to conjecture:

- The boundary stress tensor of Grey Galaxies of rank 4 in AdS_5 - with arbitrary bulk matter content - always takes the form (1.2), but with the function $h_\phi(\beta)$ replaced by the function that is read off from the gas via the analogue of (1.6).

Early in this introduction, we pointed out that the boundary stress tensor of rank 2 Grey Galaxies is completely fixed by symmetry and *thermodynamical* considerations. The conjecture of this section postulates a generalization of this fact to Grey Galaxies of higher rank; their boundary stress tensors are completely determined by symmetry and *hydrodynamical* considerations.

²⁰Note that $\gamma(\theta)$ is defined in a manner that ensures that u is a velocity vector field, i.e. that $u^2 = -1$.

²¹The function $h_\phi(\beta)$ (see (4.10) for an explicit formula) is an order unity function of the temperature.

²²This follows from the fact γ evaluates to an expression of order $N^{\frac{1}{3}}$ at such values of ω_i .

²³The main difference between the high temperature and ω near one limits lies in the analogue of the function $h_\phi(\beta)$. While this function is proportional to the simple $\frac{1}{\beta^4}$ at high temperatures, it has a complicated dependence on β in the limit $\omega \rightarrow 1$.

It is now straightforward to apply this conjecture to the bulk dual of $AdS_5 \times S^5$. The bulk gas, in this case, consists of all the fields of IIB Supergravity on $AdS_5 \times S^5$ (this is roughly 256 times the bulk stress tensor of the dilaton of the previous subsection).

Much to our surprise, we were unable to find an expression for the thermal partition function of this 10 gas, so we performed this computation ourselves; and used it to read off $h_{\text{YM}}(\beta)$, obtaining the result presented in (4.12).

The conjecture of this section thus gives us a natural guess for the boundary stress tensor of Grey Galaxies in $\mathcal{N} = 4$ Yang-Mills theory:

$$T_{\mu\nu} = \frac{2h_{\text{YM}}(\beta)}{\beta\pi^2} \gamma^4(\theta) (4u_\mu u_\nu + g_{\mu\nu}) \quad (1.7)$$

with h_{YM} listed in (4.12). Note we were able to obtain this result without performing the laborious task of actually evaluating the bulk stress tensor of the thermal IIB supergravity gas in $AdS_5 \times S^5$.

1.6 ‘ AdS_D Gregory Laflamme’ and Black Rings?

To end this introduction, we note that black holes in AdS_D (for $D \geq 5$) display some features with no counterpart in $D = 4$. In $D \geq 6$, highly spinning black holes sometimes flatten out into a thin pancake which is then subject to Gregory-Laflamme type instabilities [20, 21]. Also, in $D \geq 5$ we have new solutions (with new horizon topologies) like black rings [22, 23]. As we discuss in Appendix A, neither of these phenomena appears to be relevant to the construction of the phase diagram. The Gregory-Laflamme instability always occurs at values of ω that are greater than unity, and so for black holes that were already super radiant unstable. The black holes at the center of Grey Galaxies are never Gregory Laflamme unstable. Moreover (at least in the case that they are small, and so amenable to analytic analysis) black rings always have $\omega > 1$, and so, themselves, display a superradiant instability. Although our analysis of these points is not completely definitive, it appears that black rings - or black holes at the edge of a Gregory Laflamme instability - never appear as dominant phases.

In order to forestall confusion, we emphasize that the Gregory-Laflamme type instabilities discussed in this subsection are those that lead to clumping in the AdS_D directions. In many situations of physical interest, AdS spaces are accompanied by an internal manifold (e.g. the S^5 in $AdS_5 \times S^5$). In such contexts small black holes typically do undergo Gregory Laflamme instabilities in the internal manifold (e.g. S^5), and the resultant black holes are expected to dominate the phase diagram in appropriate parameter regimes (roughly when black holes are small). We never study this phenomenon in this paper.

1.7 Structure of this Paper

The rest of this paper is organized as follows. In section 2 we review relevant aspects of Kerr- AdS_5 Black Hole solutions and their thermodynamics. In section 3 we construct the microcanonical phase diagram of $\mathcal{N} = 4$ Yang-Mills theory (as a function of energy and angular momenta) under the assumption that black holes and Grey Galaxies are the only

relevant phases. In section 4 we study the thermodynamics of the bulk gas. In 5 we focus on the model of a single 10d massless scalar in $AdS_5 \times S^5$, and construct the bulk stress tensor at finite temperature assuming ω_1 and ω_2 to be near unity. In section 6 we compute the resultant back reaction of the metric, and read off the resultant boundary stress tensor. In section 7 we present our conjecture for the gas contribution to the boundary stress tensor for a bulk gas with arbitrary matter content (in particular for the dual of $\mathcal{N} = 4$ Yang-Mills theory). We end this paper in section 8 with a discussion of our results. Several Appendices contain material that supports the analysis of the main text.

2 Kerr - AdS₅ Black Holes

In this section, we review Kerr-AdS₅ Black hole solutions and some of their properties.

2.1 The Metric

The metric of Kerr AdS₅ Black hole is given by [24–26]

$$ds^2 = -\Delta_{\tilde{\theta}}(1+r^2)\rho^2 dt^2 + \frac{f}{\rho^4} \left(\frac{\Delta_{\tilde{\theta}} dt}{\Xi_a \Xi_b} - \omega \right)^2 + \frac{\rho^2 dr^2}{\Delta_r} + \frac{\rho^2 d\tilde{\theta}^2}{\Delta_{\tilde{\theta}}} + \frac{r^2 + a^2}{\Xi_a} \sin^2 \tilde{\theta} d\phi_1^2 + \frac{r^2 + b^2}{\Xi_b} \cos^2 \tilde{\theta} d\phi_2^2 \quad (2.1)$$

where

$$\Xi_a = 1 - a^2 \quad (2.2)$$

$$\Xi_b = 1 - b^2 \quad (2.3)$$

$$\Delta_{\tilde{\theta}} = 1 - a^2 \cos^2 \tilde{\theta} - b^2 \sin^2 \tilde{\theta} \quad (2.4)$$

$$\Delta_r = \frac{(r^2 + a^2)(r^2 + b^2)(1 + r^2)}{r^2} - 2m \quad (2.5)$$

$$\rho^2 = r^2 + a^2 \cos^2 \tilde{\theta} + b^2 \sin^2 \tilde{\theta} \quad (2.6)$$

$$f = 2m\rho^2 \quad (2.7)$$

$$\omega = a \sin^2 \tilde{\theta} \frac{d\phi_1}{\Xi_a} + b \cos^2 \tilde{\theta} \frac{d\phi_2}{\Xi_b} \quad (2.8)$$

Roughly speaking, the constants a and b determine the angular momentum of the black hole in the two planes (say ϕ_1 and ϕ_2 respectively), and the parameter m determines the mass of the black hole. The parameters a and b lie in the range :

$$a, b \in [-1, 1] \quad (2.9)$$

The parameter m is always positive but is further constrained by the requirement that the solution (2.1) should have an event horizon (and so describes a black hole rather than a naked singularity).

For Kerr-AdS₅ black holes, the positions of the event horizon are determined by solving the following algebraic equation:

$$(r_+^2 + a^2)(r_+^2 + b^2)(r_+^2 + 1) - 2mr_+^2 = 0 \quad (2.10)$$

This is a cubic equation in $r_+^2 = x$. Let us study the nature of the roots of this cubic polynomial in x :

$$x^3 + x^2(a^2 + b^2 + 1) + x(a^2b^2 + a^2 + b^2 - 2m) + a^2b^2 = 0 \quad (2.11)$$

Let the roots (2.11) be denoted by x_1 , x_2 , and x_3 . Recall that, on physical grounds, we are interested in the positive real roots of (2.11). The coefficients of x^2 and the constant, in the cubic equation (2.11) are manifestly positive. The coefficient of x , namely $a^2 + b^2 + a^2b^2 - 2m$, could be either positive or negative. Clearly no positive real roots exist if this coefficient is positive. In this case, the ‘black hole’ solution has a naked singularity, and is unphysical. In the physically interesting case

$$2m > a^2 + b^2 + a^2b^2 \quad (2.12)$$

In Appendix B we demonstrate the following. When (2.12) is just obeyed (i.e. when m is just larger than the critical value in (2.12)), (2.11) has two complex (and complex conjugate) solutions and one negative real solution. In this situation, consequently, the ‘black hole’ solution continues to have a naked singularity (and so continues to be unphysical). As m is further increased (at fixed a and b) the two complex conjugate solutions approach the real axis. At a critical value of $m = m_{\text{ext}}$ given by

$$m_{\text{ext}} = \frac{1}{2} \left(\frac{1}{6} \sqrt{(a^2 + b^2 + 1)^4 + 216a^2b^2(a^2 + b^2 + 1)} \cos\left(\frac{\alpha}{3}\right) + a^2(b^2 + 1) - \frac{1}{12} (a^2 + b^2 + 1)^2 + b^2 \right) \quad (2.13)$$

where α is given by

$$\begin{aligned} \cos(\alpha) = & \left(\frac{1}{(a^2 + b^2 + 1)^4 + 216a^2b^2(a^2 + b^2 + 1)} \right)^{3/2} \\ & \times \left(5832a^4b^4 - (a^2 + b^2 + 1)^6 + 540a^2b^2(a^2 + b^2 + 1)^3 \right) \end{aligned} \quad (2.14)$$

the two solutions merge at a positive value of $x = x_{\text{ext}}$ on the real axis, where

$$x_{\text{ext}} = \frac{1}{6} (a^2 + b^2 + 1) \left(2 \cos\left(\frac{1}{3}\xi\right) - 1 \right) \quad (2.15)$$

and ξ is given by,

$$\cos(\xi) = \left(\frac{54a^2b^2}{(a^2 + b^2 + 1)^3} - 1 \right) \quad (2.16)$$

At $m = m_{\text{ext}}$ the black hole is extremal and has nonzero horizon area (and so nonzero entropy) ²⁴

At still larger values of m , the two (newly minted) positive real roots separate away from each other on the real axis. The black hole turns non-extremal (and remains physical).

²⁴While the entropy of the extremal black hole is nonzero at generic values of a and b , it vanishes when either a or b vanishes - this follows from the fact that $\phi = \pi$ in this case. In this special case, black holes at extremality are singular; however, they can be approached as a limit of nonsingular (nonzero temperature) black holes: those with m slightly greater than m_{ext} .

As m is increased even further, the larger of the two roots increases without bound (tending to

$$x \approx \sqrt{2m} \quad (2.17)$$

while the smaller of the two roots decreases to zero (while always remaining positive). In this limit, the angular momentum is a small perturbation, and the black hole reduces to an AdS Schwarzschild black hole.

2.1.1 The special case $a = b$

All expressions presented earlier in this subsection simplify in the special case $a = b$. In this special case, the metric enjoys invariance under $SU(2)_R$, and so can be written in a simple manner in terms of right invariant one-forms.

$$ds^2 = -\Xi_a(1+r^2)(r^2+a^2)dt^2 + \frac{2m}{(r^2+a^2)\Xi_a^2} (dt - a \sigma_3)^2 + \frac{(r^2+a^2)dr^2}{\Delta_r} + \frac{(r^2+a^2)}{\Xi_a} (\sigma_1^2 + \sigma_2^2 + \sigma_3^2) \quad (2.18)$$

where

$$\begin{aligned} \sigma_1 &= \frac{1}{2} \left(\sin(\phi)d(2\tilde{\theta}) - \cos(\phi)\sin(2\tilde{\theta})d\psi \right) \\ \sigma_2 &= \frac{1}{2} \left(\cos(\phi)d(2\tilde{\theta}) + \sin(\phi)\sin(2\tilde{\theta})d\psi \right) \\ \sigma_3 &= \frac{1}{2}(d\phi - \cos(2\tilde{\theta})d\psi) \end{aligned} \quad (2.19)$$

are the usual right invariant oneforms on a (squashed) S^3 , and

$$\phi = \phi_1 + \phi_2, \quad \psi = \phi_1 - \phi_2 \quad (2.20)$$

In this case, the mass and the radius of the extremal black holes are given by the simple expressions

$$m_{\text{ext}} = \frac{1}{128} \left(\sqrt{8a^2+1} - 1 \right) \left(\sqrt{8a^2+1} + 3 \right)^3 \quad (2.21)$$

$$(r_+)_{\text{ext}}^2 = \frac{1}{4} \left(\sqrt{1+8a^2} - 1 \right) \quad (2.22)$$

2.2 Large r behaviors

While the black hole (2.1) asymptotes to AdS_5 , this fact is not manifest in the coordinates used in (2.1), but can be made manifest by changing coordinates from $r, \tilde{\theta}$ to y, θ , where y and θ are defined by the equations ([15])

$$\begin{aligned} y^2 \sin^2 \theta &= \frac{(r^2+a^2) \sin^2 \tilde{\theta}}{\Sigma_a}, \\ y^2 \cos^2 \theta &= \frac{(r^2+b^2) \cos^2 \tilde{\theta}}{\Sigma_b}. \end{aligned} \quad (2.23)$$

²⁵ In these new coordinates, the black hole metric takes the form

$$\begin{aligned}
ds^2 = & -(1+y^2)dt^2 + \frac{dy^2}{1+y^2} + y^2(d\theta^2 + \cos^2\theta d\psi^2 + \sin^2\theta d\phi^2) \\
& + \frac{2m}{y^6\Delta_\theta^3}dy^2 + \frac{2m}{y^2\Delta_\theta^3}dt^2 \\
& - \frac{4am\sin^2\theta}{y^2\Delta_\theta^3}dtd\phi - \frac{4bm\cos^2\theta}{y^2\Delta_\theta^3}dtd\psi \\
& - \frac{2ma^2\sin^4\theta}{y^2\Delta_\theta^3}d\phi^2 + \frac{2mb^2\cos^4\theta}{y^2\Delta_\theta^3}d\psi^2 \\
& + \frac{2abm\sin^2\theta\cos^2\theta}{y^2\Delta_\theta^3}d\psi d\phi,
\end{aligned} \tag{2.24}$$

At larger y this metric (2.24) reduces to

$$ds^2 = -y^2dt^2 + \frac{dy^2}{y^2} + y^2(d\theta^2 + \cos^2\theta d\psi^2 + \sin^2\theta d\phi^2). \tag{2.25}$$

We see that the metric in these coordinates is manifestly asymptotically AdS_5 , with the metric on constant y slices being the metric on a round S^3 times time.

2.3 Thermodynamics of the Black Hole

The energy, angular momenta, entropy, temperature, and the angular speeds of the Kerr AdS_5 black hole are given by [26]

$$\begin{aligned}
E &= \frac{m\pi(2\Xi_a + 2\Xi_b - \Xi_a\Xi_b)}{4\Xi_a^2\Xi_b^2} \\
J_a &= \frac{2\pi am}{4\Xi_a^2\Xi_b} \\
J_b &= \frac{2\pi bm}{4\Xi_a\Xi_b^2} \\
S &= \frac{\pi^2(r_+^2 + a^2)(r_+^2 + b^2)}{2\Xi_a\Xi_b r_+} \\
T &= \frac{r_+}{2\pi}(1+r_+^2) \left(\frac{1}{r_+^2 + a^2} + \frac{1}{r_+^2 + b^2} \right) - \frac{1}{2\pi r_+} \\
\omega_a &= \frac{a(r_+^2 + 1)}{(r_+^2 + a^2)} \\
\omega_b &= \frac{b(r_+^2 + 1)}{(r_+^2 + b^2)} \\
\Xi_a &= 1 - a^2 \\
\Xi_b &= 1 - b^2
\end{aligned} \tag{2.26}$$

²⁵On adding these two equations we find

$$y^2 = \frac{r^2(1 - a^2\cos^2\theta - b^2\sin^2\theta) + a^2\sin^2\theta + b^2\cos^2\theta - a^2b^2}{\Sigma_a\Sigma_b},$$

²⁶ Note that E , J_a and J_b diverge in the limit $a \rightarrow 1$ or $b \rightarrow 1$.

2.4 Thermodynamics at Extremality

The formulae (2.26) can be specialized to extremality by plugging (2.15) and (2.13) into those formulae. As (2.15) and (2.13) are rather complicated, the resultant thermodynamical formulae are complicated. All formulae simplify, however, if a is taken to be small (at arbitrary values of b)²⁷. Working to leading nontrivial order in a , we find

$$\begin{aligned} (r_+)_{ext} &= \frac{\sqrt{ab}}{(1+b^2)^{\frac{1}{4}}} \\ m_{ext} &= \frac{b^2}{2} + ab\sqrt{1+b^2} \end{aligned} \tag{2.27}$$

and (2.26) simplify to

$$E = -\frac{b^2(b^2 - 3\pi)}{8(b^2 - 1)^2} \tag{2.28}$$

$$J_a = \frac{ab^2\pi}{4(1-b^2)} \tag{2.29}$$

$$J_b = \frac{b^3\pi}{4(b^2 - 1)^2} \tag{2.30}$$

$$S = \frac{\sqrt{abb^2}\pi^2}{2(1+b^2)^{\frac{1}{4}}(1-b^2)} \tag{2.31}$$

The behaviour of these quantities for small b , at leading order, can, of course, be obtained by interchanging a and b .

2.5 Superradiant Instability

The Kerr AdS black hole has a superradiant instability either when $\omega_a > 1$ or $\omega_b > 1$, i.e. either when $r_+^2 < a$ or $r_+^2 < b$. Plugging these inequalities into (2.10), we find that the black hole has an ‘ a ’ type superradiant instability when

$$m \leq \frac{(1+a)^2(a+b^2)}{2} \tag{2.32}$$

(the condition for a b type instability is obtained by interchanging a and b).

The critical instability mass (lowest mass at which the black hole first suffers from a super radiant instability) always lies above extremality. This point can be seen explicitly

²⁶When a black hole is extremal, the LHS of (2.10) has a double root at its horizon. Consequently, the derivative of the LHS of (2.11) vanishes when evaluated at the horizon radius. As a check on our formulae, we have verified that imposing these conditions sets the RHS of the formula for the temperature (in (2.26)) to zero.

²⁷We could, of course, also take b to be small at arbitrary values of a .

when a is small. Working to linear order in a , the difference between the masses listed in (2.32) and (2.27) equals

$$\Delta m = a \left(\frac{1}{2} + b^2 - b\sqrt{1+b^2} \right), \quad (2.33)$$

a quantity that is everywhere positive for $b \in (0, 1)$.

While the argument presented above is only accurate at small a , the final result is correct at all values of a . We can see this by plotting the masses listed on the RHS of (2.13) and (2.32) as a function of a at various fixed values of b . We see from Fig. 1 that the mass at which the black hole becomes super radiant unstable is always larger than the mass at which it becomes extremal.

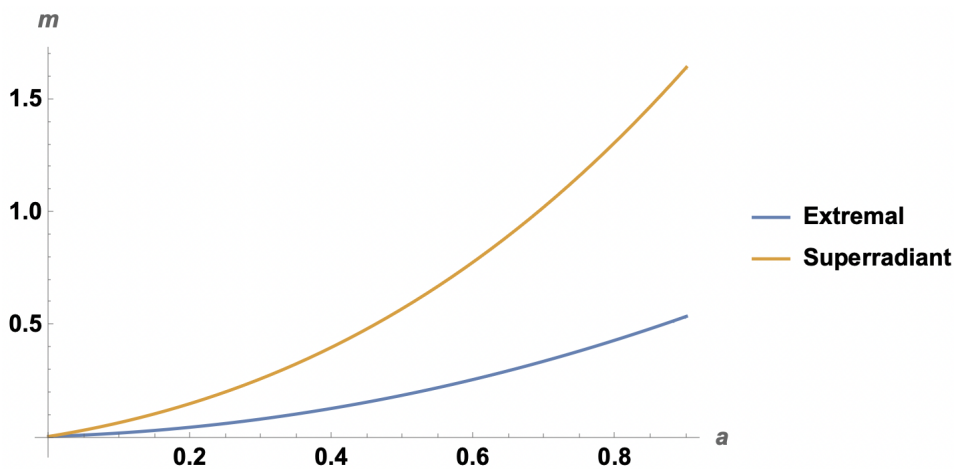


Figure 1. The plot shows that extremal BHs are below the superradiant BHs. While the plots above are presented for $\mathbf{b} = \mathbf{0.1}$, the analogous plots at all values of $b \in (0, 1)$ are qualitatively similar.

2.6 Charges at boundary of superradiance

We have seen, above, that black holes lie on the boundary of the superradiant instability when either $r_+^2 = a$ or $r_+^2 = b$ or when both of these conditions are obeyed. Black holes for which $r_+^2 = a$ and $r_+^2 = b$ have $\omega_a = \omega_b = 1$. These black holes are obtained by setting $a = b$ and by choosing m to saturate the inequality in (2.32), i.e. by choosing

$$m = \frac{a(1+a)^3}{2}. \quad (2.34)$$

These black holes appear in a one-parameter family (parameterized by a above), are of particular interest to this paper, as they will constitute the central black hole for rank 4 Grey Galaxies. In the rest of this subsection, we study these black holes in more detail.

2.6.1 Thermodynamical Formulae

As the radius of the event horizon is given by the simple formula $r_+^2 = a$, all thermodynamical formulae (2.26) simplify considerably: we find

$$\begin{aligned} T &= \frac{1}{2\pi\sqrt{a}}, \\ E &= \frac{a(3+a^2)\pi}{8(1-a)^3} \\ J &= J_a = J_b = \frac{\pi a^2}{(1-a)^3} \\ S &= \frac{\pi^2 a^{3/2}}{2(a-1)^2} \end{aligned} \tag{2.35}$$

2.6.2 Specific Heats

Along this one parameter curve, the energy as a function of temperature is given by

$$E = -\frac{\pi + 48\pi^5 T^4}{8(1-4\pi^2 T^2)^3}, \quad \frac{1}{2\pi} \leq T < \infty \tag{2.36}$$

²⁸ In the limit $T \rightarrow \infty$ (2.36) simplifies to

$$E \approx \frac{3}{32\pi T^2} \tag{2.37}$$

We can calculate the specific heat ²⁹ of these black holes by differentiating (2.36) w.r.t temperature; we find

$$c = \left(\frac{dE}{dT} \right) \Big|_{\omega_a=\omega_b=1} = -\frac{3\pi^3 T (4\pi^2 T^2 + 1)^2}{(1-4\pi^2 T^2)^4} \tag{2.38}$$

We note that the specific heat is always negative. Note that the specific heat goes to zero in the small black hole limit ($T \rightarrow \infty$) but diverges in the large black hole limit $T \rightarrow \frac{1}{2\pi}$. Quantitatively, in the limit $T \rightarrow \frac{1}{2\pi}$,

$$c \approx -\frac{3}{128\pi^2 \left(T - \frac{1}{2\pi}\right)^4} \tag{2.39}$$

while in the large T limit,

$$c \approx -\frac{3}{16\pi T^3} \tag{2.40}$$

²⁸The limit $T = \frac{1}{2\pi}$ corresponds the big black hole limit $a = 1$, while the limit $T = \infty$ corresponds to the small black hole limit $a = 0$.

²⁹Note, of course, that this specific heat is calculated at the constant values $\omega_a = \omega_b = 1$. In other words, it is a specific heat evaluated at constant ω rather than at constant J .

2.6.3 An inequality for E as a function of J

We can, in principle, use the third equation in (2.35) to solve for a in terms of J , and plug this solution into the second of (2.35) to obtain $E = E_\omega(J)$. This gives us E as a function of J along this curve. Notice that $E_\omega(0) = 0$. By differentiating the second and third of (2.35), and dividing the results, we find an exact parametric expression for the gradient of the function $E_\omega(J)$

$$\frac{dE_\omega(J)}{dJ} = \frac{3(a+1)^2}{2a(a+2)} \quad (2.41)$$

Notice that $J(a)$ varies from 0 to ∞ as a varies from 0 to unity. It is easy to convince oneself that the RHS of (2.41) is a monotonically decreasing function in the range $a \in (0, 1)$. The slope (2.41) blows up at $a = 0$ ($J = 0$), tends to 2 at $a = 1$ ($J = \infty$), and is greater than 2 at every intermediate value. It follows in particular that

$$E_\omega(J) = \int_0^J \frac{dE_\omega(J)}{dJ} > 2J \quad (2.42)$$

so that, everywhere, $E_\omega(J)$ obeys the unitarity bound $E > J_1 + J_2$ (recall that in the current context $J_1 = J_2 = J$ so the unitarity bound simplifies to (2.42)).

2.7 Boundary Stress Tensor for Black Hole

2.7.1 Components of the boundary stress tensor

The boundary stress-tensor of Kerr- AdS_5 black holes is easily read off from the form of the metric presented in (2.24), and is given by [15] :

$$\begin{aligned} T^{tt} &= \frac{m}{8\pi G_5} (4\gamma^6 - \gamma^4) \\ T^{\phi_1\phi_1} &= \frac{m}{8\pi G_5} \gamma^4 \left(4\gamma^2 a^2 + \frac{1}{\sin^2(\theta)} \right) \\ T^{\phi_2\phi_2} &= \frac{m}{8\pi G_5} \gamma^4 \left(4\gamma^2 b^2 + \frac{1}{\cos^2(\theta)} \right) \\ T^{t\phi_1} &= \frac{4m}{8\pi G_5} a\gamma^6, \quad T^{t\phi_2} = \frac{4m}{8\pi G_5} b\gamma^6 \\ T^{\phi_1\phi_2} &= \frac{4m}{8\pi G_5} ab\gamma^6, \quad T^{\theta\theta} = \frac{m}{8\pi G_5} \gamma^4 \end{aligned} \quad (2.43)$$

where $\gamma^{-2} = 1 - a^2 \sin^2 \theta - b^2 \cos^2 \theta$. The boundary stress tensor above can be rewritten in terms of N by setting $G_5 = \frac{\pi}{2N^2}$

2.7.2 Fluid nature of the boundary stress tensor

Notice that the boundary stress tensor (2.43) can be succinctly rewritten [15, 17] in the ‘fluid form’

$$\begin{aligned} T^{\mu\nu} &= \frac{N^2 m}{4\pi^2} \gamma^4(\theta) (4u_{bh}^\mu u_{bh}^\nu + g^{\mu\nu}) \\ u_{bh}^\mu &= \gamma (\partial_t - a\partial_{\phi_1} - b\partial_{\phi_2}), \quad \gamma^{-2} = 1 - a^2 \sin^2 \theta - b^2 \cos^2 \theta \end{aligned} \quad (2.44)$$

where $g^{\mu\nu}$ is the inverse metric on the unit 3 sphere (see (6.1)). Note that u_{bh}^μ is a velocity vector field, in the sense that $u_{bh}^\mu u_{bh}^\nu g_{\mu\nu} = -1$. (2.44) is the stress tensor of an equilibrated perfect fluid with fluid velocity u_{bh}^μ .

For large black holes (i.e. when $r_+ \gg 1$)³⁰ we see from (2.26) that $\omega_a \approx a$ and $\omega_b \approx b$. In this case the effective velocity field u_{bh}^μ reduces to

$$u_{bh}^\mu = \gamma (\partial_t - \omega_a \partial_{\phi_1} - \omega_b \partial_{\phi_2}), \quad \gamma^{-2} = 1 - \omega_a^2 \sin^2 \theta - \omega_b^2 \cos^2 \theta \quad (2.45)$$

i.e. to the velocity field of a fluid rotating with angular velocities ω_a and ω_b on the unit sphere. As r_+ retreats to smaller values, $a < \omega_a$. It follows that the effective angular velocity of the ‘black hole fluid’ is smaller than ω_a and ω_b when the central black hole is small, but tends to these values in the limit that the black hole radius becomes large.

The fluid discussed in this section is that of the fluid gravity correspondence [15, 17–19]

2.8 Energy Density as a function of θ

The energy density of the black hole solution is simply equal to the time-time component of the boundary stress tensor T^{tt} . Integrating this over ϕ_1 and ϕ_2 (with the usual measure factor on S^3) yields the $\rho(\theta)$, the energy per unit θ , normalized so that $E = \int d\theta \rho(\theta)$ (E is the full black hole energy). We find

$$\begin{aligned} E_5 &= \int d\Omega_3 T_0^0 \\ &= \frac{m}{8\pi G_5} \int_0^{2\pi} d\phi_1 \int_0^{2\pi} d\phi_2 \int_0^{\frac{\pi}{2}} d\theta \sin(\theta) \cos(\theta) (4\gamma^6 - \gamma^4) \\ &\equiv \int \rho(\theta) d\theta \\ &= \frac{m\pi(2 - 2a^2 + 2 - 2b^2 - (1 - a^2)(1 - b^2))}{4G_5(1 - a^2)^2(1 - b^2)^2} \end{aligned} \quad (2.46)$$

where

$$\rho(\theta) = \frac{m\pi \sin(\theta) \cos(\theta) (3 + a^2 \sin^2(\theta) + b^2 \cos^2(\theta))}{2G_5 (1 - a^2 \sin^2(\theta) - b^2 \cos^2(\theta))^3} \quad (2.47)$$

In Fig 2.8, we plot $\frac{\rho(\theta)}{E}$ versus θ for three different values of a and b , namely ($a = 0.01, b = 0.99$), ($a = 0.99, b = 0.01$) and ($a = 0.99, b = 0.99$).

Notice that the energy density is uniformly distributed on the sphere when $a = b$ (in fact, in this case, T^{tt} is exactly spherically symmetric; a result that follows from the fact that this choice of parameter preserves $SU(2)_R$). When $b \gg a$ or $a \gg b$, the energy density clumps around 0 and $\frac{\pi}{2}$ respectively.³¹

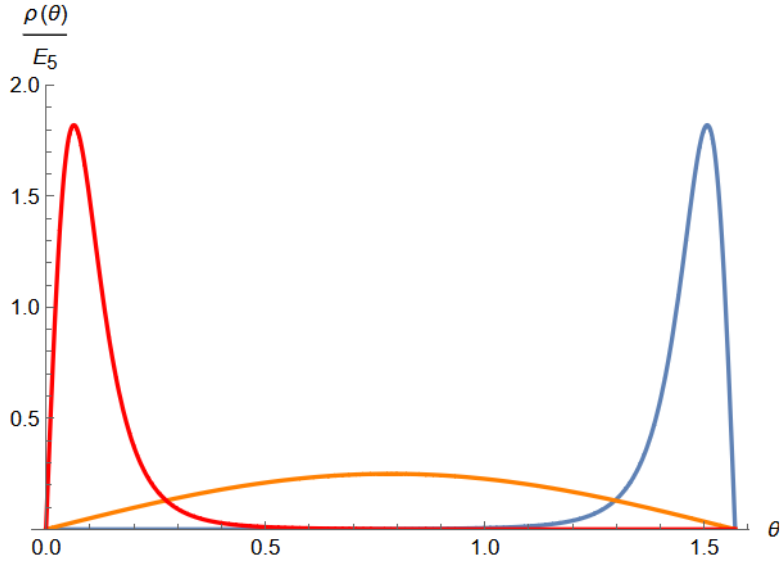


Figure 2. Here the red curve is for $b \rightarrow 0.99, a \rightarrow 0.01$ and blue curve is for $a \rightarrow 0.99, b \rightarrow 0.01$, finally the orange curve is for $a \rightarrow 0.99, b \rightarrow 0.99$.

3 The Phase diagram

In this section, we determine the phase diagram of our system as a function of the total energy E , the total angular momentum J_1 , and the total angular momentum J_2 , working under the assumption that the only relevant phases are vacuum black holes and Grey Galaxies.³²

Consider the three-dimensional space parameterized by E, J_1 and J_2 . When visualizing this space we view the energy axis as lying on the z axis and refer to points with larger values of E as lying ‘above’ points with smaller values of E .

Our charge space hosts three important two-dimensional surfaces. These are

- The unitarity plane $E = J_1 + J_2$. The unitarity bound tells us that there are no states below this plane.
- The surface S_1 on which Kerr Black holes have $\omega_1 = 1$ but $\omega_2 \leq 1$ (see (2.26) for a concrete expression).
- The surface S_2 on which Kerr Black holes have $\omega_2 = 1$ but $\omega_1 \leq 1$ (see (2.26) for a concrete expression).

The surfaces S_1 and S_2 intersect on the line C_{12} . Along this line, $J_1 = J_2 = J$ and the energy is given as a function of J by the function $E_\omega(J)$ defined above (2.41).

³⁰For all allowed values of a and b it follows from (2.10) that this inequality is equivalent $m \gg 1$.

³¹This happens because the fluid tries to move as far as possible from the axis of rapider rotation (as a consequence of its larger centrifugal force).

³²When this assumption fails - e.g. at low energies in $AdS_5 \times S^5$ (see the introduction)- only a part of the phase diagram presented in this section is physical.

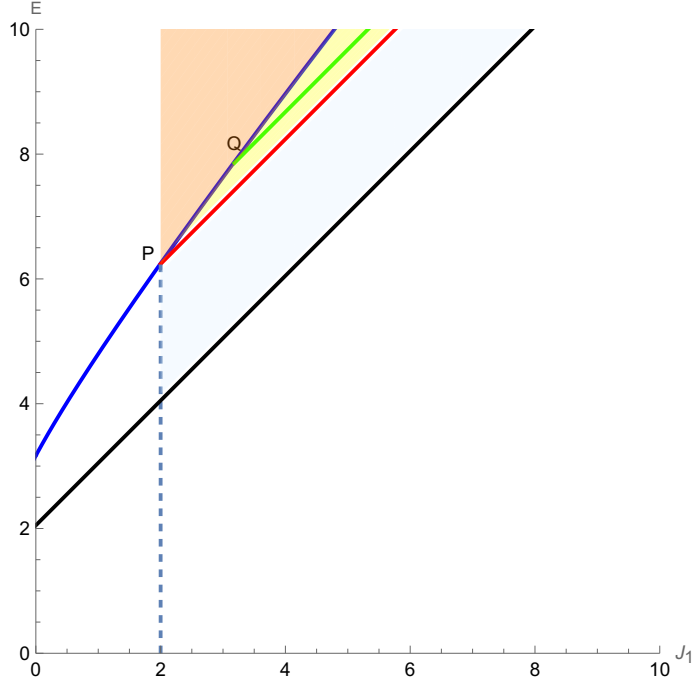


Figure 3. A constant J_2 ($J_2 = 2$) slice of the phase diagram. We have plotted E on the y axis and J_1 on the x axis. The black line is the unitarity bound $E = 2 + J_1$. The blue curve is the line $\omega_1 = 1$. When $J_1 > 2$ this curve represents a phase boundary. Above this curve, the dominant phase is the usual vacuum black hole. Below this curve (shaded yellow region) we have a rank 2 Grey Galaxy. All points on the green 45-degree line (in this phase) have the same entropy, given by the entropy of the vacuum $\omega_1 = 1$ black hole at the lower end of the green line. The rank 2 Grey Galaxy phase ends on the red 45-degree line, which meets the $\omega_1 = 1$ curve at $J_1 = 2$. Below the red curve (shaded blue region) the dominant phase is the rank four Grey Galaxy all the way down to the unitarity bound. We have not attempted to sketch the phase diagram for $J_1 < 2$; part of the phase diagram is best visualized in constant J_2 slices.

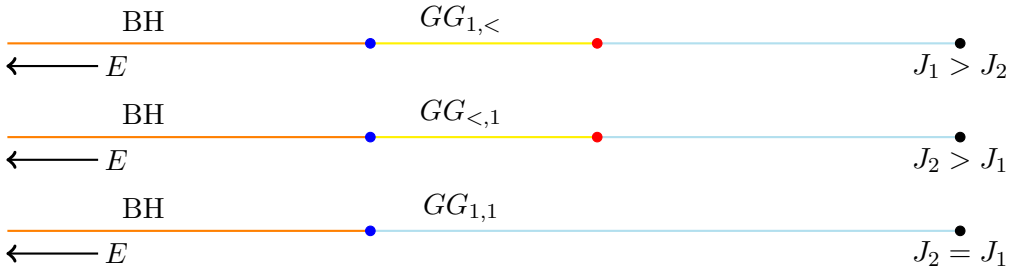


Figure 4. Here we plot the line diagram, which shows the transitions of the different phases as we lower the energy E (Keeping the J_1 and J_2 fixed) starting from the vacuum black hole phase. These plots are presented for three different cases; namely $J_1 > J_2$, $J_2 > J_1$, and $J_1 = J_2$.

Our system has four phases. The first of these is the ‘vacuum’ black hole phase, in which the bulk is described by Kerr AdS black holes. We call this the (BH) phase. This (BH) phase is stable only if $\omega_1 < 1$ and $\omega_2 < 1$, i.e. this phase exists only ‘above’ the

higher of the two sheets S_1 and S_2 .

The second phase is a Grey Galaxy (GG) with a central black hole that has $\omega_1 = 1$ and $\omega_2 < 1$, in equilibrium with a gas that has $E = J_1$. We call this the $(GG)_{1,<}$ phase. This phase only exists when $J_1 > J_2$ ³³. Points in this phase are obtained by starting on any point on S_1 with $J_1 > J_2$, and then shooting a ray upwards at 45 degrees in the $E - J_1$ plane. Note that this ray is shot at constant J_2 . This is depicted in Fig 3, where we present a plot of the $E - J_1$ plane at $J_2 = 2$. The blue curve in Fig 3 represents the intersection of S_1 with this plane. Note that the slope of this curve is always greater than 45 degrees, and asymptotes to 45 degrees at large J_1 (this can be shown to be true at all values of J_2). It follows that 45 degree lines shot out from S_1 - like the green line in Fig 3- never intersect the surface S_1 .³⁴ It follows, therefore, that no point in the space (E, J_1, J_2) lies simultaneously in the (BH) phase and the $GG_{1,<}$ phase. The point P in Fig. 3 marks the point on S_1 at which $J_1 = J_2$ (in the case of Fig 3, $J_2 = 2$). This point lies on the boundary of the surface S_1 . Note that the 45-degree lines shot out from P - the line drawn in red in Fig 3, - gives the lowest points (i.e. the points with the smallest energy for any given J_1 and J_2) that are accessed in this phase.³⁵ The union of these (red) lines for all values of J_2 makes us a second surface which we denote by B_1 . The set of points in (E, J_1, J_2) space, that make up the $(GG)_{1,<}$ phase are those bounded from above by the surface S_1 , and from below by the surface B_1 (this is the region shaded yellow in Fig 3). As is clear from Fig. 3, there is a unique ray that reaches every point in this region.

The third phase - the $(GG)_{<,1}$ phase - is a GG with a central black hole that has $\omega_2 = 1$ and $\omega_1 < 1$, in equilibrium with a gas that has $E = J_2$. This phase only exists when $J_2 > J_1$, and points in this phase are obtained by starting on any point on S_2 and then shooting a ray upwards at 45 degrees in the $E - J_2$ plane at fixed J_1 . The set of points that lie in this phase is characterized as in the previous paragraph. These points are bounded from above by S_2 and from below by B_2 (B_2 is defined in a manner entirely analogous to B_1 , but with $1 \rightarrow 2$).

The fourth phase - The $(GG)_{1,1}$ phase - consists of a GG with a central black hole that has $\omega_1 = \omega_2 = 1$, in equilibrium with a gas that has $E = J_1 + J_2$. Points in this phase are obtained starting on the curve C_{12} and shooting out rays that obey $\Delta E = \Delta J_1 + \Delta J_2$, in every positive direction³⁶ in the $J_1 J_2$ plane.

We will now demonstrate that points that lie in the fourth phase always lie below both B_1 and B_2 , and, moreover, that every point below B_1 and B_2 (but above the unitarity plane) hosts a unique GG in the $(GG)_{1,1}$ phase.

Let us consider some given values of J_1 and J_2 . For definiteness, we suppose that $J_1 = \alpha$ and $J_2 = \beta$ with $\alpha > \beta$ (the other case can be discussed analogously). Since $J_1 > J_2$, there exists a (unique) point $O_1(\alpha, \beta)$ on the sheet B_1 with the same values of

³³When $J_2 > J_1$, $\omega_2 > \omega_1$, so it is impossible to find $\omega_1 = 1$ and $\omega_2 < 1$.

³⁴The diagram in Fig 3 is qualitatively similar to Fig 1. of [1], which plots E vs J for black holes in AdS_4 . The one qualitative difference is that the unitarity curve - the black line in Fig 3 is offset from the origin (the offset is by J_2 , which has no analogue in AdS_4).

³⁵Note also that P lies on the curve C_{12} .

³⁶By a positive direction we mean a direction in which J_1 and J_2 both increase as E increases.

J_1 and J_2 , namely with $J_1 = \alpha$ and $J_2 = \beta$. Let us denote the energy of this point by $E_{B_1}(\alpha, \beta)$. It follows that the point $O_1(\alpha, \beta)$ has coordinates

$$(J_1, J_2, E) = (\alpha, \beta, E_{B_1}(\alpha, \beta)).$$

By definition, the point $(\alpha, \beta, E_{B_1}(\alpha, \beta))$ is connected - by a 45 degree line in the $E - J_1$ plane - to some point $P_{12}(\alpha, \beta)$ on C_{12} (this is the point P in Fig 3). Since this line propagates at constant J_2 , it follows that $J_2 = \beta$, and the coordinates (J_1, J_2, E) of $P_{12}(\alpha, \beta)$ are

$$(\beta, \beta, E_\omega(\beta)).$$

Since the points $O_1(\alpha, \beta)$, and the points $P_{12}(\alpha, \beta)$ are connected by a 45 degree line in the $E - J_1$ plane, it follows that

$$E_\omega(\beta) - E_{B_1}(\alpha, \beta) = \beta - \alpha \quad (3.1)$$

Let us now search for other points in this phase with $J_1 = \alpha$ and $J_2 = \beta$. Such a point must lie at the endpoints of positive rays shot out from C_{12} . As the rays must be positive, it follows that it must originate at points on C_{12} with $J < \beta$.³⁷ Let us study a point that originates at $J = \beta - x$, i.e. from the point $(\beta - x, \beta - x, E_\omega(\beta - x))$. This ray has to end up at $(J_1, J_2) = (\alpha, \beta)$. Since the ray obeys $\Delta E = \Delta J_1 + \Delta J_2$, it follows that it lands up at the point

$$(\alpha, \beta, E_\omega(\beta - x) + (\alpha - (\beta - x)) + (\beta - (\beta - x))) = (\alpha, \beta, E_\omega(\beta - x) + \alpha - \beta + 2x)$$

Using (3.1), the coordinates of this point simplify to

$$(\alpha, \beta, E_{B_1}(\alpha, \beta) + E_\omega(\beta - x) - E_\omega(\beta) + 2x)$$

Now we have already explained (see around (2.42)) that the curve $E_\omega(y)$ is monotonic with a slope everywhere greater than two. It follows, as a consequence, that the quantity $E_{B_1}(\alpha, \beta) + E_\omega(\beta - x) - E_\omega(\beta) + 2x$ starts out equal to $E_{B_1}(\alpha, \beta)$ when $x = 0$, and then decreases monotonically, (as x is increased) until it equals $\alpha + \beta$ at $x = \beta$ (this is the largest allowed value of x). We have just proved, in other words, that every point between B_1 and the unitarity plane represents a unique $(GG)_{1,1}$ black hole.

The structure of the phase diagram (in the microcanonical ensemble) is now clear. This diagram is best understood as follows. Let us sit at fixed values of J_1 and J_2 and examine which phase we occupy as we vary E (see Fig. 4). At large values of E we are always in the (BH) phase.

Let us first assume that $J_1 > J_2$. In this case, as we lower energy, we eventually hit the sheet S_1 , and transit to the $(GG)_{1,<}$ phase (see the first of Fig. 4). Upon further lowering energy we hit the sheet B_1 and transit to the $(GG)_{1,1}$ phase. Finally, further lowering the energy takes us to the unitarity sheet.³⁸ The case $J_2 > J_1$ is similar: the discussion of the previous paragraph applies unchanged $1 \leftrightarrow 2$ (see the second of Fig. 4).

³⁷Else the ray would have to proceed in a direction that decreases J_2 , which violates its positivity.

³⁸The size of the energy interval that lies in the $(GG)_{1,<}$ depends on J_1 and J_2 . In particular, this interval goes to zero when $J_1 - J_2 \rightarrow 0$.

Finally, let us consider the case $J_1 = J_2$. In this case, as we lower energy, we eventually hit the line C_{12} and transit directly into the $GG_{1,1}$ phase. Further lowering takes us to the unitarity sheet (see the last of Fig. 4).

We emphasize that the discussion above is completely quantitative. It is, for instance, a simple matter to produce a `Mathematica` file that allows the reader to input any values of the energy and two angular momenta, and outputs the phase that these charges lie in, the energy and angular momenta of the seed black hole (at those values of total charges), and the entropy of this seed black hole. We have written such a file, and would be happy to share the same upon request.

As explained in the introduction, while Grey Galaxies of rank 2 are qualitatively similar to Grey Galaxies in AdS_4 , Grey Galaxies of rank 4 have several new features. Throughout the rest of this paper, we focus on Grey Galaxies of rank 4. Over the next three sections, we will build towards a (conjectured) formula for the boundary stress tensor of such Grey Galaxies.

4 Gas thermodynamics in the canonical ensemble

In thermal AdS (and, effectively, in the gas part of a Grey Galaxy phase), the bulk partition function is a product over partition functions Z_{Δ, J_L, J_R} for each field theory single trace primary operator (here Δ , J_L , and J_R denote the scaling dimension, $SU(2)_L$ representation and $SU(2)_R$ representation of the primary). In this brief section, we determine the multiparticle partition function of

- The bulk field dual to a scalar primary operator of dimension Δ and all its descendants.
- All bulk fields arising out of the 10-dimensional dilaton in IIB supergravity.
- All bulk fields of IIB supergravity on $AdS_5 \times S^5$

In each case, we work in the limit that $1 - \omega_1$ and $1 - \omega_2$ are both small (consequently the results of this subsection will be of use when studying Grey Galaxies of rank 4).

As we explain below, a striking feature of our results is that all partition functions we study take the ‘fluid form’ even though we are not necessarily working at high temperatures.

4.1 Partition function for a single scalar in AdS_5

Consider a primary O with $J_L = J_R = 0$. Its descendants take the form

$$(\partial^2)^n \partial_{\mu_1} \dots \partial_{\mu_J} O \tag{4.1}$$

where the derivatives $\partial_{\mu_1} \dots \partial_{\mu_J}$ are understood to act in a ‘trace removed’ manner. The derivatives $\partial_{\mu_1} \dots \partial_{\mu_J}$ generate a spin $(\frac{J}{2}, \frac{J}{2})$ representation of $SU(2)_L \times SU(2)_R$. Let m_L and m_R represent the quantum numbers of J_L^z and J_R^z . Clearly m_L and m_R each run over the range $(-J/2, J/2)$. It follows that the full partition function

$$\text{Tr} e^{-\beta H + \beta(\omega_1 + \omega_2) J_L^z + \beta(\omega_1 - \omega_2) J_R^z}$$

³⁹ (obtained by multiparticling over operators in the given $SO(4, 2)$ multiplet) is given by

$$\ln Z(\beta, \omega_1, \omega_2) = - \sum_{n=0}^{\infty} \sum_{J=0}^{\infty} \sum_{m_L=-J/2}^{J/2} \sum_{m_R=-J/2}^{J/2} \ln \left(1 - e^{-\beta(\Delta+2n+J)+\beta\omega_1(m_L+m_R)+\beta\omega_2(m_L-m_R)} \right) \quad (4.2)$$

The key point here is that the partition function in (4.2) diverges when either ω_1 or ω_2 tend to unity. ⁴⁰ This point may be made explicit by expanding the logarithm in (4.2) in a Taylor series and then performing the summations over n , m_L , m_R and J (see Appendix C). Specializing to the case in which ω_1 and ω_2 are both very near unity and working to leading order both in $1 - \omega_1$ and in $1 - \omega_2$, we obtain

$$\ln Z(\beta, \omega_1, \omega_2) \approx \sum_{q=1}^{\infty} \frac{1}{q} \left[- \frac{e^{-q\beta(\Delta-6)}}{(e^{2\beta q} - 1)^4} + \frac{e^{-q\beta(\Delta-2)}}{4\beta^2 q^2 (1 - \omega_1) (1 - \omega_2) \sinh^2(\beta q)} \right] \approx \frac{h_{\Delta}(\beta)}{(1 - \omega_1) (1 - \omega_2)} \quad (4.3)$$

$$h_{\Delta}(\beta) = \sum_{q=1}^{\infty} \frac{e^{-q\beta(\Delta-2)}}{4\beta^2 q^3 \sinh^2(\beta q)} \quad (4.4)$$

While the first term in the first line of (4.3) is of order unity as $\omega_i \rightarrow 1$, the second term (again on the first line of (4.3)) diverges in this limit. When either ω_1 or ω_2 (or both) is near to unity, therefore, the gas partition function is well approximated by the second term, i.e. by the second line of (4.3).

At leading order in $1 - \omega_1$ and $1 - \omega_2$, the second line of (4.3) may equivalently be rewritten as

$$\ln Z \approx \frac{4h_{\Delta}(\beta)}{(1 - \omega_1^2) (1 - \omega_2^2)} \quad (4.5)$$

(4.5) takes precisely the form of the partition function of a ‘conformal’ fluid (with the rotational chemical potentials ω_1 and ω_2) on S^3 [15], with $4h_{\Delta}(\beta)$ playing the role of the ‘zero angular velocity partition function’ of the same fluid.

³⁹Note that J_L and J_R are related to the ‘orthogonal two plane rotation quantum numbers’ J_1 and J_2 via

$$J_L = \frac{J_1 + J_2}{2}, \quad J_R = \frac{J_1 - J_2}{2},$$

Consequently, the partition function listed above can also be written as

$$\ln Z = - \sum_{n=0}^{\infty} \sum_{J=0}^{\infty} \sum_{|m_1|+|m_2|\leq J} \ln(1 - e^{-\beta(\Delta+2n+J)+\beta\omega_1 m_1+\beta\omega_2 m_2})$$

⁴⁰In the case that ω_1 is parametrically near to unity, but $\omega_2 < \text{unity}$ (or vice versa), the divergence has its origins, respectively, in modes for which n , $\frac{J}{2} - m_L$ and $\frac{J}{2} - m_R$ are kept fixed at values of order unity, while J runs over very large values. In the case that ω_1 and ω_2 are both parametrically near to unity (the situation of main interest for this section), the divergence has its origin in modes for which n , $\frac{J}{2} - m_L$ are fixed, while J and m_R run over very large values.

The thermodynamical charges that follow from (4.5) also, of course, take the fluid form [19] and are explicitly given by

$$\begin{aligned}
E &= \frac{8h_\Delta(\beta)}{\beta} \left(\frac{1}{(1-\omega_2^2)^2(1-\omega_1^2)} + \frac{1}{(1-\omega_1^2)^2(1-\omega_2^2)} \right) \\
J_1 &= \frac{1}{\beta} \frac{8h_\Delta(\beta)}{(1-\omega_1^2)^2(1-\omega_2^2)} \\
J_2 &= \frac{1}{\beta} \frac{8h_\Delta(\beta)}{(1-\omega_2^2)^2(1-\omega_1^2)} \\
S &= \frac{(\beta\partial_\beta - 1)4h_\Delta(\beta)}{(1-\omega_1^2)(1-\omega_2^2)}
\end{aligned} \tag{4.6}$$

Note that while all the charges diverge when $\omega_i \rightarrow 1$ ($i = 1, 2$),⁴¹ the energy and two angular momenta diverge like $\frac{1}{(1-\omega)^3}$ and the entropy diverges like $\frac{1}{(1-\omega)^2}$. In both these cases, the entropy is subdominant compared to the energy, a point that will prove physically significant below.

4.2 Partition function for the 10d dilaton

The partition function for all scalars arising from the 10d dilaton can be computed from the partition function in AdS_5 evaluated in (4.3), by noting that the KK reduction of the 10d dilaton gives rise to operators of dimension $\Delta = n + 4$ with $n = 0, 1 \dots \infty$. The operators of dimension $4 + n$ transform as completely symmetric traceless tensors of the R symmetry $SO(6)$. The dimension of this irreducible representation is d_n where

$$d_n = \frac{(2n+4)(n+1)(n+2)(n+3)}{24}. \tag{4.7}$$

As a consequence, the partition function for all KK modes arising out of the dilaton is given by

$$\ln Z \approx \sum_{n=0}^{\infty} d_n \frac{4h_\Delta(\beta)}{(1-\omega_1^2)(1-\omega_2^2)} \tag{4.8}$$

$$h_\Delta(\beta) = \sum_{q=1}^{\infty} \frac{e^{-q\beta(\Delta-2)}}{4\beta^2 q^3 \sinh^2(\beta q)}, \quad \Delta = n + 4, \tag{4.9}$$

Computing the sum over n we find

$$\begin{aligned}
\ln Z &= \frac{1}{(1-\omega_1^2)(1-\omega_2^2)} \sum_{q=1}^{\infty} \frac{4\text{csch}^6\left(\frac{\beta q}{2}\right) \text{csch}(\beta q)}{128\beta^2 q^3} \\
&= \frac{4h_\phi(\beta)}{(1-\omega_1^2)(1-\omega_2^2)}.
\end{aligned} \tag{4.10}$$

All thermodynamical formulae for this case are given by (4.6) with the replacement $h_\Delta(\beta) \rightarrow h_\phi(\beta)$.

⁴¹We assume here that $\mathcal{O}(1-\omega_1) = \mathcal{O}(1-\omega_2) = \mathcal{O}(1-\omega)$.

4.3 The partition function for II SUGRA on $AdS_5 \times S^5$

In the previous subsection, we worked out the gas partition function of all modes that arose out of the Kaluza Klein reduction of the dilaton in $AdS_5 \times S^5$. It is not too difficult to repeat this exercise, for all fields of IIB SUGRA on $AdS_5 \times S^5$, i.e. work out the multi-particle gas partition function over the full spectrum of small fluctuations on $AdS_5 \times S^5$ (at arbitrary values of ω_i) and then specialize the final result to $\omega_1 \approx 1$ and $\omega_2 \approx 1$. In this subsection, we present only our final answer (the interested reader will find details in Appendix D). Once again we find a result of the fluid dynamical form

$$\ln Z = \frac{4h_{YM}(\beta)}{(1 - \omega_1^2)(1 - \omega_2^2)}. \quad (4.11)$$

where

$$h_{YM}(\beta) = h_{YM}^B(\beta) + h_{YM}^F(\beta) \quad (4.12)$$

$h_{YM}^B(\beta)$ and $h_{YM}^F(\beta)$ (which, respectively, denote the bosonic and the fermionic contributions h_{YM}) are given by

$$\begin{aligned} h_{YM}^B(\beta) &= \sum_{n=1}^{\infty} \frac{(22 \cosh(\beta n) + 17 \cosh(2\beta n) + 6 \cosh(3\beta n) + \cosh(4\beta n) + 18) \operatorname{csch}^7\left(\frac{\beta n}{2}\right) \operatorname{sech}\left(\frac{\beta n}{2}\right)}{128\beta^2 n^3} \\ h_{YM}^F(\beta) &= \sum_{n=1}^{\infty} \frac{(-1)^{n+1} \cosh(\beta n) (\cosh(\beta n) + \cosh(2\beta n) + 2) \operatorname{csch}^7\left(\frac{\beta n}{2}\right)}{8\beta^2 n^3} \end{aligned} \quad (4.13)$$

Once again, all thermodynamical formulae for this case are given by (4.6) with the replacement $h_{\Delta}(\beta) \rightarrow h_{YM}(\beta)$ (see (4.12)).

5 Bulk Gas Stress tensor

5.1 The problem addressed

Stationary black holes in AdS_5 always live in equilibrium with surrounding thermal gas. When the black hole angular velocities are less than (and well separated from) unity, the bulk gas carries energy of order unity, and so its backreaction on the bulk metric is of order G_N ⁴² $\sim \frac{1}{N^2}$ and so is negligible in the large N limit. As we have explained in section 4, however, this is no longer the case when one or both of ω_i approach unity. In particular, when we set

$$\begin{aligned} 1 - \omega_1 &= \frac{\alpha_1}{N^{\frac{2}{3}}} \\ 1 - \omega_2 &= \frac{\alpha_2}{N^{\frac{2}{3}}} \end{aligned} \quad (5.1)$$

⁴²Here G_N is Newton's constant.

(α_1 and α_2 are numbers of order unity) then the energy and angular momentum in the bulk gas are both of order N^2 . In this situation the backreaction of the bulk gas cannot be totally ignored. As in [1], we will find that this energy is distributed over a very large region (upto a radial coordinate of order $N^{\frac{1}{3}}$). As a consequence, the energy density of the bulk gas is parametrically suppressed in N . For this reason, the backreaction of the bulk gas is accurately captured by a linear order. In leading order, moreover, the total backreaction is (effectively) a superposition of the backreaction from the black hole and the back reaction of the gas (see [1] for a detailed discussion of these points which carry over unchanged to this paper).

In this section (see subsection 1.4 for a discussion) we compute the bulk stress tensor for a Grey Galaxy built out of a single 10d bulk scalar field (‘the dilaton’) in $AdS_5 \times S^5$. As explained in the introduction, we postpone a discussion of the generalization to more realistic bulk matter to section 7.

5.2 Computation in 10d Euclidean Space

5.2.1 Setting up the computation

We wish to compute the expectation value of the bulk stress tensor for the dilaton in the thermal ensemble defined by

$$\mathcal{Z} = \text{Tr} \left[e^{-\beta(H - \omega_1 J_1 - \omega_2 J_2)} \right] \quad (5.2)$$

(5.2) is computed by a Euclidean path integral with coordinate identifications given by

$$(\tau, \phi_1, \phi_2, \Omega_i) \sim (\tau + \beta, \phi_1 - i\beta\omega_1, \phi_2 - i\beta\omega_2, \Omega_i) \quad (5.3)$$

43

In this section we proceed with the computation roughly along the lines of the analysis presented in section 4.3 of [1] with one difference that we will highlight below.⁴⁴ We find the one-point function of the stress tensor by evaluating the two-point function of the bulk scalar at separated points, taking the necessary derivatives (see (5.5) below), and taking the coincident limit. After performing a temperature independent renormalization of this result, we find an unambiguous finite result for the (temperature dependent) part of the stress tensor.

The computation performed in this subsection differs qualitatively from that performed in section 4.3 of [1] in one respect. Instead of Kaluza Klein decomposing the 10-dimensional dilaton into its various distinct 5-dimensional fields, determining the stress tensor field by field, and then summing these stress tensors, we work directly with the 10-dimensional

⁴³Let us define $\omega_i = i\tilde{\omega}_i$. When rewritten in terms of $\tilde{\omega}_i$, the Boltzmann factor can be rewritten as $e^{-\beta H} e^{(i\beta\omega_1 J_1 + i\beta\omega_2 J_2)}$. Now the operator $e^{i\alpha_i J_i}$ affects a rotation by angle α_i , and the path integral identifies the fields at $\tau = 0$ with the appropriately rotated fields at $\tau = \beta$. On substituting $\tilde{\omega}_i = i\omega_i$ we recover the identification (5.3).

⁴⁴As in 4.3 of [1], it is sufficient to work with thermal AdS_5 rather than in the background of a black hole, as the dominant contribution from the gas comes from very large values of $r \sim N^{\frac{1}{3}}$, where these two spaces are essentially identical.

dilaton, and so directly find the answer for the stress tensor after the summation. Remarkably enough the answer we find for the stress tensor from this (effectively summed up) 10-dimensional procedure is considerably simpler than the contribution from any one of its 5-dimensional KK modes.⁴⁵

Let us now proceed with the computation. 10-dimensional dilaton is a minimally coupled scalar field, and its bulk stress tensor of the dilaton field is given by the simple formula

$$T_{\mu\nu} = \partial_\mu \Phi \partial_\nu \Phi - \frac{g_{\mu\nu}}{2} (\partial\Phi)^2 \quad (5.4)$$

The expectation value of $T_{\mu\nu}$ in the ensemble (5.2) is given by

$$\langle T_{\mu\nu} \rangle = \lim_{x_1 \rightarrow x_2} \left[\partial_\mu^{x_1} \partial_\nu^{x_2} \tilde{G}(x_1 - x_2) - \frac{g_{\mu\nu}}{2} \left(\partial^{\alpha, x_1} \partial_\alpha^{x_2} \tilde{G}(x_1 - x_2) \right) \right] \quad (5.5)$$

where $\tilde{G}(x_1 - x_2)$ is the propagator on $AdS_5 \times S^5$ with the identifications (5.3). Using the method of images, it follows that $\tilde{G}(x_1 - x_2)$ is given by a sum over propagators on ordinary (non-thermal) Euclidean $AdS_5 \times S^5$ via the method of images:

$$\tilde{G}(x_1, x_2) = \sum_{q=-\infty}^{\infty} G(x_1, R^q(x_2)) \quad (5.6)$$

where the symbol R^q denotes the combined action of a translation in global time by β , a rotation by angle $-qi\omega_1\beta$ in the first two planes and the angle $-qi\omega_2\beta$ in the second two plane. The propagator $G(x_1, x_2)$, in turn, is given [13, 14] by the remarkably simple formula

$$G(x_1, x_2) = \frac{\Gamma[4]}{4\pi^5} \left(\frac{1}{u+v} \right)^4$$

where v is the chordal distance between the two points on S^5 , and u is the chordal distance between the two points on AdS_5 (see Appendix E for a review of the elegant derivation [13, 14] and for a definition of these chordal distances). As we will see below, all terms in the stress tensor that involve derivatives in the S^5 directions will turn out to be subleading, and so can be ignored. For our purposes, consequently, v in (5.7) can simply be set to zero (recall that all images lie at the same point on S^5). On the other hand our image points are separated in AdS_5 , so we need the expression for the chordal distance u . Working in global coordinates (the Euclidean continuation of the coordinates used in (6.3) below), it is not difficult to verify that the chordal distance (defined in (E.16) the Appendix) between points with coordinates $(r, \theta, \phi_1, \phi_2, \tau)$ and $(r', \theta', \phi'_1, \phi'_2, \tau')$ is given by

$$u = -2 + 2 \left[\sqrt{(1+r^2)(1+r'^2)} \cosh(\tau^E - \tau'^E) - rr' (\sin \theta \sin \theta' \cos(\phi_1 - \phi'_1) + \cos \theta \cos \theta' \cos(\phi_2 - \phi'_2)) \right] \quad (5.7)$$

⁴⁵As a consistency check of the results of this subsection, however, in Appendix F we obtain the final result for the bulk stress tensor ((5.23)) using the more tedious method (i.e. by summing the contributions from each of the (infinitely many) 5d fields).

The ‘method of images’, (5.6), instructs us to evaluate the propagator between points related so that $\tau' - \tau = q\beta$, $\phi_1 - \phi'_1 = -iq\beta\omega_1$, $\phi_2 - \phi'_2 = -iq\beta\omega_2$, $r = r' = r$, $\theta = \theta' = \theta$ ⁴⁶ and $\Omega_i = \Omega'_i$ for the q^{th} image. It follows that the chordal distance between a point and its q^{th} image (in AdS_5) is given by

$$u_q = -2 + 2 \left[(1 + r^2) \cosh(q\beta + \tau' - \tau) - r^2 (\sin^2 \theta \cos(\phi_1 - \phi'_1 - iq\beta\omega_1) + \cos^2 \theta \cos(\phi_2 - \phi'_2 - iq\beta\omega_2)) \right] \quad (5.8)$$

⁴⁷ (In the formula (5.8) above we will set

$$\tau' = \tau, \quad \phi'_1 = \phi_1, \quad \phi'_2 = \phi_2 \quad (5.9)$$

after taking all relevant derivatives).

5.2.2 The large r scaling limit

We wish to evaluate the bulk stress tensor at very large values of r . As we have explained around (5.5), the stress tensor is given by evaluating various derivatives of the Greens function (5.6) evaluated between the image points described above. At large values of r , the quantity u_q above generically becomes very large so the stress tensor (at large r) generically becomes very small. This generic expectation fails (and so we receive a substantial contribution to the bulk stress tensor) only if the bulk point and its image are separated in a nearly lightlike manner. This is possible (even though we are working in Euclidean spacetime) because the angular separation between images is imaginary (in contrast to the temporal separation, which, in Euclidean spacetime, is always real). If these two separations are nearly equal and opposite, points and their images can be effectively nearly lightlike separated.

In global AdS_5 , the length of the time circle is $\sqrt{1 + r^2}\beta$. The lengths of the two angular circles are $\beta r \omega_1 \sin \theta$ and $\beta r \omega_2 \cos \theta$. When ω_1 and ω_2 are both (substantially, i.e. by order unity) less than one, the effective length of the angular circle, which equals $r\beta\sqrt{(\omega_1^2 \sin^2 \theta + \omega_2^2 \cos^2 \theta)}$, is always substantially (i.e. by an order one fraction) less than the length of the time circle, and the bulk stress tensor is very small at large r . When ω_1 is very near to unity, but ω_2 is substantially smaller than unity, the angular circle approaches the size of the time circle (at large r) in a small range of θ values around $\frac{\pi}{2}$. In this case, the stress tensor is substantial upto $r \sim \frac{1}{\sqrt{1-\omega_1}}$. In this case, we find a two-spatial dimensional disk of matter around $\theta = \frac{\pi}{2}$. Similar remarks apply to the case ω_2 near unity, and ω_1 substantially less than unity. In this section, we focus attention on the case that ω_1 and ω_2

⁴⁶In computing the stress tensor we need to take derivatives w.r.t. the coordinates 1 and 2. For this purpose we should, really, leave r_1 and r_2 as distinct until after we have taken all derivatives. As in [1], however, all derivatives w.r.t. either r or θ turn out to be subleading: the leading order stress tensor is obtained from derivatives in only the time, ϕ_1 and ϕ_2 directions. For this reason, we simply set $r = r' = r$ and $\theta = \theta' = \theta$ right at the beginning of the computation.

⁴⁷As we have mentioned above, the chordal distance between images on the sphere simply vanishes.

are both of order unity. In this case, we find a substantial contribution to the bulk stress tensor at every value of θ , upto radial coordinates of order

$$r \sim \frac{1}{\sqrt{(1 - \omega_1 \sin^2(\theta) - \omega_2 \cos^2(\theta))}}$$

For the reasons mentioned above, the bulk stress tensor of this subsection is non negligible when x^2 defined by

$$r^2(1 - \omega_1 \sin^2(\theta) - \omega_2 \cos^2(\theta)) = x^2 \quad (5.10)$$

remains of unity or smaller (even though r is taken to be very large).

To first order in $1 - \omega_1$ and $1 - \omega_2$,

$$2(1 - \omega_1 \sin^2(\theta) - \omega_2 \cos^2(\theta)) = 1 - \omega_1^2 \sin^2(\theta) - \omega_2^2 \cos^2(\theta) = \frac{1}{\gamma^2(\theta)}, \quad (5.11)$$

where $\gamma(\theta)$ was defined in (1.5). Our definition of the rescaled coordinate x may, therefore, be rewritten as

$$x^2 = \frac{r^2}{2\gamma^2(\theta)}. \quad (5.12)$$

In this scaling limit, the formula for the chordal distance u_q (with the replacement (5.9)) simplifies to

$$\begin{aligned} u_q &= 2(\cosh(\beta q) + \beta q r^2 \sinh(\beta q)(1 - \omega_1 \sin^2(\theta) - \omega_2 \cos^2(\theta)) - 1) \\ &= 2(\cosh(\beta q) + \beta q x^2 \sinh(\beta q) - 1) \end{aligned} \quad (5.13)$$

(in going from the first to the second line of (5.13) we have used (5.10)). Similarly, we find

$$\begin{aligned} \partial_\tau u_q &= -\partial_{\tau'} u_q = -2((r^2 + 1) \sinh(\beta q)) \\ \partial_{\phi_1} u_q &= -\partial_{\phi_1'} u_q = 2ir^2 \sin^2(\theta) \sinh(\beta q \omega_1) \\ \partial_{\phi_2} u_q &= -\partial_{\phi_2'} u_q = 2ir^2 \sin^2(\theta) \sinh(\beta q \omega_2) \end{aligned} \quad (5.14)$$

5.2.3 Simplification from Chirality

As in [1] the bulk gas is effectively chiral (it moves, at almost the speed of light, in the direction of the vector field ⁴⁸

$$w^\mu \partial_\mu = (\partial_t - \partial_{\phi_1} - \partial_{\phi_2}) \quad (5.16)$$

⁴⁸As written, the vector field $w^\mu \partial_\mu$ is not a velocity vector field as $w^2 \neq -1$. The velocity vector field of the gas in the bulk equals

$$\gamma(x, \theta) (\partial_t - \omega_1 \partial_{\phi_1} - \omega_2 \partial_{\phi_2}), \quad \gamma(x, \theta) = \frac{1}{\sqrt{1 + \frac{r^2}{\gamma^2(\theta)}}} = \frac{1}{\sqrt{1 + 2x^2}} \quad (5.15)$$

In the limit $\omega_1 \rightarrow 1$ and $\omega_2 \rightarrow 1$, this vector field is clearly proportional to $w^\mu \partial_\mu$, with the x dependent proportionality factor displayed above.

For this reason (as we will see below) at leading order

$$g^{\mu_1\nu_1}g^{\mu_2\nu_2}\partial_{\mu_1}\partial_{\mu_2}\langle\Phi(x_1)\Phi(x_2)\rangle_q \propto u^{\nu_1}u^{\nu_2} \quad (5.17)$$

(here q denotes the contribution from the q^{th} and $-q^{th}$ image: as in Sec 4.3 of [1] we have renormalized our answer by dropping the (temperature and ω_i independent) contribution from $q = 0$). As u^μ is an almost lightlike vector, the second term in (5.5) is of subleading order, and we find

$$T_{\mu_1\mu_2} = -2 \sum_{q=1}^{\infty} K_{\mu_1\mu_2}^q \quad (5.18)$$

$$\begin{aligned} K_{\mu_1\mu_2}^q &= \partial_{\mu_1}\partial_{\mu_2}\langle\Phi(x_1)\Phi(x_2)\rangle_q \\ &= \partial_u^2 G(u, v) \frac{\partial u_q}{\partial \mu_1} \frac{\partial u_q}{\partial \mu_2} + \partial_u G(u, v) \frac{\partial^2 u_q}{\partial \mu_1 \partial \mu_2} \end{aligned}$$

(After all derivatives are taken, u_q is evaluated on the configuration (5.9))

The expression on the RHS of (5.19) has two kinds of terms: those proportional to a second derivative of u_q and those proportional to the square of the first derivatives of u_q . It is not difficult to verify that terms of the first sort are subleading (in the large r limit) to terms of the second sort. ⁴⁹

5.2.4 Final Result at leading order

From the discussion of the previous subsection, we see that $K_{\tau\tau}^q$ simplifies, at leading order, to

$$K_{\tau\tau}^q = \partial_u^2 G(u, v) \frac{\partial u_q}{\partial \tau} \frac{\partial u_q}{\partial \tau'} \Big|_{u=u_q} \quad (5.19)$$

Putting everything together, in leading order we find

$$\begin{aligned} K_{\tau\tau}^q &= -16\gamma^4(\theta)x^4 \sinh^2(q\beta) \partial_u^2 G(u, v) \Big|_{v \rightarrow 0} \\ &= -\frac{4\gamma^4(\theta)x^4 \sinh^2(\beta q) \Gamma[6]}{\pi^5 u_q^6} \end{aligned} \quad (5.20)$$

⁴⁹For instance,

$$\begin{aligned} \frac{\partial u}{\partial \tau^E} \frac{\partial u}{\partial \tau'^E} &= -4r^4 \sinh^2(q\beta) \\ &= -16\gamma^4(\theta)x^4 \sinh^2(q\beta) \\ \frac{\partial^2 u}{\partial \tau^E \partial \tau'^E} &= -2r^2 \cosh(q\beta) \\ &= -4\gamma^2(\theta)x^2 \cosh(q\beta) \end{aligned}$$

Note that while the RHS of the first line of (5.19) is of order r^4 , the second line is of order r^2 , illustrating the fact that terms of the schematic form $\partial^2 u$ are subleading (and so can be ignored) compared to terms of the schematic form $(\partial u)^2$.

$$\langle T_{00} \rangle = \sum_{q=1}^{\infty} \frac{8\gamma^4(\theta)x^4 \sinh^2(q\beta)\Gamma[6]}{\Gamma[2]\pi^5 u_q^6} \quad (5.21)$$

Other components of the stress tensor are computed in a similar manner. At leading order we find

$$\begin{aligned} \langle T_{0\phi_1} \rangle &= \sum_{q=1}^{\infty} \frac{4\gamma^4(\theta)x^4 \sinh^2(q\beta) \sin^2 \theta \Gamma[6]}{\pi^5 u_q^6} \\ \langle T_{0\phi_2} \rangle &= \sum_{q=1}^{\infty} \frac{4\gamma^4(\theta)x^4 \sinh^2(q\beta) \cos^2 \theta \Gamma[6]}{\pi^5 u_q^6} \\ \langle T_{\phi_1\phi_1} \rangle &= \sum_{q=1}^{\infty} \frac{4\gamma^4(\theta)x^4 \sinh^2(q\beta) \sin^4 \theta \Gamma[6]}{\pi^5 u_q^6} \\ \langle T_{\phi_2\phi_2} \rangle &= \sum_{q=1}^{\infty} \frac{4\gamma^4(\theta)x^4 \sinh^2(q\beta) \cos^4 \theta \Gamma[6]}{\pi^5 u_q^6} \\ \langle T_{\phi_1\phi_2} \rangle &= \sum_{q=1}^{\infty} \frac{4\gamma^4(\theta)x^4 \sinh^2(q\beta) \sin^2 \theta \cos^2 \theta \Gamma[6]}{\pi^5 u_q^6} \\ \langle T_{\theta i} \rangle &= 0, \quad i \in \{\tau_E, \theta, \phi_1, \phi_2\} \\ \langle T_{r i} \rangle &= 0 \\ \langle T_{\alpha\beta} \rangle &= 0 \\ \langle T_{\mu\alpha} \rangle &= 0, \quad y_\alpha, y_\beta \in S^5, \quad x_\mu \in AdS_5 \end{aligned} \quad (5.22)$$

In the matrix form,

$$\langle T_{\mu\nu} \rangle = 4\mathcal{F}(x)\gamma^4(\theta) \begin{pmatrix} 1 & 0 & 0 & \sin^2(\theta) & \cos^2(\theta) \\ 0 & 0 & 0 & 0 & 0 \\ 0 & 0 & 0 & 0 & 0 \\ \sin^2(\theta) & 0 & 0 & \sin^4(\theta) & \sin^2(\theta) \cos^2(\theta) \\ \cos^2(\theta) & 0 & 0 & \sin^2(\theta) \cos^2(\theta) & \cos^4(\theta) \end{pmatrix} \quad (5.23)$$

here, $\mu, \nu \in \{t, r, \theta, \phi_1, \phi_2\}$ and

$$\begin{aligned} \mathcal{F}(x) &= \sum_{q=1}^{\infty} \frac{2x^4 \Gamma[6] \sinh^2 \beta q}{\pi^5 u_q^6} \\ &= \sum_{q=1}^{\infty} \frac{x^4 \Gamma[6] \sinh^2 \beta q}{2^5 \pi^5 ((\cosh(\beta q) + \beta q x^2 \sinh(\beta q) - 1))^6} \end{aligned} \quad (5.24)$$

The final form of the bulk stress tensor can be succinctly rewritten as

$$T_{\mu\nu} = 4\mathcal{F}(x)\gamma^4(\theta)w_\mu w_\nu \quad (5.25)$$

where w_μ was defined in (5.16). Note this stress tensor takes the form (5.17) as foreshadowed above.⁵⁰

We will find it useful below to have explicit expressions for $\mathcal{F}(x)$ at large and small values of x . At small values of x we find

$$\begin{aligned}\mathcal{F}(x) &= x^4 D + \mathcal{O}(x^6) \\ D &= \left(\frac{\Gamma[6]}{2^6 \pi^5} \sum_{q=1}^{\infty} \frac{1}{2 \sinh^2 \beta q (\cosh(\beta q) - 1)^6} \right)\end{aligned}\quad (5.26)$$

whereas at large values of x

$$\begin{aligned}\mathcal{F}(x) &= \frac{B}{x^8} + \mathcal{O}\left(\frac{1}{x^{10}}\right) \\ B &= \frac{15\Gamma[6]}{4\pi^5 \beta^6} \sum_{q=1}^{\infty} \frac{\operatorname{csch}^4(\beta q)}{q^6}\end{aligned}\quad (5.27)$$

5.3 Matching the total energy with the thermodynamical prediction

It is easy to compute the total energy E contained in the bulk stress tensor. The energy is the charge associated with the conserved current $T_{\mu\alpha}\zeta^\alpha$, where ζ^α is the killing vector corresponding to global time translations. In our coordinates $\zeta^t = 1$, with all other $\zeta^\mu = 0$. Consequently, $J_\mu = T_{\mu 0}$ and so $J^\mu = g^{\mu\alpha}T_{\alpha 0}$. The charge associated with this current equals the integral of $\sqrt{-g}g^{0\alpha}T_{\alpha 0}$ over a slice of constant time. As our background metric is diagonal, it follows that

$$\begin{aligned}E &= \int d^{10}x \sqrt{-g}g^{00}T_{00} \\ &= \Omega_5 \int d\Omega_3 dr r \times 4\gamma^4(\theta)\mathcal{F}(x) \\ &= \Omega_5 \int_{S^3} \gamma^6(\theta) \int_0^\infty dx x \times 8\mathcal{F}(x)\end{aligned}$$

⁵¹The integral over S^3 is easily evaluated

$$\begin{aligned}\int_{S^3} \gamma^6(\theta) &= 4\pi^2 \int_0^{\frac{\pi}{2}} \frac{d\theta \sin \theta \cos \theta}{(1 - \omega_1^2 \sin^2 \theta - \omega_2^2 \cos^2 \theta)^3} \\ &= \pi^2 \left(\frac{1}{(1 - \omega_1^2)(1 - \omega_2^2)^2} + \frac{1}{(1 - \omega_1^2)(1 - \omega_2^2)^2} \right)\end{aligned}\quad (5.28)$$

⁵⁰Using (5.15) this stress tensor can be rewritten in terms of the local fluid velocity. This rewriting is not very useful, however as $T_{\mu\nu}$ in (6.11) is more simply written in terms of $\gamma(\theta)$ rather than $\gamma(x, \theta)$ in (5.15). In other words (6.11) does not admit a particularly natural rewriting in terms of the bulk local fluid velocity.

⁵¹In going from the first to the second line we have used that $\int r dr = 2\gamma^2(\theta) \int x dx$.

The integral over x can also be computed

$$\begin{aligned}
& \int_0^\infty dx x \mathcal{F}(x) \\
&= \sum_{q=1}^\infty \int_0^\infty \frac{2\Gamma(6) \sinh^2 \beta q dx x^5}{\pi^5 (2 (\cosh(\beta q) + \beta q x^2 \sinh(\beta q) - 1))^6} \\
&= \sum_{q=1}^\infty \frac{\operatorname{csch}^6\left(\frac{\beta q}{2}\right) \operatorname{csch}(\beta q)}{128\pi^5 \beta^3 q^3} \\
&= \frac{h_\phi(\beta)}{\pi^5 \beta}
\end{aligned}$$

Putting it all together and using $\Omega_5 = \pi^3$ we find

$$\begin{aligned}
E &= \left(\frac{1}{(1-\omega_1^2)(1-\omega_2^2)^2} + \frac{1}{(1-\omega_1^2)(1-\omega_2^2)^2} \right) \sum_{q=1}^\infty \frac{\operatorname{csch}^6\left(\frac{\beta q}{2}\right) \operatorname{csch}(\beta q)}{16\beta^3 q^3} \\
&= \frac{8h_\phi(\beta)}{\beta} \left(\frac{1}{(1-\omega_1^2)(1-\omega_2^2)^2} + \frac{1}{(1-\omega_1^2)(1-\omega_2^2)^2} \right)
\end{aligned} \tag{5.29}$$

in perfect agreement with (4.6) with $h_\Delta(\beta) \rightarrow h_\phi(\beta)$.

6 Back-reactions on the metric

In this section, we compute the response (the backreaction) of the bulk metric to the bulk stress tensor (6.11) computed in the previous section. We continue to work within the model of the previous section (the bulk matter is given by a single massless 10d scalar field). We discuss the generalization to a more realistic bulk matter content in the next subsection.

6.1 AdS_5 metric in terms of right invariant one forms

The metric on a unit S^3

$$ds^2 = d\theta^2 + \sin(\theta)^2 d\phi_1^2 + \cos(\theta)^2 d\phi_2^2 \tag{6.1}$$

⁵² can be rewritten as

$$ds^2 = (\sigma_1)^2 + (\sigma_2)^2 + (\sigma_3)^2 \tag{6.2}$$

where σ_i are right invariant oneforms ⁵³ defined in (2.19) and (2.20). It follows that the metric of AdS_5 , in global coordinates, can be written as

$$ds_{AdS_5}^2 = -(1+r^2)dt^2 + \frac{dr^2}{1+r^2} + r^2 ((\sigma_1)^2 + (\sigma_2)^2 + (\sigma_3)^2) \tag{6.3}$$

⁵²Here ϕ_1 and ϕ_2 represent rotations in the two orthogonal two planes in the embedding R^4

⁵³This means that they are annihilated by the Lie derivatives corresponding to $SU(2)_R$ generators. This fact will, however, play no essential role in our computation.

6.2 Bulk Stress tensor in terms of right invariant oneforms

It is not difficult to check that the bulk stress tensor (5.23) can be succinctly rewritten in the form

$$T = 4\mathcal{F}(x)\gamma^4(\theta) (dt - \sigma_3) (dt - \sigma_3) \quad (6.4)$$

where x (see (5.10)) is defined as

$$x = \frac{r}{\sqrt{2\gamma(\theta)}} \quad (6.5)$$

6.3 Computation of the backreaction

As we have explained in subsection 1.4, the computation of the back reaction to the bulk stress tensor is a simple exercise because it can be performed in a manner that is ‘point by point’ from a boundary viewpoint. In this subsection, we perform this computation. In comparing the discussion below with that of subsection 1.4, it is useful to keep in mind that we are working at values of ω_1 and ω_2 such that $1 - \omega_1$ and $1 - \omega_2$ are both $\sim \frac{1}{N^{\frac{2}{3}}}$, so that $\gamma \sim N^{\frac{1}{3}}$.

As we see from (5.5), the stress the bulk gas stress tensor is a nontrivial function of the coordinate $x = \frac{r}{\sqrt{2\gamma(\theta)}}$.⁵⁴ Recall that, in the limit of interest, $\gamma(\theta)$ is parametrically large. For this reason (and as in [1]) it is convenient to rewrite the metric of AdS_5 (6.3) in this coordinate. In order to remove all explicit factors of $\gamma(\theta)$ from the resultant metric, we also focus on the neighborhood of some time t_0 , and some angular coordinates ϕ_0, ψ_0 and θ_0 , work with the scaled coordinates (for deviations away from our central coordinate)

$$\begin{aligned} t &= t_0 + \frac{\tau}{\sqrt{2\gamma(\theta_0)}} \\ \phi &= \phi_0 + \frac{\phi'}{\sqrt{2\gamma(\theta_0)}} \\ \psi &= \psi_0 + \frac{\psi'}{\sqrt{2\gamma(\theta_0)}} \\ \theta &= \theta_0 + \frac{\theta'}{\sqrt{2\gamma(\theta_0)}} \end{aligned} \quad (6.6)$$

Working to leading order in $\frac{1}{\sqrt{2\gamma(\theta_0)}}$, the metric of AdS_5 becomes

$$ds^2 = -x^2 d\tau^2 + \frac{dx^2}{x^2} + x^2 ((\sigma'_1)^2 + (\sigma'_2)^2 + (\sigma'_3)^2) + d\Omega_5^2 \quad (6.7)$$

⁵⁴The coordinate x is proportional (with an order one proportionality constant) to r' in (1.1).

where $\sigma'_i = \sqrt{2}\gamma(\theta_0)\sigma_i$. The explicit factor of $\sqrt{2}\gamma(\theta_0)$ disappears when these forms are written in terms of differentials of primed coordinates: explicitly

$$\begin{aligned}\sigma'_1 &= \frac{1}{2} \left(\sin\left(\phi_0 + \frac{\phi'}{\sqrt{2}\gamma(\theta_0)}\right) d(2\theta') - \cos\left(\phi_0 + \frac{\phi'}{\sqrt{2}\gamma(\theta_0)}\right) \sin\left(2\theta_0 + \frac{2\theta'}{\sqrt{2}\gamma(\theta_0)}\right) d\psi' \right) \\ \sigma'_2 &= \frac{1}{2} \left(\cos\left(\phi_0 + \frac{\phi'}{\sqrt{2}\gamma(\theta_0)}\right) d(2\theta') + \sin\left(\phi_0 + \frac{\phi'}{\sqrt{2}\gamma(\theta_0)}\right) \sin\left(2\theta_0 + \frac{2\theta'}{\sqrt{2}\gamma(\theta_0)}\right) d\psi' \right) \\ \sigma'_3 &= \frac{1}{2} \left(d\phi' - \cos\left(2\theta_0 + \frac{2\theta'}{\sqrt{2}\gamma(\theta_0)}\right) d\psi' \right)\end{aligned}\quad (6.8)$$

We would now like to define the coordinates w, y and z s.t.

$$dw = \sigma'_1, \quad dy = \sigma'_2, \quad dz = \sigma'_3 \quad (6.9)$$

Locally, this is possible if and only if $d\sigma'_i$ vanish. In the current context (always working in rescaled coordinates), $d\sigma'_i$ are of order $\frac{1}{2\gamma(\theta_0)}$, and so vanish at leading order. It follows that we can (in leading order) find coordinates that satisfy (6.9). In these coordinates the metric of AdS_5 can be rewritten in the ‘Poincare Patch form’

$$ds^2 = \frac{dx^2}{x^2} + x^2 (-d\tau^2 + dw^2 + dy^2 + dz^2) \quad (6.10)$$

The bulk stress tensor can be rewritten as

$$T = \mathcal{F}(x) 2\gamma^2(\theta_0) (d\tau - dz) (d\tau - dz) \quad (6.11)$$

We would now like to compute the backreaction on AdS space by solving the Einstein equation

$$R_{\mu\nu} - \frac{1}{2} R g_{\mu\nu} - 6g_{\mu\nu} = 8\pi G_N^{(10)} T_{\mu\nu} \quad (6.12)$$

In order to make the RHS of (6.12) concrete, we recall that the 10-dimensional Newton constant equals $G^{(10)} = 2^3 \pi^6 g_s^2 \alpha'^4$,⁵⁵ while R_{AdS} (in the case of $\mathcal{N} = 4$ Yang Mills theory) is $R_{AdS}^4 = 4\pi g_s N \alpha'^2$. It follows that

$$G^{(10)} = \frac{\pi^4 R_{AdS}^8}{2N^2} \quad (6.13)$$

so that

$$G^{(5)} = \frac{G^{(10)}}{\Omega_5 R_{AdS}^5} = \frac{\pi^4 R_{AdS}^3}{2N^2 \pi^3} = \frac{\pi R_{AdS}^3}{2N^2} \quad (6.14)$$

⁵⁶ We are working in units in which $R_{AdS} = 1$. Using (6.11) and (6.13) we see that (6.15) can be rewritten as

$$\begin{aligned}\left(R_{\mu\nu} - \frac{1}{2} R g_{\mu\nu} - 6g_{\mu\nu} \right) dx^\mu dx^\nu &= 8\pi \left(\frac{\pi^4}{2N^2} \right) \mathcal{F}(x) (2\gamma^2(\theta_0)) (d\tau - dz) (d\tau - dz) \\ &= \left(\frac{8\pi^5 \gamma^2(\theta_0)}{N^2} \right) \mathcal{F}(x) (d\tau - dz) (d\tau - dz)\end{aligned}\quad (6.15)$$

⁵⁵ So that the coefficient of $\int \sqrt{g} R$ equals $\frac{1}{(2\pi)^7 g_s (\alpha')^4} = \frac{1}{16\pi G_N}$

⁵⁶ We have used the fact that the volume of a unit S^5 is π^3 .

We see that the RHS of (6.15) is of order $\frac{\gamma^2(\theta_0)}{N^2}$. As we have explained in earlier sections, we will be interested in values of ω so that $\gamma^2(\theta_0) \sim N^{\frac{2}{3}}$. Consequently, the RHS of (6.15) is of order $\frac{1}{N^{\frac{4}{3}}}$ and so is parametrically small in the large N limit. Consequently, we can solve this backreaction in a linearized order. In this order, the correction to bulk AdS_5 metric takes the form

$$\delta ds^2 = \frac{8\pi^5 \gamma^2(\theta_0)}{N^2} x^2 f(x) (d\tau - dz) (d\tau - dz) \quad (6.16)$$

where the function $f(x)$ obeys the sourced minimally coupled scalar equation

$$\frac{1}{x^3} \partial_x (x^5 \partial_x f) = -2 \frac{x \mathcal{F}(x)}{x^3} \quad (6.17)$$

This equation can be solved by integration. We find

$$f(x) = 2 \int_x^\infty dy \left(\frac{1}{y^5} \int_0^y dz z \mathcal{F}(z) \right) \quad (6.18)$$

where, we have fixed the integration constants by demanding normalizability of our solution (at $x = \infty$) and regularity of the solution at $x = 0$.

We conclude that our final bulk metric is given by

$$ds_{AdS_5}^2 = -(1+r^2)dt^2 + \frac{dr^2}{1+r^2} + r^2 ((\sigma_1)^2 + (\sigma_2)^2 + (\sigma_3)^2) + \frac{8\pi^2 \gamma^2(\theta)}{N^2} r^2 f\left(\frac{r}{\gamma(\theta)}\right) (dt - \sigma_3) (dt - \sigma_3) \quad (6.19)$$

where the function $f(x)$ is given by (6.18) (and $\mathcal{F}(x)$ was listed in (5.24)).

We will find it useful, below, to know the behaviour of $f(x)$ at large and small values of x . When x is large, y in (6.18) is also everywhere large. Consequently the quantity

$$\begin{aligned} \int_0^y dz z \mathcal{F}(z) &= \int_0^\infty dz z \mathcal{F}(z) - \int_y^\infty dz z \mathcal{F}(z) \\ &= C - \frac{B}{6y^6} + \mathcal{O}(1/y^8) \end{aligned} \quad (6.20)$$

where B was defined in (5.27) and

$$\begin{aligned} C &= \int_0^\infty dz z \mathcal{F}(z) \\ &= \sum_{q=1}^\infty \frac{\text{csch}^6\left(\frac{\beta q}{2}\right) \text{csch}(\beta q)}{128\pi^5 \beta^3 q^3} \end{aligned} \quad (6.21)$$

(We obtain the second line of (6.21) by substituting (5.24) into the first line.)⁵⁷ Comparing with (4.10) we see that

$$C = \frac{h_\phi(\beta)}{\beta \pi^5} \quad (6.22)$$

⁵⁷The fact that integral that evaluates C (first line of (6.21)) converges follows from (5.26) and (5.27).

Inserting (5.27) into (6.18) yields the large x expansion

$$f(x) = \frac{h_\phi(\beta)}{2\pi^5 x^4 \beta} - \frac{B}{60x^{10}} + \mathcal{O}\left(\frac{1}{x^{12}}\right) \quad (6.23)$$

Note that C and B are both constants independent of all coordinates (they are also independent of the chemical potentials ω_i , but are functions of the temperature).

In order to obtain an expansion of $f(x)$ at small x it is useful to rewrite (6.18) (after an integration by parts) as

$$\begin{aligned} f(x) &= \frac{1}{2} \int_x^\infty dy \frac{\mathcal{F}(y)}{y^3} + \frac{1}{2x^4} \int_0^x dy y \mathcal{F}(y) \\ &= \frac{1}{2} \int_0^\infty dy \frac{\mathcal{F}(y)}{y^3} - \frac{1}{2} \int_0^x dy \frac{\mathcal{F}(y)}{y^3} + \frac{1}{2x^4} \int_0^x dy y \mathcal{F}(y) \\ &= \frac{1}{2} \int_0^\infty dy \frac{\mathcal{F}(y)}{y^3} - \frac{D}{6} x^2 + \mathcal{O}(x^4) \end{aligned} \quad (6.24)$$

where D was defined in (5.26).⁵⁸

6.4 Boundary Stress Tensor

We can now use the expansion of $f(x)$ at large x to evaluate the boundary stress tensor of our solution. Inserting (6.23) into (6.16), we see that for $r \gg \gamma(\theta)$, our bulk metric simplifies to

$$ds_{AdS_5}^2 = -(1+r^2)dt^2 + \frac{dr^2}{1+r^2} + r^2((\sigma_1)^2 + (\sigma_2)^2 + (\sigma_3)^2) + r^2(dt - \sigma_3)(dt - \sigma_3) \frac{16h_\phi(\beta)\gamma^6(\theta)}{N^2 r^4 \beta} \quad (6.25)$$

The usual formulae [27] allow us to read off the boundary stress tensor from (6.25); we find

$$\begin{aligned} T_{\text{bdry}} &= \left(\frac{4}{16\pi G_5}\right) \frac{16h_\phi(\beta)\gamma^6(\theta)}{\beta N^2} (dt - \sigma_3)(dt - \sigma_3) \\ &= \frac{8h_\phi(\beta)\gamma^6(\theta)}{\pi^2 \beta} (dt - \sigma_3)(dt - \sigma_3) \end{aligned} \quad (6.26)$$

The boundary stress tensor can be rewritten as follows. Let us define the four-velocity vector

$$u^\mu \partial_\mu = \gamma(\theta) (\partial_t - \omega_1 \partial_{\phi_1} - \omega_2 \partial_{\phi_2}) \quad (6.27)$$

Note that u^μ has been defined in a way that ensures that $u^\mu u_\mu = -1$. To leading order in the large $\gamma(\theta)$ expansion,

$$u^\mu \partial_\mu = \gamma(\theta) \left(\partial_t - \partial_{\phi_1} - \partial_{\phi_2} + \mathcal{O}\left(\frac{1}{\gamma(\theta)}\right) \right) \quad (6.28)$$

Ignoring the subleading correction, it follows that velocity one-form (obtained by lowering indices on the velocity vector field) takes the form

$$u_u dx^\mu = \gamma(\theta) (-dt + \sin^2 \theta d\phi_1 + \cos^2 \theta d\phi_2) = \gamma(\theta) (dt - \sigma_3) \quad (6.29)$$

⁵⁸The integral in the first term in the last line of (6.24) is convergent (this follows because $\mathcal{F}(y) \sim y^4$ at small y (see (5.26)) and $\sim \frac{1}{y^8}$ at large y (see (5.27)).

(where σ_3 was defined in (6.8)). Consequently, the stress tensor (6.26) can be rewritten as

$$(T_{\text{bdry}})_{\mu\nu} = \frac{2h_\phi(\beta)\gamma^4(\theta)}{\beta\pi^2} (4u_\mu u_\nu + g_{\mu\nu}) \quad (6.30)$$

(6.30) has precisely the spatial dependence of the equilibrium configuration of a four-dimensional conformal fluid rotating with the velocity (6.28) (see equations 28 and 14 of [15]). This is a satisfying result.

We can re-evaluate the energy of the gas by integrating the (00) component of (6.30) over the boundary sphere. Using the fact that $u_0^2 = \gamma^2$ we find

$$\begin{aligned} E &= \frac{h_\phi(\beta)}{\beta\pi^5} \pi^3 \int_{S^3} 8\gamma^6(\theta) \\ &= \frac{8h_\phi(\beta)}{\beta} \left(\frac{1}{(1-\omega_1^2)(1-\omega_2^2)^2} + \frac{1}{(1-\omega_1^2)(1-\omega_2^2)^2} \right) \end{aligned} \quad (6.31)$$

The final expression in (6.31) is in perfect agreement with (5.29).

7 Conjectured Boundary Stress Tensor for general bulk matter

In sections 5 and 6 we have computed the detailed bulk solution corresponding to a rank 4 Grey Galaxy supported by the bulk gas from all bulk fields emerging from the Kaluza Klein decomposition of the 10d dilaton. It is natural to ask how the computations of the previous two sections would be modified if the bulk matter that supported the Grey Galaxy was different (for instance if the bulk matter consisted of all the fields of IIB supergravity in 10 dimensions).

We expect that any reasonable choice for bulk matter would give rise to a bulk stress tensor of the form (6.11), but with the function $\mathcal{F}(x)$ replaced by some new function $\mathcal{F}'(x)$, whose detailed form depends on the details of the bulk matter content. We have explicitly verified that this is the case, both for 5d scalar field of any mass (see (F.14) in Appendix F) as well as for a massive 5d vector field or arbitrary mass (see (H.16) in Appendix H), and see no obstruction to this result holding for matter of arbitrary spin. While the precise form of $\mathcal{F}'(x)$ depends on the details of the bulk matter content and requires a computation, one particular moment of this function can be determined on general grounds. We now illustrate this point (which applies -with minor modifications- for any bulk matter content) in the context of an important example, namely the case in which the bulk is IIB Supergravity, the bulk dual to $\mathcal{N} = 4$ Yang-Mills theory on $AdS_5 \times S^5$.

In the particular example of IIB supergravity on $AdS_5 \times S^5$, we have already computed the thermodynamics of the bulk gas in (4.11). The energy of this gas is given by the first of (4.6), with $h_\Delta(\beta)$ replaced by $h_{YM}(\beta)$. But this total energy may also be obtained by

⁵⁹The term in (6.30) proportional to $g_{\mu\nu}$ has been added by hand to make the stress tensor traceless: this can be done because this term is proportional to $\gamma^4(\theta)$, and so is subleading compared to the term proportional to $u_\mu u_\nu$ (which is proportional to $\gamma^6(\theta)$).

integrating over the bulk stress tensor, which is given in terms of \mathcal{F}_{YM} (the name we give to \mathcal{F}' in this particular case). This constraint tells us (see around (5.29)) that

$$\int_0^\infty dx x \mathcal{F}_{YM}(x) = \frac{h_{YM}(\beta)}{\pi^5 \beta} \quad (7.1)$$

The analysis of section 6 now continues to apply with minor modifications. The back reaction of the metric to the full gas continues to be given by (6.19), but with $f(r/\gamma) \rightarrow f_{YM}(r/\gamma)$, with

$$f_{YM}(x) = 2 \int_x^\infty dy \left(\frac{1}{y^5} \int_0^y dz z \mathcal{F}_{YM}(z) \right) \quad (7.2)$$

Repeating the analysis around (6.20) and (6.21) we find that $f_{YM}(x)$ admits the large x expansion

$$f_{YM}(x) = \frac{h_{YM}(\beta)}{2\pi^5 x^4 \beta} - \frac{B_{YM}}{60x^{10}} + \mathcal{O}\left(\frac{1}{x^{12}}\right) \quad (7.3)$$

Here B_{YM} is a constant whose precise value we do not know but will not need.⁶⁰ It follows that the leading deviation of the metric from the metric of pure AdS_5 is given by (6.25) with $h_\phi(\beta) \rightarrow h_{YM}(\beta)$. Consequently, the gas component of the boundary stress tensor dual to the full Grey Galaxy (sourced by all gas fields in IIB supergravity on $AdS_5 \times S^5$) is given by (6.30) with $h_\phi(\beta) \rightarrow h_{YM}(\beta)$, i.e. by

$$(T_{\text{bdry}}^{YM})_{\mu\nu} = \frac{2h_{YM}(\beta)\gamma^4(\theta)}{\beta\pi^2} (4u_\mu u_\nu + g_{\mu\nu}) \quad (7.4)$$

In summary, our final prediction is that the boundary stress tensor of the Grey Galaxy in IIB theory on $AdS_5 \times S^5$ is the sum of the black hole boundary stress tensor (described in detail in subsection 2.7) and the gas boundary stress tensor (7.4). A similar result applies to any bulk theory on $AdS_5 \times M$ where, the internal manifold M could, for instance, be a $Y^{p,q}$.

8 Conclusion and Discussion

Grey Galaxies in AdS_D were studied exhaustively in [1] for the special case $D = 4$. In this paper, we have investigated Grey Galaxies in AdS_D for $D \geq 5$, with a special focus on the case $D = 5$. In this dimension, rotating black holes are parameterized by two angular velocities, ω_1 and ω_2 . We find Grey Galaxy phases when either ω_1 or ω_2 or both are taken parametrically near unity. When only one of ω_1 or ω_2 is near unity, we obtain a Grey Galaxy of rank 2. The gas contribution to the boundary stress tensor of this solution turns out to be sharply localized around a boundary equator (a similar behavior was noticed in AdS_4).

When both ω_i are parametrically near unity, the Grey Galaxy is qualitatively different from its four-dimensional cousin. In this case, the gas contribution to the boundary stress

⁶⁰Determination of this quantity - the analogue of (5.27) - which requires more knowledge of the distribution of the bulk gas stress tensor than we have without performing a computation.

tensor is smooth. A key result of this paper is that this stress tensor takes the fluid dynamical form (1.7), where the ‘fluid velocity’ u_μ is given in (1.4), and the function $h_{YM}(\beta)$ can be read off from the partition function of the bulk gas by comparison with (4.11). In the special case of $AdS_5 \times S^5$ (the bulk dual to $\mathcal{N} = 4$ Yang-Mills at strong coupling) we have explicitly computed $h_{YM}(\beta)$ (see (4.12)). We emphasize that the gas component of the boundary stress tensor takes a fluid dynamical form even at values of the temperature of order unity (in units of the radius of the boundary S^3).⁶¹

Although we have mainly focused on the study of rank 4 Grey Galaxies in AdS_5 , the structure of these solutions strongly suggests that the (obvious generalization of) form (1.2) always accurately captures the form of the boundary stress tensor for an odd D Grey Galaxy of maximum rank (of course with $h_{YM}(\beta)$ replaced by the function read off from the partition function of the relevant theory). In the case of Grey Galaxies of non-maximal rank (or of maximal rank but in even D) the boundary fluid is sharply localized on some part of the boundary. Even in these cases, we continue to expect the variation of the boundary stress tensor *along* the localizing manifold to be captured by the fluid model. It would be interesting to perform computations to verify these guesses.

From the boundary point of view, the black hole represents the bulk dual to a ‘gluon plasma’. The gas of gravitons in the Grey Galaxy is a gas of ‘glueballs’ (or, more accurately, single trace fields). The Grey Galaxy can be thought of as a phase in which the fast-rotating gluon plasma dynamically spits out an order one fraction of its energy into glueballs; it does so because the entropy it loses (due to loss of energy) is more than compensated for by the entropy it gains (due to the angular momentum loss). The final boundary stress tensor is effectively a sum of the boundary stress tensor of gluon plasma and the glueball gas. We suspect that the glueball gas takes a precisely fluid form (even at temperatures of order unity) due to relativistic boost effects, which make the effective rest volume of the sphere much larger than the lab frame rest volume, and so make the temperature effectively large in units of the effective rest frame size of the sphere. It would be interesting to investigate this point further.

All Grey Galaxies in AdS_D for even D - and all Grey Galaxies of non maximal rank in AdS_D at odd values of D - have a striking feature. Their boundary stress tensor is sharply localized on a submanifold of the boundary S^{D-2} . This feature can be used as an order parameter that sharply distinguishes these solutions from other phases like vacuum black holes. At odd values of D and maximal rank, however, the gas contribution to the

⁶¹As we take, say, ω_2 away from unity, the fluid dynamical form of the stress tensor becomes increasingly localized around an equator (over angular scale $1 - \omega_1 = \frac{\delta^2}{4}$) in qualitative agreement with the boundary stress tensor of a rank 2 Grey Galaxy. This follows because, in this limit,

$$\gamma = \frac{1}{\sqrt{1 - \omega^2 \sin^2 \theta}} \approx \frac{\sqrt{2}}{\sqrt{\delta^2 + \delta\theta^2}}, \quad 1 - \omega^2 \approx \frac{\delta^2}{2}$$

While the fluid model gets the localization scale right, it should not be expected to (and does not) get the details of the localization function correct (see equations 5.33-5.39 of [1]) as dynamics at these length scales are not properly captured by hydrodynamics (from a boundary point of view) or by the ‘point by point’ method of obtaining the bulk solution of this paper (contrast with the more complicated bulk evaluation in [1])

boundary stress tensor is as smooth as the black hole contribution. It would be interesting to find a sharp order parameter that distinguishes such Grey Galaxy phases from vacuum black holes. The key physical difference between the two phases lies in the fact that Grey Galaxies host a high energy gas at parametrically large values of the bulk radial coordinate (such a gas is absent in black hole phases). It should be possible to detect this gas using the boundary two point functions evaluated at parametrically small distances. It would be interesting to make this expectation precise.

It is, of course, a well-known result of the fluid gravity correspondence that the gluon plasma is a rather perfect fluid, that obeys the equations of relativistic hydrodynamics with a relatively small viscosity [16]. We emphasize that the glueball fluid studied in this paper is entirely different. It is composed of glueballs not gluons, is weakly interacting, and is characterized by parametrically large thermalization time scales (in comparison, the thermalization time scale of the gluon fluid is of the order of the inverse temperature). Moreover, a gas of gluons (on the boundary sphere) is accurately described by hydrodynamics only at large temperatures. This point can be seen even in equilibrium in our Grey Galaxy solutions. In any of our solutions, the boundary stress tensor of the rotating black hole is accurately captured by the perfect fluid hydrodynamical form only at small β . On the other hand the stress tensor of the glueball gas takes the fluid form at every value of β .

In the bulk, the graviton gas and the black hole are parametrically well separated in the radial coordinate. For this reason the black hole and the gravitons (i.e. the gluon ‘fluid’ and the glueball fluid) are essentially non-interacting. This fact would lead to rather striking phenomena from the boundary point of view. For instance, we could excite or force a Grey Galaxy by turning on a time dependent boundary source for any single trace operator - say the stress tensor - over distance and time scales of order unity. Such a forcing would excite the black hole in the usual manner: at late times all excitations would die down in a manner governed by the usual black hole quasi-normal modes. Through all of this, the bulk graviton gas (gas of glueballs) would carry on its perfect hydrodynamical motion, serenely unaffected, even though it lives in the same field theory location as the excited plasma.

It would, of course, be fascinating to understand the existence of Grey Galaxies - and the details of all these fascinating phenomena - from a direct analysis of the field theory. While Grey Galaxies are only sharply defined at large N , we see no reason for them not to exist at all values of λ , even down to $\lambda = 0$, and so may be accessible in perturbation theory, suggesting an exciting research program for the future.

In section 3 of this paper, we have used the Grey Galaxies constructed in this paper to present a fully quantitative conjecture for one part of the phase diagram of $\mathcal{N} = 4$ Yang-Mills theory as a function of energy and its two angular momenta. As we have explained in the introduction, the low energy part of the relevant phase diagram is dominated by small 10d black holes. It would be interesting to put 10d black holes (e.g. along the lines of [28]) and Grey Galaxies together, to construct a complete quantitative phase diagram for $\mathcal{N} = 4$ Yang Mills theory as a function of energy and angular momenta. It would also be interesting to generalize these results (and their counterparts for a charge without

angular momentum, [11]) to a conjectured phase diagram for $\mathcal{N} = 4$ Yang Mills theory as a function of all 6 Cartan charges (energy, two angular momenta, and three $SO(6)$ charges). Finally, it would be interesting to search for checks of this phase diagram, perhaps from exact computations performed in the BPS limit.

Our construction of the phase diagram in section 3 proceeded under the assumption that all relevant phases in the phase diagram are usual black holes and Grey Galaxies. We have seen above that this assumption fails when our background has internal manifolds (like S^5), in addition to the AdS_D solutions. In subsection 1.6 (and Appendix A) we have briefly investigated the question of whether other purely AdS higher topology black solutions - and associated phenomena - might be relevant for our phase diagram even in the absence of internal manifolds. Our tentative conclusion was that these solutions and phenomena appear irrelevant from the viewpoint of leading order thermodynamics, but this important question deserves a more careful investigation.

In this paper we have presented a complete bulk solution for rank 4 AdS_5 Grey Galaxies for only one choice of bulk matter, namely a single massless scalar field in $AdS_5 \times S^5$. Our physical interpretation of the results of this computation allowed us to come up with an educated guess for the boundary stress tensor for a Grey Galaxy in a theory with arbitrary bulk matter, for instance in full IIB supergravity in $AdS_5 \times S^5$. It would nonetheless be of interest to perform an honest computation of the full bulk solution with this matter content. Such a computation would allow us to verify our guesses, and would also give us the full bulk solution rather than just its boundary stress tensor. This exercise may be less daunting than it first sounds, as (in the limit of interest) the bulk gas stress tensor is completely determined from a (sum over) two-point functions between points that are almost lightlike separated. It seems likely that the relevant propagators simplify at these short proper distances, simplifying the computation. We leave further investigation of this point to future work.

Acknowledgments

We would like to thank S. Choi, A. Gadde, D. Jain, S. Kim, V. Krishna, S. Kundu, G. Mandal, O. Parrikar, and S. Trivedi and especially E. Lee and C. Patel for the very useful discussions. The work of K.B., V.K., S.M., J.M. and A.R. was supported by the J C Bose Fellowship JCB/2019/000052 and the Infosys Endowment for the study of the Quantum Structure of Spacetime. We would also like to acknowledge the debt to the people of India for their steady support to the study of the basic science.

A Black Rings and Gregory Laflamme Instabilities

In this Appendix, we investigate the role of Gregory Laflamme-type instabilities and black rings (and other similar solutions) in the phase diagram of the relevant gravitational theory. We argue that Gregory-Laflamme type instabilities only occur for black holes that are already super radiant unstable: the black hole components of Grey Galaxies are never

super radiant unstable. As a consequence, Gregory-Laflamme’s instabilities play no role in the phase diagram of the theory. Our analysis for black rings is less conclusive because these solutions are not analytically known except in the case that they are small (in units of the AdS radius). In this case (i.e. in the case of small black rings) we demonstrate that these solutions always have $\omega > 1$ and so are super radiant unstable. While we suspect that this conclusion also holds for large black rings, the lack of solutions for these objects stops us from reaching a definite conclusion here.

A.1 Gregory Laflamme Type instabilities

A.1.1 GL instabilities in flat space

Spinning black holes in bulk dimensions $D \geq 6$ are qualitatively different from their lower dimensional cousins in one important respect. This difference can already be seen in flat space as we now explain.

Let us consider a spinning flat space black hole in $D = 4$ or $D = 5$. Let us imagine that we hold the angular momentum (or angular momenta, in $D = 5$) of this black hole fixed and lower its energy. Both in $D = 4$ and $D = 5$ we find that this process cannot be continued indefinitely: there is a minimum energy (determined by the black hole angular momenta: roughly $GM \sim (GJ)^{\frac{D-3}{D-2}}$) at which the black hole becomes extremal. Black holes with energies lower than this extremal black hole do not exist⁶². It is also interesting to track the temperature of these black holes as their energy is decreased at fixed angular momentum. At large values of the energy the black holes in question are similar to Schwarzschild black holes and have negative specific heat. Starting at large energies, it follows that the black hole temperature increases (from zero) as we lower their energy. At a critical value of the energy (once again roughly of order $GM \sim (GJ)^{\frac{D-3}{D-2}}$), this temperature reaches a maximum. Upon further lowering the energy, the temperature of the black hole decreases, until it approaches zero at extremality.

In the case $D \geq 6$, on the other hand, Kerr black holes at fixed angular momentum exist at all energies ≥ 0 . Let us suppose we have turned on only one of the angular momenta (let’s say J_1) and that all other angular momenta are zero. As we lower the energy down to zero (at fixed J), the horizon of the black hole is a thin but large disk (at the center, the horizon is approximately $R^2 \times S^{D-4}$). As we approach zero energy (more precisely at energies $GM \ll (GJ)^{\frac{D-3}{D-2}}$) the radius of the disk increases, and its angular velocity decreases (in such a manner so that the product of the radius and angular velocity is roughly constant). The thickness of the disk - i.e. the radius of the S^{D-4} also decreases⁶³ - reaching zero when $M = 0$.⁶⁴

⁶²The corresponding solutions have a naked singularity, and so are unphysical

⁶³Quantitatively, the ratio of the thickness to the radius of the disk scales like $\frac{(GM)^{\frac{D-2}{D-3}}}{(GJ)}$ when M is small. The thickness scales like $r^{D-3} = GM$, and therefore the size of the disk scales like $\frac{J}{M}$.

⁶⁴Upon lowering the mass, the temperature of the black increases monotonically, from zero at very large mass, to infinity at very small mass. This statement may be verified as follows. Recall that the combined transformation $g_{\mu\nu} \rightarrow \lambda^2 g_{\mu\nu}$, $x^\mu \rightarrow \frac{x^\mu}{\lambda}$ is an invariance of the classical Einstein action. Physically, this transformation represents a stretching (by scale factor λ) of all spacetime features of the solution: for

The important point here is the following. As we have mentioned above, the black hole solution at low mass begins, locally, to resemble the product of a Schwarzschild black hole in $D - 2$ dimensions times a disk. It is, however, well known ([20],[21]) that configurations this sort are Gregory Laflamme unstable whenever the radius of the disk is much larger than the radius of the S^{D-4} . In other words, the black holes described above become unstable before they reach zero mass.

A.1.2 Gregory Laflamme instabilities in AdS space

The flat space discussion above has an analogue in AdS space. Once again the moduli space of spinning black holes in AdS_D is qualitatively different in $D = 4, 5$ and $D \geq 6$. In $D = 4, 5$, black holes at every fixed J become extremal⁶⁵ at an energy E_{ext} , whose value is such that $R_{AdS}E_{\text{ext}} > J$. Black holes do not exist at sub extremal energies, and so do not exist all the way down to the unitarity bound. In $D \geq 6$, however, black holes with a single rotational angular momentum exist all the way down to the unitarity bound $R_{AdS}E = J$ ([21]). At small values of GJ ($GJ \ll R_{AdS}^{D-2}$), the approach to this limiting black hole may be understood as follows. As we have seen above, for $GM \ll (GJ)^{\frac{D-3}{D-2}}$, the black hole horizon behaves like the thin flat space pancake of radius $\frac{J}{M}$. As we further decrease the mass of the black hole, its radius increases (and angular velocity decreases, proportional to the radius) until the radius of the pancake becomes $\sim R_{AdS}$ at $R_{AdS}E \sim J$. At this energy AdS space significantly modifies the flat space-like behaviour. The energy of the black hole can be further lowered all the way down to the unitarity bound $R_{AdS}E = J$, at which point the thickness of the pancake shrinks to zero, while, somewhat surprisingly, its radius continues to grow without bound (notwithstanding the AdS potential barrier).

As in flat space, pancake like black holes in AdS_D ($D \geq 6$) suffer from a Gregory-Laflamme like instability whenever the thickness of the pancake is much smaller than the minimum radius of the pancake and the AdS radius. When $GJ \ll R_{AdS}^{D-2}$, this happens for $GM \lesssim (GJ)^{\frac{D-3}{D-2}}$. Note that the ratio of the critical energy for the Gregory Laflamme instability, $(GJ)^{\frac{D-3}{D-2}}$ to the unitarity bound $\frac{J}{R_{AdS}}$ equals $\frac{R_{AdS}}{(GJ)^{\frac{1}{D-2}}}$. As we have assumed $GJ \ll R_{AdS}^{D-2}$, this ratio is very large, indicating that the Gregory Laflamme instability happens over a large range of energies.

We will now argue that the Gregory Laflamme instability never shows up in the phase diagram of the relevant gravitational theories. This happens because black holes go super

instance, it takes a Schwarzschild black hole of radius r_0 to a black hole of radius λr_0 . It follows from the usual ADM formulae (and the Bekenstein formula) that, under this transformation the mass, angular momenta, temperature and entropy transform like $M \rightarrow \lambda^{D-3}M$, $J \rightarrow \lambda^{D-2}J$, $T \rightarrow \frac{T}{\lambda}$ and $S \rightarrow \lambda^{D-2}S$. Consequently, for flat space black holes with a single rotational angular momentum J , the temperature as a function of mass, at fixed J can be read off from the single-scale invariant relationship

$$TJ^{\frac{1}{D-2}} = f\left(\frac{M}{J^{\frac{D-3}{D-2}}}\right)$$

We have computed the function f numerically in $D = 6$ and verified it decreases monotonically. We believe that this monotonic decrease is true (of black holes with a single rotation) for all $D \geq 6$.

⁶⁵i.e. have zero temperature

radiant unstable much before they go Gregory Laflamme unstable - and the endpoint of the superradiant instability - namely a black hole with $\omega = \frac{1}{R_{AdS}}$ in equilibrium with a rotating gas - is never itself Gregory-Laflamme unstable.

When J is small, scale invariance tells us that the angular velocity of spinning black holes must be given by a scale-invariant relation very similar to the temperature

$$\omega J^{\frac{1}{D-2}} = g \left(\frac{M}{J^{\frac{D-3}{D-2}}} \right) \quad (\text{A.1})$$

It turns out that g is a linear function, so that

$$\omega \sim \frac{M}{J} \quad (\text{A.2})$$

In the regime that the approximations above are valid, however, we have already argued that M is parametrically larger than the unitarity bound $\frac{1}{R_{AdS}}$. At least when $GJ \ll R_{AdS}^{D-2}$, consequently, it follows that black holes only suffer from the Gregory Laflamme instability when ω is parametrically larger than the superradiant bound.

From a more general analysis as depicted in Figure 2 of [21], one can see that for singly spinning black holes in AdS, the Gregory Laflamme instability sets in after the superradiant instability, and the surface is ultraspinning regime is well separated from the superradiant curve, even for spinning black holes whose size is comparable to the AdS radius or larger.

A.2 Black Rings

Another new feature in $D \geq 5$, with no known analogue in $D = 4$, is the existence of black solutions with (spatial) horizon topologies more complicated than S^{D-2} . The simplest of these solutions is a black ring ([29]), with horizon topology $S^{D-3} \times S^1$. It is natural to wonder whether the large ‘centrifugal forces’ associated with highly spinning black holes tend to thermodynamically favour black rings over black holes at large angular momenta.

At large values of the energy, a detailed investigation of whether black rings dominate over black holes is complicated by the fact that the relevant black ring solutions are not (yet) analytically known. At small values of the energy, however, the situation is better. At these values of the energy, all relevant solutions are characterized by a length scale l with $l \ll R_{AdS}$. At these length scales, AdS is well approximated by flat space and the length scale R is irrelevant for local analysis. Notice, however, that black holes suffer from the superradiant instability at $\omega = \frac{1}{R}$, i.e. when $l\omega \ll 1$. In other words, the superradiant solution already occurs at values of ω that are extremely small in units of the proper size of the black holes. On the other hand, (effectively) flat space black rings only exist for $\omega \gtrsim \frac{1}{l}$ (as might have been anticipated on either physical or dimensional grounds). It follows, in other words, all black rings (at small energies) are themselves super radiant unstable. Since black rings with $\omega = \frac{1}{R}$ do not exist (at small energies) they never play a dominant role in the thermal ensemble.

As we have mentioned above, the situation is less clear at energies of order (or greater than) $1/R$. It is possible that black ring solutions play a key role in the phase diagram at these energies, and even that ‘grey black ring’ solutions exist at these energies. We leave clarification of this point to future work.

B Mass and the radius of the extremal Kerr- AdS_5 black holes

If r_1, r_2, r_3 are the three roots (not necessarily distinct nor real) of the cubic $ax^3 + bx^2 + cx + d = 0$ then the discriminant of this equation is defined as

$$\Delta = a^4(r_1 - r_2)^2(r_1 - r_3)^2(r_2 - r_3)^2. \quad (\text{B.1})$$

This definition immediately tells us that, $\Delta > 0$ if and only if the cubic has three distinct real roots.⁶⁶ Similarly, $\Delta < 0$ if and only if cubic has one real root and two complex conjugate roots, and $\Delta = 0$ if and only if it has degenerate roots.

Using standard manipulations it is easy to verify (and well known) that the discriminant of the cubic equation $ax^3 + bx^2 + cx + d$ is given in terms of coefficients a, b, c, d by

$$\Delta = 18abcd - 4b^3d + b^2c^2 - 4ac^3 - 27a^2d^2 \quad (\text{B.2})$$

Recall, now, that a black hole is extremal when its inner and outer horizon coincide, i.e. when the equation that determines the location of its horizon has a double root. The relevant equation is (2.10) which we reproduce here for convenience:

$$(r^2 + a^2)(r^2 + b^2)(r^2 + 1) - 2mr^2 = 0 \quad (\text{B.3})$$

Note, of course, that (B.3) is a cubic in r^2 . Using (B.2), we find that the discriminant of (B.3) is given by,

$$\begin{aligned} \Delta = & -27a^4b^4 - 18a^2b^2(a^2 + b^2 + 1)(a^2(-b^2) - a^2 - b^2 + 2m) + 4(a^2(-b^2) - a^2 - b^2 + 2m)^3 \\ & + (a^2 + b^2 + 1)^2(a^2(-b^2) - a^2 - b^2 + 2m)^2 - 4a^2b^2(a^2 + b^2 + 1)^3 \end{aligned} \quad (\text{B.4})$$

When $\Delta = 0$ our black hole is extremal. From (B.4), we see that the equation $\Delta = 0$ is itself a cubic equation in m (one of the roots of this equation equals m_{ext} , the mass of the extremal black hole). Once again by studying the discriminant of this new cubic equation, we can find the nature of its roots.

Once again using (B.2), we find that the discriminant of the equation $\Delta = 0$ (viewed as a cubic equation in m) is given by

$$\frac{1}{16}a^2b^2 \left(a^6 + 3a^4(b^2 + 1) + 3a^2(b^4 - 7b^2 + 1) + (b^2 + 1)^3 \right)^3 \geq 0 \quad (\text{B.5})$$

(we have checked that the inequality in (B.5) holds for all $|a|, |b| \leq 1$ by 3d plotting the expression on the LHS on Mathematica).

It thus follows that (B.5) has three real roots for all physically allowed values of a and b , i.e. $|a|, |b| \leq 1$. We have evaluated and plotted the three real roots of this equation for all values of $|a|, |b| \leq 1$, and verified that exactly one of these is positive (while the other

⁶⁶The ‘only if’ part of this statement may be verified as follows. Let the three roots be $\alpha + i\beta$, $\alpha - i\beta$ and γ where α , β and γ are all real. In this case $\Delta = a^4(i\beta)^2|\alpha - \gamma + i\beta|^4$ and so is negative.

two are negative or zero) for all values of a and b in the allowed range. The formula for the positive real root is

$$m_{\text{ext}} = \frac{1}{2} \left(\frac{1}{6} \sqrt{(a^2 + b^2 + 1)^4 + 216a^2b^2(a^2 + b^2 + 1)} \cos\left(\frac{\theta}{3}\right) + a^2(b^2 + 1) - \frac{1}{12} (a^2 + b^2 + 1)^2 + b^2 \right) \quad (\text{B.6})$$

where θ is given by

$$\cos(\theta) = \left(\frac{1}{(a^2 + b^2 + 1)^4 + 216a^2b^2(a^2 + b^2 + 1)} \right)^{3/2} \times \left(5832a^4b^4 - (a^2 + b^2 + 1)^6 + 540a^2b^2(a^2 + b^2 + 1)^3 \right) \quad (\text{B.7})$$

as reported in (2.13).

While the formula for m_{ext} is complicated in general, it simplifies when $a = b$. In this case (B.4) simplifies to

$$\Delta_{a=b} = 4m(2a^2(-1 + a^2)^3 + m - 4a^2(5 + 2a^2)m + 8m^2) \quad (\text{B.8})$$

In this case the equation $\Delta_{a=b} = 0$ is effectively quadratic, and its unique the positive root is given by

$$m_{\text{ext}} = \frac{1}{128} \left(\sqrt{8a^2 + 1} - 1 \right) \left(\sqrt{8a^2 + 1} + 3 \right)^3 \quad (\text{B.9})$$

in agreement with Eq 5.28 of [24]. It is possible, after some work, to check that the complicated expressions (B.6) and (B.7) reduce to (B.9) when $a = b$.

In this simple special case, we can evaluate the value of the radius of the extremal black hole as follows. We differentiate (B.3) w.r.t. r^2 , substitute the value of $m = m_{\text{ext}}$ from (B.9), and equate the result to zero (the derivative must vanish because the LHS of (B.3) has a double root at extremality). This procedure gives us the following expression for the horizon radius of the extremal black hole,

$$(r_+)_{\text{ext}}^2 = \frac{1}{4} \left(\sqrt{1 + 8a^2} - 1 \right) \quad (\text{B.10})$$

again in agreement with Eq. 5.28 of [24].

C Partition function of a single scalar in AdS_5

In this brief appendix, we supply a detailed derivation of (4.3). We see from (4.2) that

$$\begin{aligned}
\ln Z &= - \sum_{n=0}^{\infty} \sum_{J=0}^{\infty} \sum_{m_L, m_R = -\frac{J}{2}}^{\frac{J}{2}} \ln(1 - e^{-\beta(\Delta+2n+J)+\beta(\omega_1+\omega_2)m_L+\beta(\omega_1-\omega_2)m_R}) \\
&= - \sum_{n=0}^{\infty} \sum_{J=0}^{\infty} \sum_{a,b=0}^J \ln(1 - e^{-\beta(\Delta+2n+a(\omega_1+\omega_2)+b(\omega_1-\omega_2))+\beta(1-\omega_1)J}) \\
&= \sum_{n=0}^{\infty} \sum_{J=0}^{\infty} \sum_{a,b=0}^J \sum_{q=1}^{\infty} \frac{e^{-q\beta(\Delta+2n+a(\omega_1+\omega_2)+b(\omega_1-\omega_2))+q\beta(1-\omega_1)J}}{q}
\end{aligned} \tag{C.1}$$

In the final line, we use the Taylor expansion of logarithm. We can now perform sum over a and b which simplifies to

$$\begin{aligned}
\ln Z &= \sum_{n,J=0}^{\infty} \sum_{q=1}^{\infty} \frac{1}{q} \left[- \frac{\exp(\beta(J+1)q\omega_1 - \beta q(\Delta + J\omega_1 + J\omega_2 + J + 2n))}{(e^{\beta q\omega_1} - e^{\beta q\omega_2})(e^{\beta q(\omega_1+\omega_2)} - 1)} \right. \\
&\quad + \frac{\exp(\beta(J+1)q\omega_2 - \beta q(\Delta + J\omega_1 + J\omega_2 + J + 2n))}{(e^{\beta q\omega_1} - e^{\beta q\omega_2})(e^{\beta q(\omega_1+\omega_2)} - 1)} \\
&\quad + \frac{\exp(-\beta q(\Delta + J\omega_1 + J\omega_2 + J + 2n) + \beta(J+1)q\omega_1 + \beta(J+1)q(\omega_1 + \omega_2))}{(e^{\beta q\omega_1} - e^{\beta q\omega_2})(e^{\beta q(\omega_1+\omega_2)} - 1)} \\
&\quad \left. - \frac{\exp(-\beta q(\Delta + J\omega_1 + J\omega_2 + J + 2n) + \beta(J+1)q\omega_2 + \beta(J+1)q(\omega_1 + \omega_2))}{(e^{\beta q\omega_1} - e^{\beta q\omega_2})(e^{\beta q(\omega_1+\omega_2)} - 1)} \right]
\end{aligned} \tag{C.2}$$

We can now perform sum over n and J easily and obtain

$$\begin{aligned}
\ln Z &= \sum_{q=1}^{\infty} \frac{1}{q} \left[- \frac{(\coth(\beta q) - 1)e^{\beta q(-\Delta+\omega_1+\omega_2+4)}}{2(e^{\beta q(\omega_1+1)} - 1)(e^{\beta q(\omega_2+1)} - 1)(e^{\beta q(\omega_1+\omega_2)} - 1)} \right. \\
&\quad \left. + \frac{(\coth(\beta q) - 1)e^{\beta q(-\Delta+\omega_1+\omega_2+4)}}{2(e^{\beta q} - e^{\beta q\omega_1})(e^{\beta q} - e^{\beta q\omega_2})(e^{\beta q(\omega_1+\omega_2)} - 1)} \right]
\end{aligned} \tag{C.3}$$

The first term of (C.3) is obtained after summing over n and J of the first two terms of (C.2) which is clearly finite when both ω_1 and ω_2 approach to unity. However, the last term of (C.3) obtained from the last two terms of (C.2) exhibits divergences when both ω_i approaches to unity.

To extract the divergences, we explicitly expand (C.2) and (C.3) in the limit $\omega_1 \rightarrow 1$ and $\omega_2 \rightarrow 1$.

$$\begin{aligned}
\ln \mathcal{Z} &= \sum_{q=1}^{\infty} \frac{1}{q} \left[- \frac{e^{\beta(\Delta-6)(-q)}}{(e^{2\beta q} - 1)^4} + \frac{e^{\beta(\Delta-4)(-q)}}{\beta^2 q^2 (\omega_1 - 1)(\omega_2 - 1)(e^{2\beta q} - 1)^2} + O\left(\frac{1}{1 - \omega_1}\right) + O\left(\frac{1}{1 - \omega_2}\right) \right] \\
&\approx \frac{e^{-q\beta(\Delta-2)}}{4\beta^2 q^3 (1 - \omega_1)(1 - \omega_2) \sinh^2(\beta q)}
\end{aligned} \tag{C.4}$$

D The Gas partition function in $AdS_5 \times S^5$

In this Appendix, we compute the partition function (at the free level) of a gas of gravitons on $AdS_5 \times S^5$. As a consistency check on our computation, we use our answer to compute the superconformal index of the gas and verify that it reproduces the answer previously computed in [30]. As the last step, we shut off all $SO(6)$ chemical potentials, and set $\omega_1 \approx 1$, $\omega_2 \approx 1$, to obtain the partition function in the fluid form of interest to this paper.

Our computation of the gas partition function proceeds as follows. In subsection D.1 we recall the character formulae for long and short representations of the conformal group $SO(4,2)$. In subsection D.2 we recall the Schur formula for $SU(N)$ characters, specialized to $SU(4)$. In subsection D.3 we combine these results with the listing of particles in $AdS_5 \times S^5$ of [31] to obtain the full Bosonic single particle partition function, as well as the full Fermionic single particle partition function in $AdS_5 \times S^5$. We present our answer as a function of all 6 chemical potentials. In subsection D.4 (as a check on our answer) we restrict our single particle partition function to the values of chemical potentials that compute the superconformal index and find the result previously reported in [30]. Finally, in subsection D.5 we shut off all $SO(6)$ chemical potentials, set $\omega_1 \approx 1$, $\omega_2 \approx 1$, and multiparticle the answer, obtaining a formula for the partition function that takes the fluid form.

D.1 Review of conformal characters

Recall that the isometry group of the $AdS_5 \times S^5$ is $SO(2,4) \times SO(6)$. So states in this background space-time are labeled by the eigenvalues of the Cartans of the compact subgroup $SO(2) \times SO(4) \times SO(6)$, which can also be written as, $SO(2) \times SU_L(2) \times SU_R(2) \times SO(6) = SO(2) \times SU_L(2) \times SU_R(2) \times SU(4)$. The labels for the quantum states are then conformal dimension Δ , corresponding to $SO(2)$ Cartan, j_1/j_2 angular momentum corresponding to the Cartans of $SU_L(2)/SU_R(2)$, and the $SU(4)$ Cartan charges, $[R_1, R_2, R_3]$ (as in [30], R_i are eigenvalues under the diagonal $SU(4)$ matrices with 1 in the i^{th} diagonal entry, and -1 in the $(i+1)^{th}$ diagonal).

In this subsection, we focus on the $SO(4,2)$ part of this algebra. Single particle states in the bulk dual transform in given irreducible representations of $SO(4,2)$. These representations are conveniently labeled by the scaling dimension Δ and angular momenta j_1/j_2 (see above). Let us recall that generic (or long) unitary representations representations of $SO(4,2)$ occur for scaling dimensions that obey [32]

$$\Delta > j_1 + j_2 + 2 - \delta_{j_1,0} - \delta_{j_2,0} + \delta_{j_1,0}\delta_{j_2,0} \quad (D.1)$$

Modules of this sort have no null states. Their character

$$\text{Tr} (s^H x^{j_1^z} y^{j_2^z}) \quad (D.2)$$

⁶⁷ is obtained by the free action of derivatives on the primary, and is given by

$$z_{B/F}^{\Delta j_1 j_2}(s, x, y) = \frac{s^\Delta \chi_{j_1}^L(x) \chi_{j_2}^R(y)}{\left(1 - sx^{\frac{1}{2}} y^{-\frac{1}{2}}\right) \left(1 - sx^{-\frac{1}{2}} y^{\frac{1}{2}}\right) \left(1 - sx^{-\frac{1}{2}} y^{-\frac{1}{2}}\right) \left(1 - sx^{\frac{1}{2}} y^{\frac{1}{2}}\right)} \quad (\text{D.3})$$

where, $\chi_j(x)$ is $SU(2)$ characters in the spin j representation.

In addition to long representations, $SO(4, 2)$ also admits three families of nontrivial short representations. The most special of these is the single representation at $\Delta = 1, j_1 = j_2 = 0$. This ‘free scalar’ representation has character

$$z_{B/F}^{100}(s, x, y) = \frac{s(1 - s^2)}{\left(1 - sx^{\frac{1}{2}} y^{-\frac{1}{2}}\right) \left(1 - sx^{-\frac{1}{2}} y^{\frac{1}{2}}\right) \left(1 - sx^{-\frac{1}{2}} y^{-\frac{1}{2}}\right) \left(1 - sx^{\frac{1}{2}} y^{\frac{1}{2}}\right)} \quad (\text{D.4})$$

(the subtraction in the numerator is a consequence of the free equation of motion). A less special family short representation has $j_2 = 0, j_1 \neq 0, \Delta = j_1 + 1$. The character of this family of representations is given by [33]

$$z_{B/F}^{j_1+1, j_1 0}(s, x, y) = \frac{s^{j_1+1} \left(\chi_{j_1}^L(x) - s \chi_{j_1-1/2}^L(x) \chi_{1/2}^R(y) + s^2 \chi_{j_1-1}^L(x) \right)}{\left(1 - sx^{\frac{1}{2}} y^{-\frac{1}{2}}\right) \left(1 - sx^{-\frac{1}{2}} y^{\frac{1}{2}}\right) \left(1 - sx^{-\frac{1}{2}} y^{-\frac{1}{2}}\right) \left(1 - sx^{\frac{1}{2}} y^{\frac{1}{2}}\right)} \quad (\text{D.5})$$

(the subtraction in the numerator is a consequence of a ‘Bianchi Identity’ type null state). Of course the analogous formula for short representations with $j_1 = 0, j_2 \neq 0$ are obtained by acting with $1 \leftrightarrow 2$ on (D.5).

Finally, the character of short representations with $j_1 \neq 0, j_2 \neq 0, \Delta = j_1 + j_2 + 2$ is given by

$$z_{B/F}^{j_1+j_2+2, j_1 j_2}(s, x, y) = \frac{s^{j_1+j_2+2} \left(\chi_{j_1}^L(x) \chi_{j_2}^R(y) - s \chi_{j_1-1/2}^L(x) \chi_{j_2-1/2}^R(y) \right)}{\left(1 - sx^{\frac{1}{2}} y^{-\frac{1}{2}}\right) \left(1 - sx^{-\frac{1}{2}} y^{\frac{1}{2}}\right) \left(1 - sx^{-\frac{1}{2}} y^{-\frac{1}{2}}\right) \left(1 - sx^{\frac{1}{2}} y^{\frac{1}{2}}\right)} \quad (\text{D.6})$$

D.2 $SU(4)$ character formula

In this subsection, we briefly review the Schur formula for $SU(4)$ characters in terms of determinants. Consider the $SU(4)$ character

$$\text{Tr} e^{i(\theta_1 R_1 + \theta_2 R_2 + \theta_3 R_3)} = \text{Tr}(\mathbf{p}^{R_1} \mathbf{q}^{R_2} \mathbf{r}^{R_3}) \quad (\text{D.7})$$

where the Cartan charges R_i were defined above. ⁶⁸ Let us note, in particular, that the weights (R_1, R_2, R_3) of the four vectors in the fundamental representation are, respectively

$$[1, 0, 0], [-1, 1, 0], [0, -1, 1], \text{ and } [0, 0, -1].$$

⁶⁷Note the s, x and y are related to the chemical temperature and angular velocities in other parts of this paper by $s = e^{-\beta}$, $x = e^{\beta(\omega_1 + \omega_2)}$, $y = e^{\beta(\omega_1 - \omega_2)}$.

⁶⁸When evaluated on highest weight states, R_i equals the number of columns of length i in the Young Tableaux corresponding to the given representation.

The contribution of these states to (D.7), respectively, are

$$v_1 = e^{i\theta_1}, \quad v_2 = e^{i(\theta_2-\theta_1)}, \quad v_3 = e^{i(\theta_3-\theta_2)}, \quad v_4 = e^{-i\theta_3}. \quad (\text{D.8})$$

69

Let us now recall that the Schur formula that asserts that

$$\chi = \frac{\det[v_i^{l_j+n-j}]}{\det[v_i^{n-j}]} \quad (\text{D.9})$$

where v_i are the ‘weight vectors’ of the fundamental representation listed in (D.8), and l_i are the number of boxes in the i^{th} row of the Young Tableaux (with the convention $l_4=0$).

While representations of $SU(4)$ are conveniently specified by the row lengths l_i , a second specification (the Dynkin specification) is commonly used in the literature. In this convention, representations are specified by the values of R_1 , R_2 and R_3 acting on the highest weight state of the representation. Let these values be denoted by r_i . A little thought will convince the reader that r_i denotes the number of columns of length i in the Young Tableaux⁷⁰. The relationship between l_i (the length of the i^{th} row) and r_i (the number of columns of length i) is clearly given by

$$\begin{aligned} l_1 &= r_1 + r_2 + r_3 \\ l_2 &= r_2 + r_3 \\ l_3 &= r_3 \\ l_4 &= 0 \end{aligned} \quad (\text{D.10})$$

Rewritten in terms of the column lengths or Dynkin labels r_i , it follows that

$$\chi_{(r_1, r_2, r_3)}(p, q, r) = \frac{\det \begin{pmatrix} v_1^{r_1+r_2+r_3+3} & v_2^{r_1+r_2+r_3+3} & v_3^{r_1+r_2+r_3+3} & v_4^{r_1+r_2+r_3+3} \\ v_1^{r_2+r_3+2} & v_2^{r_2+r_3+2} & v_3^{r_2+r_3+2} & v_4^{r_2+r_3+2} \\ v_1^{r_3+1} & v_2^{r_3+1} & v_3^{r_3+1} & v_4^{r_3+1} \\ 1 & 1 & 1 & 1 \end{pmatrix}}{\det \begin{pmatrix} v_1^3 & v_2^3 & v_3^3 & v_4^3 \\ v_1^2 & v_2^2 & v_3^2 & v_4^2 \\ v_1 & v_2 & v_3 & v_4 \\ 1 & 1 & 1 & 1 \end{pmatrix}} \quad (\text{D.11})$$

As a check, the fundamental representation is labeled by $(r_1, r_2, r_3) = (1, 0, 0)$. It is easy to check that plugging these values into (D.11) yields $v_1 + v_2 + v_3 + v_4$ as expected.

⁶⁹Note the product $v_1 v_2 v_3 v_4 = 1$ carries zero charge under all three Cartans; this is a consequence of the fact that the contraction of four vectors with the ϵ tensor is a singlet.

⁷⁰The argument goes as follows. Recall that the Young Tableaux can be thought of as a tensor product of fundamentals, in a particular symmetry channel. The highest weight state associated with a Young is obtained by occupying the first row by the highest weight state in the fundamental (namely the column with 1 in the first row and zero every where else), the second highest weight state in the second row, and the third highest wt state in the third row. By the definition of this Cartan element, the action of R_1 on this state equals the number of boxes in the first row minus the number of boxes in the second row, i.e. the number of columns of length 1. The action of R_2 equals the number of boxes in the second row minus the number of boxes in the third row, i.e. the number of columns of length 2, and so on.

D.3 Full Single Particle Partition Function

The spectrum of supergravitons in $AdS_5 \times S^5$ is the spectrum of chiral primaries $\text{Tr} Z^p$ $p = 1 \dots \infty$ and their descendents. Each of the chiral primaries described above can be decomposed into a finite number of primaries of the conformal algebra. A full listing of this decomposition is provided in table 1 of [31]. All conformal multiplets that appear in this listing for $p \geq 3$ are long representations. When $p = 1$ and $p = 2$, on the other hand, some of the conformal representations that appear in this listing are short. We list all these short representations in Table 1 and Table 2.

Taking the products of $SO(4,2)$ and $SU(4)$ characters (described in detail in the previous two subsections) we obtain a definite character formula for each field listed in Table 1 of [31]. It is then a simple matter to sum over the full spectrum of [31] and find the full single-letter partition function. We now present our final (unfortunately rather unwieldy) answer for this partition function, separately for bosonic and fermionic letters.

(j_1, j_2)	2Δ	Fields	$SU(4)$ Dynkin labels
$(0, 0)$	2	$\varphi^{(1)}$	$(0, 1, 0)$
$(\frac{1}{2}, 0)$	3	$\lambda^{(1)}$	$(0, 0, 1)$
$(0, \frac{1}{2})$	3	$\lambda^{(1)}$	$(1, 0, 0)$
$(1, 0)$	4	$A_{\mu\nu}^{(1)}$	$(0, 0, 0)$
$(0, 1)$	4	$\tilde{A}_{\mu\nu}^{(1)}$	$(0, 0, 0)$

Table 1. $p = 1$ multiplet

$SO(4)$ Labels	2Δ	Fields	$SU(4)$ Dynkin Labels
$(\frac{1}{2}, \frac{1}{2})$	$2p + 2 = 6$	$A_{\mu}^{(1)}$	$(1, p - 2, 1) = (1, 0, 1)$
$(1, \frac{1}{2})$	$2p + 3 = 7$	$\psi_{+\mu}^{(1)}$	$(1, p - 2, 0) = (1, 0, 0)$
$(\frac{1}{2}, 1)$	$2p + 3 = 7$	$\psi_{-\mu}^{(1)}$	$(0, p - 2, 1) = (0, 0, 1)$
$(1, 1)$	$2p + 4 = 8$	$h_{\mu\nu}$	$(0, p - 2, 0) = (0, 0, 0)$

Table 2. $p = 2$ multiplet

$$\begin{aligned}
z_B = & \mathcal{D}s(-s^2(s^2-1)xyr^4 + (s(s-q)(qs-1)(x+1)\sqrt{xy}^{3/2} + s^3(1-qs)xy^2 - (q(s-q)x^2s^3 \\
& + q(s-q)s^3 + (s^2+1)((q^2+1)s^3 + qs^2 - 2(q^2+1)s+q)x)y + s^3(1-qs)x \\
& + s(s-q)(qs-1)(x+1)\sqrt{x}\sqrt{y})r^2 - q^2s^2(s^2-1)xy)p^4 + (s^2(s-q)(qs-1)(r^4 + q(s^2+1)^2r^2 \\
& + q^2)(x+1)\sqrt{xy}^{3/2} + qs(q^3xs^3 + r^2(-sr^2 + s^2+1)xs^3 + q^2(r^2(s^2+1) - s)xs^3 \\
& + qr^2((-2xs^4 - (x(x+3)+1)s^2 + r^2xs + x^2+1)s^2 + x))y^2 + (s^2(2-s(r^2+s)(s^2-1))xq^4 \\
& + (r^2(s^2+1) - s)((x^2+x+1)s^4 + 2xs^2 + x)q^3 + s(s(-s^4 + s^2+2)xr^4 - (xs^8 + (x(2x+3)+2)s^6 \\
& + (x(3x+7)+3)s^4 + 3xs^2 - (x-1)^2)r^2 + s^3 + sx(-s^4 + (x+1)s^2+2))q^2 \\
& + r^2(-sr^2 + s^2+1)((x^2+x+1)s^4 + 2xs^2 + x)q + r^4s^4 + r^4s^4x^2 + r^2s^2(-s^3 + s+ \\
& r^2(-s^4 + s^2+2))x)y + qs(q^3xs^3 + r^2(-sr^2 + s^2+1)xs^3 + q^2(r^2(s^2+1) - s)xs^3 \\
& + qr^2((-2xs^4 - (x(x+3)+1)s^2 + r^2xs + x^2+1)s^2 + x)) + s^2(s-q)(qs-1)(r^4 + q(s^2+1)^2r^2 \\
& + q^2)(x+1)\sqrt{x}\sqrt{y})p^2 - qr(r^2+q)(s^2(s^2+1)(q(s^3+s-q) - 1)(x+1)\sqrt{xy}^{3/2} \\
& - s^4(s-q)(qs-1)xy^2 + (q-s)(qs-1)((x^2+x+1)s^4 + 2xs^2 + x)y - s^4(s-q)(qs-1)x \\
& + s^2(s^2+1)(q(s^3+s-q) - 1)(x+1)\sqrt{x}\sqrt{y})p - p^3r(r^2+q)(s^2(s^2+1)(q(s^3+s-q) \\
& - 1)(x+1)\sqrt{xy}^{3/2} - s^4(s-q)(qs-1)xy^2 + (q-s)(qs-1)((x^2+x+1)s^4 + 2xs^2 + x)y \\
& - s^4(s-q)(qs-1)x + s^2(s^2+1)(q(s^3+s-q) - 1)(x+1)\sqrt{x}\sqrt{y}) + q^2s(-s^2(s^2-1)xyr^4 \\
& + (s(s-q)(qs-1)(x+1)\sqrt{xy}^{3/2} + s^3(1-qs)xy^2 - (q(s-q)x^2s^3 + q(s-q)s^3 + (s^2+1)((q^2+1)s^3 \\
& + qs^2 - 2(q^2+1)s+q)x)y + s^3(1-qs)x + s(s-q)(qs-1)(x+1)\sqrt{x}\sqrt{y})r^2 - q^2s^2(s^2-1)xy))
\end{aligned} \tag{D.12}$$

$$\begin{aligned}
z_F = & -\mathcal{D}(s^{3/2}(s^2+1)(p^4rs^2\sqrt{x}\sqrt{y}(q+r^2)(\sqrt{x}(y+1)(qs-1) + x\sqrt{y}(s-q) + \sqrt{y}(s-q)) \\
& + p^3(y^{3/2}(q-s)(q^2s^2x(r^2s-1) - qr^2(s^2(x(s^2+x+4)+1)+x) + r^2sx(1-r^2s)) \\
& + \sqrt{y}(q-s)(q^2s^2x(r^2s-1) - qr^2(s^2(x(s^2+x+4)+1)+x) + r^2sx(1-r^2s)) \\
& + (x+1)\sqrt{xy}(qs-1)(q^2s(s-r^2) + qr^2(s^4+4s^2+1) + r^2s^2(r^2-s)) + qr^2s^2(x+1)\sqrt{xy}^2(qs-1) \\
& + qr^2s^2(x+1)\sqrt{x}(qs-1) + p^2r(q+r^2)(-y^{3/2}(qs-1)(q^2sx - q(s^2(x(s^2+x+4)+1)+x) \\
& + s^3x)) - \sqrt{y}(qs-1)(q^2sx - q(s^2(x(s^2+x+4)+1)+x) + s^3x) + (x+1)\sqrt{xy}(q-s)(q^2s^3 \\
& - q(s^4+4s^2+1)+s) - qs^2\sqrt{x}(x+1)y^2(q-s) - qs^2(x+1)\sqrt{x}(q-s) + pq(y^{3/2}(q-s)(q^2s^2x(r^2s-1) \\
& - qr^2(s^2(x(s^2+x+4)+1)+x) + r^2sx(1-r^2s)) + \sqrt{y}(q-s)(q^2s^2x(r^2s-1) \\
& - qr^2(s^2(x(s^2+x+4)+1)+x) + r^2sx(1-r^2s)) + (x+1)\sqrt{xy}(qs-1)(q^2s(s-r^2) + qr^2(s^4+4s^2 \\
& + 1) + r^2s^2(r^2-s)) + qr^2s^2(x+1)\sqrt{xy}^2(qs-1) + qr^2s^2(x+1)\sqrt{x}(qs-1)) \\
& + q^2rs^2\sqrt{x}\sqrt{y}(q+r^2)(\sqrt{x}(y+1)(qs-1) + x\sqrt{y}(s-q) + \sqrt{y}(s-q))).
\end{aligned} \tag{D.13}$$

where \mathcal{D} equals

$$\frac{1}{\mathcal{D}} = (q-s)(qs-1)(ps-r)(rs-p) (s\sqrt{x} - \sqrt{y}) (s\sqrt{y} - \sqrt{x}) (s - \sqrt{x}\sqrt{y}) (s\sqrt{x}\sqrt{y} - 1) (qs-pr)(q-prs) \tag{D.14}$$

D.4 Matching with the superconformal index

The single particle superconformal index is defined in [30] as,

$$i_{s,p} = \text{Tr}_{s,p}[(-1)^F u^\delta t^{2(E+j_1)} \bar{y}^{2j_2} v^{R_2} w^{R_3}] \quad (\text{D.15})$$

where, $\delta = E - 2j_1 - \frac{1}{2}(3R_1 + 2R_2 + R_3)$.

We can obtain the single letter superconformal index from (D.12) (D.13) by computing $z_B - z_F$ with the replacements

$$s \rightarrow ut^2, x \rightarrow u^{-2}t^2, y \rightarrow \bar{y}^2, p \rightarrow u^{-3/2}, q \rightarrow u^{-1}v, r \rightarrow u^{-1/2}w \quad (\text{D.16})$$

Magically, we find that the ugly expressions (D.12) and (D.13) collapse into the extremely simple

$$i_{s,p} = -\frac{t^3}{\bar{y} \left(1 - \frac{t^3}{\bar{y}}\right)} - \frac{t^3 \bar{y}}{1 - t^3 \bar{y}} + \frac{t^2 w}{v \left(1 - \frac{t^2 w}{v}\right)} + \frac{t^2 v}{1 - t^2 v} + \frac{t^2}{w \left(1 - \frac{t^2}{w}\right)}, \quad (\text{D.17})$$

an expression that agrees perfectly with the single letter superconformal index computed in [30](eqn. 4.14). We view this agreement as a highly nontrivial consistency check of (D.12) and (D.13).

D.5 Turning $SU(4)$ chemical potentials off

Our rather complicated single-letter partition functions, (D.12) and (D.13) simplify somewhat when we set all $SU(4)$ fugacities to unity. Upon setting $p, q, r = 1$ we find

$$\begin{aligned} z_B(s, x, y, 1, 1, 1) &= \mathcal{N} s \left(-s^3(s+1)x^2 - s^3(s+1) + s^2 \left((s((s-5)s-2) - 14)s^2 + s - 13 \right) (x+1)\sqrt{xy}^{3/2} \right. \\ &\quad + s^2 \left((s((s-5)s-2) - 14)s^2 + s - 13 \right) (x+1)\sqrt{x}\sqrt{y} - y \left(s \left(s \left(s \left(s \left(s \left(s^2 + s + 4 \right) + 6 \right) \right. \right. \right. \right. \right. \\ &\quad \left. \left. \left. \left. + 31 \right) + 5 \right) + 26 \right) x + s \left((2(s-2)s+11)s^2 + s + 1 \right) + \left((2(s-2)s+11)s^3 + s^2 + s + 1 \right) x^2 \right. \\ &\quad \left. - 8x + 1 \right) + 6x - s \left((2(s-2)s+11)s^3 + s^2 + s + 1 \right) x \\ &\quad \left. - sy^2 \left(s \left(s \left((s+1)x^2 + s(2(s-2)s+11)x + s + x + 1 \right) + x \right) + x \right) \right) \\ z_F(s, x, y, 1, 1, 1) &= -4\mathcal{N} s^{3/2} (s^2 + 1) \left(\sqrt{x}(y+1) + x\sqrt{y} + \sqrt{y} \right) \left(s^2(x+1)y + s^2(x+1) \right. \\ &\quad \left. + (s(s((s-1)s+4) - 1) + 1)\sqrt{x}\sqrt{y} \right) \end{aligned} \quad (\text{D.18})$$

where \mathcal{N} equals,

$$\mathcal{N} = \frac{1}{(s-1)^5 (s\sqrt{x} - \sqrt{y}) (s\sqrt{y} - \sqrt{x}) (s - \sqrt{x}\sqrt{y}) (s\sqrt{x}\sqrt{y} - 1)}$$

D.5.1 Partition function at $\omega_1 \rightarrow 1, \omega_2 \rightarrow 1$

We can multi-particle the single-particle partition functions (D.18) (with Bose and Fermi statistics respectively) using the formulae

$$\begin{aligned}\ln Z_B &= \sum_{n=1}^{\infty} \frac{1}{n} z_B(s^n, x^n, y^n, p^n, q^n, r^n) \\ \ln Z_F &= \sum_{n=1}^{\infty} \frac{(-1)^{n+1}}{n} z_F(s^n, x^n, y^n, p^n, q^n, r^n)\end{aligned}\tag{D.19}$$

In the limit $\omega_1 \rightarrow 1, \omega_2 \rightarrow 1$ and putting $p, q, r = 1$ we get,

$$\begin{aligned}\ln Z_B &= \sum_{n=1}^{\infty} \frac{(22 \cosh(\beta n) + 17 \cosh(2\beta n) + 6 \cosh(3\beta n) + \cosh(4\beta n) + 18) \operatorname{csch}^7\left(\frac{\beta n}{2}\right) \operatorname{sech}\left(\frac{\beta n}{2}\right)}{32\beta^2 n^3 (1 - \omega_1^2) (1 - \omega_2^2)} \\ \ln Z_F &= \sum_{n=1}^{\infty} \frac{(-1)^{n+1} \cosh(\beta n) (\cosh(\beta n) + \cosh(2\beta n) + 2) \operatorname{csch}^7\left(\frac{\beta n}{2}\right)}{2\beta^2 n^3 (1 - \omega_1^2) (1 - \omega_2^2)}\end{aligned}\tag{D.20}$$

(D.20) is the final result of this Appendix.

E The Dilaton Propagator in $AdS_5 \times S^5$

In this Appendix we review the elegant derivation of [13, 14] of the dilaton propagator in $AdS_5 \times S^5$.

To start with let us work in coordinates in which the metric of $AdS_5 \times S^5$ takes the form

$$\begin{aligned}ds^2 &= R_{AdS_5}^2 \left(\frac{dz^2}{z^2} + \frac{dx_i^2}{z^2} + d\Omega_5^2 \right) \\ &= \frac{R_{AdS_5}^2}{z^2} (dx_i^2 + dz^2 + z^2 d\Omega_5^2) \\ &= \frac{R_{AdS_5}^2}{z^2} (dx_i^2 + dy_j^2)\end{aligned}\tag{E.1}$$

where $i = 1 \dots 4, j = 1 \dots 6$, and y_j are 6 Cartesian coordinates in the space whose polar coordinate line element is given by $dz^2 + z^2 d\Omega_5^2$. We see that the metric $AdS_5 \times S^5$ is Weyl equivalent to flat 10-dimensional spacetime.

Now recall that, in D spacetime dimensions, the conformally coupled Laplacian

$$\nabla_{\text{conf}, g_{\mu\nu}}^2 \equiv \left(g^{\mu\nu} \nabla_\mu \nabla_\nu - \frac{D-2}{4(D-1)} R \right)\tag{E.2}$$

obeys the property

$$\nabla_{x, \text{conf}, e^{2\chi} g_{\mu\nu}}^2 \left(e^{-\chi \frac{D-2}{2}} \phi \right) = e^{-\frac{(D+2)\chi}{2}} \nabla_{\text{conf}, g_{\mu\nu}}^2 (\phi)\tag{E.3}$$

Now let us suppose we have found a Green's function G for the operator $\nabla_{\text{conf}, g_{\mu\nu}}^2$. By definition, G obeys the equation

$$\nabla_{\text{conf}, g_{\mu\nu}}^2 G(x, y) = \frac{1}{\sqrt{-g}} \delta^D(x - y) \quad (\text{E.4})$$

Using (E.3), it follows that

$$\begin{aligned} \nabla_{\text{conf}, e^{2\chi}g_{\mu\nu}}^2 \left(e^{-\chi(x)\frac{D-2}{2}} G(x, y) \right) &= \frac{e^{-\frac{(D+2)\chi(y)}{2}} \times e^{\chi(y)D}}{\sqrt{-ge^{2\chi(x)}}} \delta^D(x - y) \\ &= \frac{e^{\frac{(D-2)\chi(y)}{2}}}{\sqrt{-ge^{2\chi(x)}}} \delta^D(x - y) \end{aligned} \quad (\text{E.5})$$

The key point here is that while the derivatives on the LHS are derivatives w.r.t. x_μ , the δ function allows us to view every χ on the RHS as a function of y^μ . As functions of y^μ are just constants as far as the differential operator on the RHS is concerned. As a consequence, it follows that

$$\nabla_{\text{conf}, e^{2\chi}g_{\mu\nu}}^2 \left(e^{-\chi(x)\frac{D-2}{2}} G(x, y) e^{-\chi(y)\frac{D-2}{2}} \right) = \frac{1}{\sqrt{-ge^{2\chi(x)}}} \delta^D(x - y) \quad (\text{E.6})$$

and so we conclude that [13, 14]

$$G_{ge^{2\chi}}(x, y) = e^{-\chi(x)\frac{D-2}{2}} G_{g_{\mu\nu}}(x, y) e^{-\chi(y)\frac{D-2}{2}} \quad (\text{E.7})$$

is the Greens function of the operator ∇_{conf}^2 in the metric $e^{2\chi}g_{\mu\nu}$.

In summary

$$g_{\mu\nu} \rightarrow e^{2\chi}g_{\mu\nu} \implies G(x, y) \rightarrow e^{-\chi(x)\frac{D-2}{2}} G(x, y) e^{-\chi(y)\frac{D-2}{2}} \quad (\text{E.8})$$

Viewing the propagator as a two-point function $\langle \phi(x)\phi(y) \rangle$, we see that this two-point function transforms exactly as we would expect of a field of Weyl weight $\frac{D-2}{2}$, which, of course, is also the scaling dimension of ϕ .

Now recall that the scalar curvature of $AdS_5 \times S^5$ vanishes (because the positive scalar curvature of S^5 exactly cancels the negative scalar curvature of AdS_5). The scalar curvature of 10-dimensional flat space also, of course, vanishes. So in the particular case of flat space and $AdS_5 \times S^5$, it follows that ∇_{conf}^2 is simply the (minimally coupled) Laplacian operator, the kinetic term of the dilaton. It follows, therefore, that in the coordinate (E.1), the propagator dilaton propagator is given by

$$\langle \phi(x)\phi(y) \rangle = z_x^4 G(x, y) z_y^4 \quad (\text{E.9})$$

where $G(x, y)$ is the well known propagator in flat space given by

$$G(x, x') = \frac{\Gamma[4]}{4\pi^5} \left(\frac{1}{(x_i - x'_i)^2} \right)^4 \quad (\text{E.10})$$

Given (E.10), we evaluate

$$\begin{aligned}
\langle \phi(\tilde{x}_1)\phi(\tilde{x}_2) \rangle &= z_1^4 G(\tilde{x}_1, \tilde{x}_2) z_2^4 & (E.11) \\
&= \frac{\Gamma[4]}{4\pi^5} z_1^4 \left(\frac{1}{(x_1 - x_2)^2 + (y_1 - y_2)^2} \right)^4 z_2^4 \\
&= \frac{\Gamma[4]}{2^6 \pi^5} \left(\frac{1}{\frac{(x_1 - x_2)^2}{2z_1 z_2} + \frac{(y_1 - y_2)^2}{2z_1 z_2}} \right)^4 \\
&= \frac{\Gamma[4]}{2^6 \pi^5} \left(\frac{1}{\frac{(x_1 - x_2)^2}{2z_1 z_2} + \frac{(z_1 y'_1 - z_2 y'_2)^2}{2z_1 z_2}} \right)^4 \\
&= \frac{\Gamma[4]}{2^6 \pi^5} \left(\frac{1}{\frac{(x_1 - x_2)^2}{2z_1 z_2} + \frac{(z_1 - z_2)^2 + 2z_1 z_2 - 2z_1 z_2 y'_1 \cdot y'_2}{2z_1 z_2}} \right)^4 \\
&= \frac{\Gamma[4]}{2^6 \pi^5} \left(\frac{1}{\frac{(x_1 - x_2)^2}{2z_1 z_2} + \frac{(z_1 - z_2)^2}{2z_1 z_2} + 1 - y'_1 \cdot y'_2} \right)^4 \\
&= \frac{\Gamma[4]}{4\pi^5} \left(\frac{1}{u + v} \right)^4
\end{aligned}$$

where $y'_i = \frac{y_i}{z}$ ⁷¹ and

$$v = 2 \left(1 - y'_1 \cdot y'_2 \right), \quad u = 2 \left(\frac{(x_1 - x_2)^2 + (z_1 - z_2)^2}{2z_1 z_2} \right) \quad (E.12)$$

We will now explain the geometric meaning of the quantities v and u . We will verify that v is the chordal distance between two points on the unit sphere, while u is the chordal distance between two points on the unit AdS_5 ⁷²

That v is the chordal distance on the unit sphere follows immediately from

$$(y'_1 - y'_2)^2 = 2 \left(1 - y'_1 \cdot y'_2 \right) = v \quad (E.13)$$

As we have parameterized AdS_5 in coordinates adapted to the Poincare Patch, it takes a little more effort to verify that u is the AdS_5 chordal distance. Recall that the Poincare patch coordinates x_i and u are related to embedding space coordinates

$$-X_{-1}^2 - X_0^2 + \sum_1^{d-1} X_i^2 = -1 \quad (E.14)$$

⁷¹Recall y_i 's are embedding space Cartesian coordinates (in \mathbb{R}^6) of a sphere of radius z so that

$$\sum y_i^2 = z^2$$

It follows that y'_i lie on a unit sphere.

⁷²The chordal distance is defined to be the distance between the points as measured (by the usual Pythagorean formula) in the relevant $\mathbb{R}^{4,2}$ or $\mathbb{R}^{6,0}$ embedding space. It gets its name because it is the distance of the chord - the shortest straight line between the two points - in embedding space.

via

$$\begin{aligned}
X_i &= \frac{x_i}{z}, \quad i = 0, \dots, d-2 \\
X_{-1} &= \frac{1}{2} \left(\frac{(z^2 + x^2)}{z} + \frac{1}{z} \right) \\
X_{d-1} &= \frac{1}{2} \left(\frac{(z^2 + x^2)}{z} - \frac{1}{z} \right)
\end{aligned} \tag{E.15}$$

It follows that

$$(X_1 - X_2)^2 = -2 - 2X_1 \cdot X_2 = -2 + 2 \left(1 + \frac{(x_1 - x_2)^2}{2z_1 z_2} + \frac{(z_1 - z_2)^2}{2z_1 z_2} \right) = u \tag{E.16}$$

F Sum over KK modes

In this Appendix, we study the relationship between the 10-dimensional dilaton propagator and the propagators of its five-dimensional descendants. We also demonstrate that the bulk stress tensor, computed using the 10-dimensional dilaton propagator, agrees with the sum of the bulk stress tensors (computed from the various 5-dimensional propagators).

F.1 Decomposition of the 10d propagator

Let us consider the metric of $AdS_5 \times S^5$ with equal radius (unity)

$$ds^2 = -(1 + r^2)dt^2 + \frac{dr^2}{1 + r^2} + r^2(d\theta^2 + \sin^2 \theta d\phi_1^2 + \cos^2 \theta d\phi_2^2) + d\Omega_5^2. \tag{F.1}$$

Consider a massless minimally coupled scalar field propagating on this space. We can KK decompose this field on S^5 . The KK masses so obtained are the eigenvalues of $-\nabla^2$ (acting on S^5). Now the eigenstates of $-\nabla^2$ on S^5 are the spherical harmonics Y_l^α , with eigenvalue $l(l+4)$ and degeneracy labels running over $d_l = \frac{(2l+4)(l+1)(l+2)(l+3)}{24}$ values. Consequently, the 10 dimensional Greens function $G^{(10)}$ on the space (F.1) can be

$$G^{(10)}((x, \theta), (x', \theta')) = \sum_{l=0}^{\infty} \sum_{\alpha=1}^{d_l} G_l^{(5)}(x, x') Y_l^\alpha(\theta) Y_l^{*\alpha}(\theta') \tag{F.2}$$

where

$$-\nabla_{10}^2 G^{(10)}((x, \theta), (x', \theta')) = \delta^{(10)}(x - x', \theta - \theta') \tag{F.3}$$

$$-\nabla_5^2 G_l^{(5)}(x, x') = \delta^{(5)}(x - x') \tag{F.4}$$

and our spherical harmonics are normalized so that

$$\int_{S^5} Y_l^\alpha(\theta) Y_l^{*\alpha}(\theta) = 1 \tag{F.5}$$

⁷³ As in the main text, we can obtain the bulk stress tensor by acting on (F.2) with the appropriate derivatives. In the limit of interest to this paper, the variation of g in factors of \sqrt{g} don't contribute to the stress tensor and the 5 and 10-dimensional stress tensors are computed via the same derivative operations (all derivatives are in the AdS_5 direction). It thus follows from (F.2) that

$$T_{\mu\nu}^{(10)} = \sum_{l=0}^{\infty} \sum_{\alpha=1}^{d_l} (T_l)_{\mu\nu}^{(5)} Y_l^\alpha(\theta) Y_l^{*\alpha}(\theta) \quad (\text{F.6})$$

(In this section we interchangeably use angles on the sphere, and unit vectors in embedding space, as coordinates on S^5).

In order to further process this relation, we use the completeness formula

$$\sum_{\alpha} Y_l^\alpha(\hat{n}) Y_l^{*\alpha}(\hat{n}') = \frac{d_l}{\Omega_5 P^l(\hat{n} \cdot \hat{n}' = 1)} P^l(\hat{n} \cdot \hat{n}') \quad (\text{F.7})$$

⁷⁴ where $P^l(\hat{n} \cdot \hat{n}')$ is the unique l^{th} spherical harmonic that preserves $SO(5)$ (and is normalized to obey (F.5)). Setting $\hat{n} = \hat{n}'$ in (F.7), and substituting in (F.6) gives

$$T_{\mu\nu}^{(10)} = \sum_{l=0}^{\infty} d_l \frac{(T_l)_{\mu\nu}^{(5)}}{\Omega_5} \quad (\text{F.8})$$

Integrating the LHS over S^5 (recall the stress tensor is independent of the coordinates on the S^5) gives

$$\int_{S^5} T_{\mu\nu}^{(10)} = \sum_{l=0}^{\infty} d_l (T_l)_{\mu\nu}^{(5)} \quad (\text{F.9})$$

(F.9) tells us that the energy computed using the full 10 dimensional propagator the sum over energies of each of the 5 dimensional particles.

F.2 Explicit check of equality of 10d and 5d stress tensors

In this subsection, we explicitly perform the summation on the RHS of (F.8), and demonstrate that the result equals the LHS (already computed in (5.22)).

The mass of a minimally coupled scalar in $AdS_5 \times S^5$ is related to its conformal dimension can be obtained

$$M^2 = \Delta(\Delta - 4) = m_{KK}^2 = l(l + 4), \quad (\text{F.10})$$

The particles of interest to this paper have $\Delta = l + 4$ and $M^2 = l(l + 4)$.

⁷³(F.2) can be established by acting on both sides of this equation with $-\nabla_{10}^2$, and using the completeness relation

$$\sum_{l,\alpha} Y_l^\alpha(\theta) Y_l^{*\alpha}(\theta') = \delta^{(5)}(\theta - \theta')$$

⁷⁴We obtain the proportionality constant on the RHS by setting $\hat{n} = \hat{n}'$.

The bulk to bulk propagator (defined by (F.4)) (for a scalar in AdS_5 with any given value of Δ) is given by well known [34]

$$\begin{aligned} G_l^{(5)}(y, y') &= \frac{\Gamma(\Delta)}{2\pi^2\Gamma(\Delta-1)} \frac{1}{u^\Delta} {}_2F_1\left(\Delta, \Delta - \frac{3}{2}, 2\Delta - 3, -\frac{4}{u}\right) \\ &= \frac{\Gamma(l+4)}{2\pi^2\Gamma(l+3)} \frac{1}{u^{l+4}} {}_2F_1\left(l+4, l+5/2, 2l+5, -\frac{4}{u}\right) \end{aligned} \quad (\text{F.11})$$

Consequently (F.2) takes the explicit form

$$G^{(10)}(x, x') = \sum_{l=0}^{\infty} \sum_{\alpha=1}^{d_l} \frac{\Gamma(l+4)}{2\pi^2\Gamma(l+3)} \frac{1}{u^{l+4}} {}_2F_1\left(l+4, l+5/2, 2l+5, -\frac{4}{u}\right) Y_l^\alpha(\Omega) Y_l^{*\alpha}(\Omega') \quad (\text{F.12})$$

As explained in the main text, the stress tensor is obtained by taking appropriate derivatives on $\tilde{G}(x, x')$ as in (5.19). As in the main text (see around (5.19)), when working at leading order, we need only retain those terms $(\partial_\mu u)^2$ (and can ignore terms proportional to $\partial_\mu \partial_\nu u$). Acting on (F.12) we find an answer of the form

$$\langle T_{\mu\nu}^{(10)} \rangle = -2 \sum_{q=1}^{\infty} \sum_{l=0}^{\infty} \sum_{\alpha=1}^{d_l} K_{l,\mu\nu}^q Y_l^\alpha(\Omega) Y_l^{*\alpha}(\Omega) \quad (\text{F.13})$$

Let us first explicitly compute $\langle T_{00}^{(10)} \rangle$.

$$\begin{aligned} -K_{l,\tau\tau}^q &= -\frac{4x^4 \gamma^4(\theta) \sinh^2(q\beta)}{2\pi^2} \frac{\Gammal+4}{\Gamma[l+3](4+u_q)u_q^{l+6}} \left[5(u_q+2) {}_2F_1\left(l+\frac{5}{2}, l+5; 2l+5; -\frac{4}{u_q}\right) \right. \\ &\quad \left. + (lu_q) {}_2F_1\left(l+\frac{5}{2}, l+4; 2l+5; -\frac{4}{u_q}\right) \right] \\ &= -\frac{4x^4 \gamma^4(\theta) \sinh^2(q\beta)}{2\pi^2} \frac{\Gamma[l+5]}{\Gamma[l+3]u_q^{l+6}} \left[(l+5) {}_2F_1\left(l+\frac{5}{2}, l+6; 2l+5; -\frac{4}{u_q}\right) \right] \end{aligned} \quad (\text{F.14})$$

In the last line, we use (15.2.11) identity of [35] that relates derivatives of the relevant hypergeometric functions to linear combinations of other such functions. Since (F.14) only depends on the quantum number l , we can sum over other quantum numbers on S^5 using the ‘addition theorem of spherical harmonics’

$$\sum_{l=0}^{\infty} \sum_{\alpha=1}^{d_l} Y_l^\alpha(\Omega) Y_l^{*\alpha}(\Omega') = \sum_{l=0}^{\infty} \frac{(2l+4)\Gamma(2)}{4\Omega_5} C_l^{(2)}(\cos\Theta), \quad \cos\Theta = 1 - \frac{v}{2}. \quad (\text{F.15})$$

where $C_l^{(2)}(\cos\Theta)$ are the Gegenbauer polynomials and v is the chordal distance on S^5 . Note that, in the limit $\Theta \rightarrow 0$, the Gegenbauer polynomial $C_l^{(2)}(1)$ becomes $\frac{(l+3)(l+2)(l+1)}{6}$. Therefore the addition theorem in (F.15) precisely matches with (F.7). Substituting the

addition formula in (F.14), we obtain

$$\begin{aligned}
\langle T_{00}^{(10)} \rangle &= \lim_{\Theta \rightarrow 0} \sum_{q=1}^{\infty} \sum_{l=0}^{\infty} \frac{4x^4 \gamma^4(\theta) \sinh^2(q\beta)(2l+4)}{8\pi^5} \frac{\Gamma[(l+6)]}{\Gamma[l+3]u_q^{l+6}} \\
&\quad \times \left[{}_2F_1 \left(l + \frac{5}{2}, l+6; 2l+5; -\frac{4}{u_q} \right) C_l^{(2)}(\cos \Theta) \right] \\
&= \lim_{\Theta \rightarrow 0} \sum_{q=1}^{\infty} \sum_{l=0}^{\infty} \frac{x^4 \gamma^4(\theta) \sinh^2(q\beta)}{\pi^5} \frac{\Gamma[(l+6)]}{\Gamma[l+2](u_q+2)^{l+6}} \\
&\quad \times \left[{}_2F_1 \left(\frac{l}{2} + 3, \frac{l}{2} + \frac{7}{2}; l+3; \frac{4}{(u_q+2)^2} \right) C_l^{(2)}(\cos \Theta) \right] \quad (\text{F.16})
\end{aligned}$$

To obtain the last line, we use the identity given in equation (15.3.16) of [35]⁷⁵

We now perform sum over l using the following identity given in (B.9) of [13]

$$\sum_{l=0}^{\infty} \frac{\Gamma(l+\alpha)}{\Gamma(l+\beta)} \left(\frac{z}{2} \right)^l F \left(\frac{l}{2} + \frac{\alpha}{2}, \frac{l}{2} + \frac{\alpha}{2} + \frac{1}{2}; l + \beta + 1; z^2 \right) C_l^{(\beta)}(\cos \Theta) = \frac{\Gamma(\alpha)}{\Gamma(\beta)} \frac{1}{(1 - z \cos \Theta)^\alpha}, \quad (\text{F.17})$$

In our case, $\alpha = 6$, $\beta = 2$ and $z = \frac{2}{u_q+2}$.

$$\langle T_{00}^{(10)} \rangle = \lim_{\Theta \rightarrow 0} 2 \sum_{q=1}^{\infty} \frac{x^4 \gamma^4(\theta) \sinh^2(q\beta) \Gamma[6]}{\Gamma[2] \pi^5 (u_q+2)^6 \left(1 - \frac{2}{u_q+2} \cos \Theta \right)^6} \quad (\text{F.18})$$

Since, all the angles on S^5 have to be identified with each other, $\Theta \rightarrow 0$ and finally we obtain

$$\langle T_{00}^{(10)} \rangle = \sum_{q=1}^{\infty} \frac{2x^4 \gamma^4(\theta) \sinh^2(q\beta) \Gamma[6]}{\Gamma[2] \pi^5 u_q^6} \quad (\text{F.19})$$

Similarly, we compute all other components of the stress tensor and they agree with (5.22).

G Stress tensor of conformally coupled free scalar on $S^1 \times S^3$

In this section, we evaluate the one-point function of the stress tensor of a free conformally coupled scalar field on S^3 . After presenting a formal result for this object, we specialize to two limits

- The limit ‘ $\omega_1 \rightarrow 1, \omega_2 \rightarrow 1$ ’.
- The high temperature limit ($\beta \rightarrow 0$).

We demonstrate that the one-point function of the stress tensor takes the fluid dynamical form in both these limits, and also verify that these two limits commute with each other.

⁷⁵ ${}_2F_1(a, b, 2b, z) = (1 - \frac{z}{2})^{-a} {}_2F_1(a/2, a/2 + 1/2, b + 1/2, \frac{z^2}{(2-z)^2})$

G.1 Two Point function on $S^3 \times$ time

Consider a conformally coupled scalar on S^3 times time in Euclidean space. The metric $S^3 \times$ time can be rewritten as

$$\begin{aligned} ds^2 &= dt^2 + d\Omega_3^2 \\ &= \frac{dr^2}{r^2} + d\Omega_3^2 \\ &= \frac{1}{r^2} (dr^2 + r^2 d\Omega_3^2) \end{aligned} \tag{G.1}$$

(where we have defined $r = e^t$) demonstrating the (well known) fact that $S^3 \times$ time is Weyl equivalent to R^4 .

By construction, a conformally coupled scalar is Weyl invariant, where the scalar has Weyl weight one. This means that we get the same correlators from the ‘couples’ $(\phi, g_{\mu\nu})$ and $(e^\sigma \phi, e^{2\sigma} g_{\mu\nu})$ ⁷⁶.

We can apply this rule to the current situation. Let us parameterize points on S^3 by the unit vector \hat{n} (which, itself, can be written as a function of any convenient angular coordinates on S^3). Consequently, our coordinates on $S^3 \times$ time are \hat{n} and t . Let us parameterize points on R^4 by the four-dimensional position vector \vec{r} from the origin. We see that from (G.1) the map from $S^3 \times$ time to R^4 is given by

$$\vec{r} = e^t \hat{n} \tag{G.2}$$

Let us now apply the rule of the previous paragraph. Let $g_{\mu\nu}$ be the flat metric. Let $e^\sigma g_{\mu\nu}$ be the metric on $S^3 \times$ time. it follows from (G.1) that $e^\sigma = \frac{1}{r} = e^{-t}$. We conclude that

$$\begin{aligned} e^{-t} G_{S^3 \times R}(t, \hat{n}; t', \hat{n}') e^{-t'} &= \frac{\mathcal{N}}{|e^t \hat{n}_1 - e^{t'} \hat{n}'|^2} \\ \implies G_{S^3 \times R}(t, \hat{n}; t', \hat{n}') &= \frac{\mathcal{N} e^t e^{t'}}{|e^t \hat{n} - e^{t'} \hat{n}'|^2} = \frac{\mathcal{N}}{\left| e^{\frac{t-t'}{2}} \hat{n} - e^{\frac{t'-t}{2}} \hat{n}' \right|^2} \end{aligned} \tag{G.3}$$

where

$$\mathcal{N} = \frac{1}{4\pi^2}. \tag{G.4}$$

⁷⁷ In what follows we will use coordinate on S^3 s.t.

$$\hat{n} = (\sin \theta \cos \phi_1, \sin \theta \sin \phi_1, \cos \theta \cos \phi_2, \cos \theta \sin \phi_2) \tag{G.5}$$

In these coordinates the Greens function takes the form

$$G_{S^3 \times R}(t, \hat{n}; t', \hat{n}') = \frac{\mathcal{N}}{e^{t-t'} + e^{t'-t} - 2(\cos \theta \cos \theta' \cos(\phi_1 - \phi'_1) + \sin \theta \sin \theta' \cos(\phi_2 - \phi'_2))} \tag{G.6}$$

⁷⁶The first term in the couple is the field, while the second term is base space on which it propagates.

⁷⁷We have used the fact that the Greens for a massless scalar on $R^4 = \frac{\mathcal{N}}{r^2}$.

G.2 Greens function on (twisted) $S^3 \times S^1$

It is now a simple matter to evaluate the Greens function of our field on $S^3 \times S^1$, twisted with the angular velocities ω_1 and ω_2 . As in the main text we use the method of images, the q^{th} image is displaced by $\delta t = \beta q$, $\delta\phi_1 = -iq\beta\omega_1$, and $\delta\phi_2 = -iq\beta\omega_2$. It follows that Green's function is given by summing over images, and so is given by

$$G_{S^3 \times S^1}(t, \hat{n}; t', \hat{n}') = G_{S^3 \times R}(t, \hat{n}; t', \hat{n}') + \sum_{q=-\infty; q \neq 0}^{\infty} \frac{\mathcal{N}}{(e^{t-t'+q\beta} + e^{t'-t-q\beta} - 2(\cos\theta \cos\theta' \cos(\phi_1 - \phi'_1 - iq\beta\omega_1) + \sin\theta \sin\theta' \cos(\phi_2 - \phi'_2 - iq\beta\omega_2)))} \quad (\text{G.7})$$

where the first line of (G.7) is the contribution of the 0^{th} image, and the second line corresponds to contributions from all the non-zero images.

We are interested in this Green's function in the limit that $\theta' = \theta$, $\phi'_1 = \phi_1$, and $\phi'_2 = \phi_2$. Inserting these coordinate choices, and also taking the 'near extremal limit' $\omega_1 \rightarrow 1$ and $\omega_2 \rightarrow 1$, we find that at leading order in $(1 - \omega_1)$ and $(1 - \omega_2)$, the two-point function is given by ⁷⁸

$$G_{S^3 \times S^1}(t, \hat{n}; t', \hat{n}') - G_{S^3 \times R}(t, \hat{n}; t', \hat{n}') = \gamma^2(\theta) \sum_{q=1}^{\infty} \frac{2\mathcal{N}}{\beta q \sinh(\beta q)} \quad (\text{G.8})$$

where $\gamma(\theta)$ was defined in (1.5). The factor of $\gamma^2(\theta)$ tells us that the propagator is taking the 'fluid form'. It is interesting this happens when $\omega_1 \sim 1$ and $\omega_2 \sim 1$, even though we are at a temperature of order unity (rather than at high temperatures, at which fluid dynamics traditionally emerges).

As an aside, we can, once again set $\theta' = \theta$, $\phi'_1 = \phi_1$, and $\phi'_2 = \phi_2$ and evaluate the two-point function in the high-temperature limit $\beta \rightarrow 0$. We find

$$\begin{aligned} \lim_{\beta \rightarrow 0} G_{S^3 \times S^1}(t, \hat{n}; t', \hat{n}') - G_{S^3 \times R}(t, \hat{n}; t', \hat{n}') &= 2 \sum_{q=1}^{\infty} \frac{\mathcal{N}}{q^2 \beta^2 (1 - \omega_2^2 \sin^2(\theta) - \omega_1^2 \cos^2(\theta))} \\ &= 2 \sum_{q=1}^{\infty} \frac{\mathcal{N} \gamma^2(\theta)}{q^2 \beta^2} \end{aligned} \quad (\text{G.9})$$

The factors of $\gamma^2(\theta)$ are expected here as $T \rightarrow \infty$ takes us to the fluid limit. It is not difficult to check that the $\beta \rightarrow 0$ limit of (G.8) agrees with the $\omega_1 \rightarrow 1$ and $\omega_2 \rightarrow 1$ limit of (G.9). It follows, therefore, that (G.8) is genuinely fluid dynamical in nature.

⁷⁸It is easy to verify that the denominator of each of the terms in (G.8) simply vanishes when $\omega_1 = \omega_2 = 1$ and $\theta' = \theta$, $\phi'_1 = \phi_1$, and $\phi'_2 = \phi_2$. When ω_1 and ω_2 are not quite unity (but differ slightly from unity) the denominators do not quite vanish but are small.

G.3 Derivative structures required to compute the stress tensor in the $\omega_i \rightarrow 1$ limit

To compute the stress tensor, we follow the same strategy discussed in 5.2.4 which is by taking appropriate derivatives on the two-point function (G.7). We first take the derivatives on the Greens function (G.7) and then take the limit $t = t'$, $\theta' = \theta$, $\phi'_1 = \phi_1$, and $\phi'_2 = \phi_2$. As discussed in 5.2.3, we have renormalized our answers by subtracting the zero temperature answer (i.e. by dropping the $q = 0$ contribution; recall that this is independent of the temperature and ω_i). On performing the computation for the ‘time time’ derivative we find that (to leading order of the $\omega_i \rightarrow 1$)

$$\begin{aligned} & \partial_t \partial_{t'} G_{S^3 \times S^1}(t, \hat{n}, t', \hat{n}')|_{(t, \hat{n}) \rightarrow (t', \hat{n}')} \\ & \approx \sum_{q=1}^{\infty} -\frac{8\gamma^6(\theta) \operatorname{csch}(\beta q) \left(2 - \beta q \coth(\beta q) \left(\frac{1}{2\gamma^2(\theta)}\right)\right)}{4\pi^2 \beta^3 q^3} \\ & \approx \sum_{q=1}^{\infty} -\frac{4\gamma^6(\theta) \operatorname{csch}(\beta q)}{\pi^2 \beta^3 q^3} \end{aligned} \quad (\text{G.10})$$

Note that, the leading order term goes as $\gamma^6(\theta)$. In a similar manner all (double) derivatives of the propagator can be evaluated; at leading order we find

$$\partial_{\phi_1} \partial_{\phi'_1} G_{S^3 \times S^1}(t, \hat{n}, t', \hat{n}')|_{(t', \hat{n}') \rightarrow (t, \hat{n})} \approx \gamma^6(\theta) \sum_{q=1}^{\infty} \frac{4\omega_1^2 \cos^4(\theta) \operatorname{csch}(\beta q)}{\pi^2 \beta^3 q^3} \quad (\text{G.11})$$

$$\partial_{\phi_2} \partial_{\phi'_2} G_{S^3 \times S^1}(t, \hat{n}, t', \hat{n}')|_{(t, \hat{n}) \rightarrow (t', \hat{n}')} \approx \gamma^6(\theta) \sum_{q=1}^{\infty} \frac{4\omega_2^2 \sin^4(\theta) \operatorname{csch}(\beta q)}{\pi^2 \beta^3 q^3} \quad (\text{G.12})$$

$$\begin{aligned} \partial_{\phi_1} \partial_{\phi'_2} G_{S^3 \times S^1}(t, \hat{n}, t', \hat{n}')|_{(t, \hat{n}) \rightarrow (t', \hat{n}')} &= \partial_{\phi_2} \partial_{\phi'_1} G_{S^3 \times S^1}(t, \hat{n}, t', \hat{n}')|_{(t, \hat{n}) \rightarrow (t', \hat{n}')} \\ &\approx \gamma^6(\theta) \sum_{q=1}^{\infty} \frac{4\omega_1 \omega_2 \sin^2(2\theta) \operatorname{csch}(\beta q)}{\pi^2 (\beta q)^3} \end{aligned} \quad (\text{G.13})$$

$$\begin{aligned} \partial_t \partial_{\phi'_2} G_{S^3 \times S^1}(t, \hat{n}, t', \hat{n}')|_{(t, \hat{n}) \rightarrow (t', \hat{n}')} &= \partial_{\phi_2} \partial_{t'} G_{S^3 \times S^1}(t, \hat{n}, t', \hat{n}')|_{(t, \hat{n}) \rightarrow (t', \hat{n}')} \\ &\approx \gamma^6(\theta) \sum_{q=1}^{\infty} \frac{i4\omega_2 \sin^2(\theta) \operatorname{csch}(\beta q)}{\pi^2 \beta^3 q^3} \end{aligned} \quad (\text{G.14})$$

$$\begin{aligned} \partial_t \partial_{\phi'_1} G_{S^3 \times S^1}(t, \hat{n}, t', \hat{n}')|_{(t, \hat{n}) \rightarrow (t', \hat{n}')} &= \partial_{\phi_1} \partial_{t'} G_{S^3 \times S^1}(t, \hat{n}, t', \hat{n}')|_{(t, \hat{n}) \rightarrow (t', \hat{n}')} \\ &\approx \gamma^6(\theta) \sum_{q=1}^{\infty} \frac{i4\omega_1 \cos^2(\theta) \operatorname{csch}(\beta q)}{\pi^2 \beta^3 q^3} \end{aligned} \quad (\text{G.15})$$

$$\partial_\theta \partial_{\phi'_1} G_{S^3 \times S^1}(t, \hat{n}, t', \hat{n}')|_{(t, \hat{n}) \rightarrow (t', \hat{n}')} = \partial_\theta \partial_{\phi'_2} G_{S^3 \times S^1}(t, \hat{n}, t', \hat{n}')|_{(t, \hat{n}) \rightarrow (t', \hat{n}')} \approx O\left(\frac{1}{\gamma^2(\theta)}\right) \quad (\text{G.16})$$

$$\partial_\theta \partial_{\theta'} G_{S^3 \times S^1}(t, \hat{n}, t', \hat{n}')|_{(t, \hat{n}) \rightarrow (t', \hat{n}')} \approx \gamma^4(\theta) \sum_{q=1}^{\infty} \frac{\text{csch}^2(\beta q)}{\pi^2 \beta^2 q^2} \quad (\text{G.17})$$

$$\partial_t \partial_{\theta'} G_{S^3 \times S^1}(t, \hat{n}, t', \hat{n}')|_{(t, \hat{n}) \rightarrow (t', \hat{n}')} \approx O\left(\frac{1}{\gamma^2(\theta)}\right) \quad (\text{G.18})$$

G.4 The stress tensor

The action of a conformally coupled free scalar on an arbitrary curved spacetime is given by

$$S = \frac{1}{2} \int \sqrt{-g} d^4x \left(-g^{\mu\nu} \nabla_\mu \phi \nabla_\nu \phi - \xi R \phi^2 \right), \quad \xi = \frac{1}{6}. \quad (\text{G.19})$$

By varying the action with respect to metric one can determine the stress tensor for this theory to be (see, e.g. equation (3.190) of [36])

$$T_{\mu\nu} = \nabla_\mu \phi \nabla_\nu \phi - \frac{1}{2} g_{\mu\nu} \nabla_\alpha \phi \nabla^\alpha \phi + \xi G_{\mu\nu} \phi^2 + \xi (g_{\mu\nu} \nabla^\alpha \nabla_\alpha - \nabla_\mu \nabla_\nu) \phi^2 \quad (\text{G.20})$$

Tracelessness of the stress tensor in (G.20) can be verified immediately (this verification works in any bulk dimension D once we use the appropriate value of ξ , namely, $\xi = \frac{D-2}{4(D-1)}$)

$$\begin{aligned} T^\mu{}_\mu &= \left(1 - \frac{D}{2}\right) \nabla_\alpha \phi \nabla^\alpha \phi + \xi R \left(1 - \frac{D}{2}\right) \phi^2 + \xi (2(D-1) \nabla_\alpha \phi \nabla^\alpha \phi + 2(D-1) \phi \nabla^2 \phi) \\ &= \left(1 - \frac{D}{2}\right) \phi (-\nabla^2 + \xi R) \phi \\ &= 0 \end{aligned} \quad (\text{G.21})$$

In the last line, we have used the equation of motion.

From the derivative structures presented in the G.3, it is easy to write the non-zero

components of the stress tensor in the $\omega_i \rightarrow 1$ in the leading order.

$$\langle T_{00} \rangle = \gamma^6(\theta) \sum_{q=1}^{\infty} \frac{4\text{csch}(\beta q)}{\pi^2 \beta^3 q^3} \quad (\text{G.22})$$

$$\langle T_{\phi_1 \phi_1} \rangle = \gamma^6(\theta) \sum_{q=1}^{\infty} \frac{4\omega_1^2 \cos^4(\theta) \text{csch}(\beta q)}{\pi^2 \beta^3 q^3} \quad (\text{G.23})$$

$$\langle T_{\phi_2 \phi_2} \rangle = \gamma^6(\theta) \sum_{q=1}^{\infty} \frac{4\omega_2^2 \sin^4(\theta) \text{csch}(\beta q)}{\pi^2 \beta^3 q^3} \quad (\text{G.24})$$

$$\langle T_{\theta\theta} \rangle = \gamma^4(\theta) \sum_{q=1}^{\infty} \frac{\text{csch}^2(\beta q)}{\pi^2 \beta^2 q^2} \quad (\text{G.25})$$

$$\langle T_{0\phi_1} \rangle = \gamma^6(\theta) \sum_{q=1}^{\infty} \frac{4\omega_1 \cos^2(\theta) \text{csch}(\beta q)}{\pi^2 \beta^3 q^3} \quad (\text{G.26})$$

$$\langle T_{0\phi_2} \rangle = \gamma^6(\theta) \sum_{q=1}^{\infty} \frac{4\omega_2 \sin^2(\theta) \text{csch}(\beta q)}{\pi^2 \beta^3 q^3} \quad (\text{G.27})$$

$$\langle T_{\phi_1 \phi_2} \rangle = \gamma^6(\theta) \sum_{q=1}^{\infty} \frac{4\omega_1 \omega_2 \sin^2(2\theta) \text{csch}(\beta q)}{\pi^2 (\beta q)^3} \quad (\text{G.28})$$

These results agree (at leading order in γ) with the ‘fluid form’ stress tensor

$$T_{\mu\nu} = \gamma^4(\theta) (4u_\mu u_\nu + g_{\mu\nu}) \sum_{q=1}^{\infty} \frac{1}{\pi^2 \beta^3 \sinh(q\beta) q^3} \quad (\text{G.29})$$

In a similar manner, we can also compute the one-point function of the stress tensor in the small β limit (but at finite values of γ). This is the limit in which we expect to recover the usual results of fluid dynamics. Performing the computation we find

$$\lim_{\beta \rightarrow 0} \langle T_{\mu\nu} \rangle = \frac{\pi^2}{90\beta^4} \gamma^4(\theta) (g_{\mu\nu} + 4u_\mu u_\nu), \quad u_\mu = \gamma(-1, 0, \omega_1 \cos^2 \theta, \omega_2 \sin^2 \theta). \quad (\text{G.30})$$

Using $\sum_{q=1}^{\infty} \frac{1}{q^4} = \frac{\pi^4}{90}$, it is straightforward to verify that the small β limit of (G.29) matches with (G.30).

H Spin-1 contribution to the bulk stress tensor

In this Appendix we compute the expectation value of the thermal stress tensor (at nonzero values of ω_i) for a five dimensional massive vector field. We work with a bulk field dual to a boundary operator of dimension Δ (so that the mass of the bulk field is given by $M^2 = (\Delta - 1)(\Delta - 3)$). The main qualitative take away from this Appendix is that this thermal stress tensor takes the form (6.11) (for an appropriate choice of the function $\mathcal{F}(x)$), giving evidence for the conjecture made at the beginning of section 7.

We remind the reader that the stress tensor of massive vector field is given by

$$T_{\mu\nu} = g^{\alpha\beta} F_{\mu\alpha} F_{\nu\beta} + M^2 A_\mu A_\nu - g_{\mu\nu} \left(\frac{1}{4} F_{\alpha\beta} F^{\alpha\beta} + \frac{M^2}{2} A_\alpha A^\alpha \right) \quad (\text{H.1})$$

H.1 Stress tensor in thermal AdS_5

The expectation value of (H.1) is given by

$$\begin{aligned}
\langle T_{\mu\nu} \rangle &= \lim_{x_1 \rightarrow x_2} \left[\langle F_{\mu\alpha}(x_1) F_\nu{}^\alpha(x_2) + M^2 \langle A_\mu(x_1) A_\nu(x_2) \rangle - \frac{g_{\mu\nu}}{4} \left(\langle F_{\alpha\beta}(x_1) F^{\alpha\beta}(x_2) \rangle + \langle A_\alpha(x_1) A^\alpha(x_2) \rangle \right) \right] \\
&= \lim_{x_1 \rightarrow x_2} \left[\partial_\mu^{x_1} \partial_\nu^{x_2} \tilde{\Pi}_\alpha{}^\alpha(x_1, x_2) - \partial_\mu^{x_1} \partial^{x_2, \alpha} \tilde{\Pi}_{\alpha, \nu}(x_1, x_2) - \partial_\alpha^{x_1} \partial_\nu^{x_2} \tilde{\Pi}_\mu{}^\alpha(x_1, x_2) + \partial_\alpha^{x_1} \partial^{x_2, \alpha} \tilde{\Pi}_{\mu, \nu}(x_1, x_2) \right. \\
&\quad - \frac{g_{\mu\nu}}{4} \left(\partial_\alpha^{x_1} \partial^{x_2, \alpha} \tilde{\Pi}_\beta{}^\beta(x_1, x_2) + \partial_\beta^{x_1} \partial^{x_2, \beta} \tilde{\Pi}_\alpha{}^\alpha(x_1, x_2) - \partial_\alpha^{x_1} \partial^{x_2, \beta} \tilde{\Pi}_\beta{}^\alpha(x_1, x_2) - \partial_\beta^{x_1} \partial^{x_2, \alpha} \tilde{\Pi}_\alpha{}^\beta(x_1, x_2) \right) \\
&\quad \left. + M^2 \tilde{\Pi}_{\mu, \nu}(x_1, x_2) - \frac{g_{\mu\nu}}{4} M^2 \tilde{\Pi}_\alpha{}^\alpha(x_1, x_2) \right] \tag{H.2}
\end{aligned}$$

where $\tilde{\Pi}_{\mu\nu}(x_1, x_2)$ is massive vector propagator on AdS_5 with the identifications mentioned in (5.3). Using the method of images, it follows that $\tilde{\Pi}(x_1, x_2)$ is given by a sum over propagators on ordinary (non-thermal) Euclidean AdS_5 :

$$\tilde{\Pi}_{\mu, \nu}(x_1, x_2) = \sum_{q=-\infty}^{\infty} \Pi_{\mu, \nu}(x_1, R^q(x_2)) \tag{H.3}$$

where R^q was defined under (5.6). The expression of the bulk to bulk propagator of massive vector field in Euclidean (non-thermal) AdS_5 is known [37]

$$\langle A_\mu(x_1) A_\nu(x_2) \rangle = \Pi_{\mu, \nu}(x_1, x_2) = -\frac{\partial^2 u}{\partial x_1^\mu \partial x_2^\nu} g_0(u) + \frac{\partial u}{\partial x_1^\mu} \frac{\partial u}{\partial x_2^\nu} g_1(u) \tag{H.4}$$

In AdS_5 , the expressions of $g_0(u)$ and $g_1(u)$ are given by [37]

$$\begin{aligned}
g_0(u) &= \frac{\mathcal{N}}{(u)^\Delta} \left[(4 - \Delta) {}_2F_1 \left(\Delta, \frac{1}{2}(-3 + 2\Delta); -3 + 2\Delta; -\frac{1}{u} \right) \right. \\
&\quad \left. - \frac{2 + u}{u} {}_2F_1 \left(\Delta + 1, \frac{1}{2}(-3 + 2\Delta); -3 + 2\Delta; -\frac{1}{u} \right) \right] \\
g_1(u) &= \frac{\mathcal{N}}{(u)^\Delta} \left[\frac{2(2 + u)(4 - \Delta)}{u(u + 4)} {}_2F_1 \left(\Delta, \frac{1}{2}(-3 + 2\Delta); -3 + 2\Delta; -\frac{1}{u} \right) \right. \\
&\quad \left. - 2 \frac{4 + (u + 2)^2}{u^2(u + 4)} {}_2F_1 \left(\Delta + 1, \frac{1}{2}(-3 + 2\Delta); -3 + 2\Delta; -\frac{1}{u} \right) \right]
\end{aligned}$$

where the normalization constant \mathcal{N} for AdS_5 is given by

$$\mathcal{N} = \frac{\Gamma(\Delta + 1)}{2\pi^2(3 - \Delta)(\Delta - 1)\Gamma(\Delta - 1)}. \tag{H.5}$$

We compute the two-point function of the field strengths by acting with appropriate derivatives first on the correlator (H.3) and then take the coincident limit. As we already discussed in 5.2.4, we renormalize the two-point function of the field strengths by removing the temperature independent ($q = 0$) term. We present our results for the thermal two-point function of the field strengths in the leading order of $\omega_i \rightarrow 1$.

$$\lim_{x_1 \rightarrow x_2} \langle F_{0\lambda}(x_1) F_0{}^\lambda(x_2) \rangle = 4x^4 \gamma^4(\theta) f^{(1)}(x) \tag{H.6}$$

$$\lim_{x_1 \rightarrow x_2} \langle F_{0\lambda}(x_1) F_{\phi_1}^\lambda(x_2) \rangle = 4x^4 \gamma^4(\theta) \sin^2(\theta) f^{(1)}(x) \quad (\text{H.7})$$

$$\lim_{x_1 \rightarrow x_2} \langle F_{0\lambda}(x_1) F_{\phi_2}^\lambda(x_2) \rangle = 4x^4 \gamma^4(\theta) \cos^2(\theta) f^{(1)}(x) \quad (\text{H.8})$$

$$\lim_{x_1 \rightarrow x_2} \langle F_{\phi_1\lambda}(x_1) F_{\phi_1}^\lambda(x_2) \rangle = 4x^4 \gamma^4(\theta) \sin^4(\theta) f^{(1)}(x) \quad (\text{H.9})$$

$$\lim_{x_1 \rightarrow x_2} \langle F_{\phi_2\lambda}(x_1) F_{\phi_2}^\lambda(x_2) \rangle = 4x^4 \gamma^4(\theta) \cos^4(\theta) f^{(1)}(x) \quad (\text{H.10})$$

$$\lim_{x_1 \rightarrow x_2} \langle F_{\phi_1\lambda}(x_1) F_{\phi_2}^\lambda(x_2) \rangle = 4x^4 \gamma^4(\theta) \sin^2(\theta) \cos^2(\theta) f^{(1)}(x) \quad (\text{H.11})$$

where $f^{(1)}(x)$ is given in terms of the chordal distance u_q (see equation (5.24))

$$f^{(1)}(x) = \sum_{q=1}^{\infty} \sinh^2(\beta q) (g_0''(u_q) + g_1'(u_q)) (3 \cosh(\beta q) + \beta q x^2 \sinh(\beta q)) + 2g_0'(u_q) + 2g_1(u_q) \quad (\text{H.12})$$

We also compute the term which turns out to be subleading

$$g_{\mu\nu} \lim_{x_1 \rightarrow x_2} \langle F_{\alpha\beta}(x_1) F^{\alpha\beta}(x_2) \rangle = O(\gamma^2(\theta)) \quad (\text{H.13})$$

From the two-point functions of the field strengths, it is now easy to evaluate the stress tensor

$$\langle T_{\mu\nu} \rangle = 4\mathcal{F}_\Delta^{(1)}(x) \gamma^4(\theta) \begin{pmatrix} 1 & 0 & 0 & \sin^2(\theta) & \cos^2(\theta) \\ 0 & 0 & 0 & 0 & 0 \\ 0 & 0 & 0 & 0 & 0 \\ \sin^2(\theta) & 0 & 0 & \sin^4(\theta) & \sin^2(\theta) \cos^2(\theta) \\ \cos^2(\theta) & 0 & 0 & \sin^2(\theta) \cos^2(\theta) & \cos^4(\theta) \end{pmatrix} \quad (\text{H.14})$$

where $\mathcal{F}_\Delta^{(1)}(x)$ is given by

$$\begin{aligned} \mathcal{F}_\Delta^{(1)}(x) &= \sum_{q=1}^{\infty} \left[\sinh^2(\beta q) (g_0''(u_q) + g_1'(u_q)) (3 \cosh(\beta q) + \beta q x^2 \sinh(\beta q)) \right. \\ &\quad \left. + 2g_0'(u_q) + 2g_1(u_q) + M^2 g_1(u_q) \right] \\ &= \sum_{q=1}^{\infty} \left[\sinh^2(\beta q) (g_0''(u_q) + g_1'(u_q)) (3 \cosh(\beta q) + \beta q x^2 \sinh(\beta q)) \right. \\ &\quad \left. + 2g_0'(u_q) + 2g_1(u_q) + (\Delta - 1)(\Delta - 3)g_1(u_q) \right] \end{aligned} \quad (\text{H.15})$$

In the last line, we use $M^2 = (\Delta - 1)(\Delta - 3)$.

The final form of the stress tensor is manifestly fluid in nature

$$T_{\mu\nu} = \mathcal{F}_\Delta^{(1)}(x) \gamma^4(\theta) 4w_\mu w_\nu \quad (\text{H.16})$$

and so, once again, takes the form (6.11) (with $\mathcal{F}_\Delta^{(1)}(x)$ replacing $\mathcal{F}(x)$).

References

- [1] S. Kim, S. Kundu, E. Lee, J. Lee, S. Minwalla and C. Patel, *Grey Galaxies' as an endpoint of the Kerr-AdS superradiant instability*, *JHEP* **11** (2023) 024 [[2305.08922](#)].
- [2] V. Cardoso and O.J.C. Dias, *Small Kerr-anti-de Sitter black holes are unstable*, *Phys. Rev. D* **70** (2004) 084011 [[hep-th/0405006](#)].
- [3] O.J.C. Dias, J.E. Santos and B. Way, *Black holes with a single Killing vector field: black resonators*, *JHEP* **12** (2015) 171 [[1505.04793](#)].
- [4] T. Ishii and K. Murata, *Black resonators and geons in AdS₅*, *Class. Quant. Grav.* **36** (2019) 125011 [[1810.11089](#)].
- [5] P.M. Chesler and D.A. Lowe, *Nonlinear Evolution of the AdS₄ Superradiant Instability*, *Phys. Rev. Lett.* **122** (2019) 181101 [[1801.09711](#)].
- [6] T. Ishii, K. Murata, J.E. Santos and B. Way, *Superradiant instability of black resonators and geons*, *JHEP* **07** (2020) 206 [[2005.01201](#)].
- [7] P.M. Chesler, *Hairy black resonators and the AdS₄ superradiant instability*, *Phys. Rev. D* **105** (2022) 024026 [[2109.06901](#)].
- [8] H.K. Kunduri, J. Lucietti and H.S. Reall, *Gravitational perturbations of higher dimensional rotating black holes: Tensor perturbations*, *Phys. Rev. D* **74** (2006) 084021 [[hep-th/0606076](#)].
- [9] K. Murata, *Instabilities of Kerr-AdS(5) x S^{**5} Spacetime*, *Prog. Theor. Phys.* **121** 1099 [[0812.0718](#)].
- [10] V. Cardoso, O.J.C. Dias, G.S. Hartnett, L. Lehner and J.E. Santos, *Holographic thermalization, quasinormal modes and superradiance in Kerr-AdS*, *JHEP* **04** (2014) 183 [[1312.5323](#)].
- [11] S. Choi, D. Jain, S. Kim, V. Krishna, E. Lee, S. Minwalla et al., *Dual Dressed Black Holes as the end point of the Charged Superradiant instability in $\mathcal{N} = 4$ Yang Mills*, [2409.18178](#).
- [12] V.E. Hubeny and M. Rangamani, *Unstable horizons*, *JHEP* **05** (2002) 027 [[hep-th/0202189](#)].
- [13] H. Dorn, M. Salizzoni and C. Sieg, *On the propagator of a scalar field on AdS x S and on the BMN plane wave*, *JHEP* **02** (2005) 047 [[hep-th/0307229](#)].
- [14] P. Dai, R.-N. Huang and W. Siegel, *Covariant propagator in AdS(5) x S^{**5} superspace*, *JHEP* **03** (2010) 001 [[0911.2211](#)].
- [15] S. Bhattacharyya, S. Lahiri, R. Loganayagam and S. Minwalla, *Large rotating AdS black holes from fluid mechanics*, *JHEP* **09** (2008) 054 [[0708.1770](#)].
- [16] S. Bhattacharyya, R. Loganayagam, S. Minwalla, S. Nampuri, S.P. Trivedi and S.R. Wadia, *Forced Fluid Dynamics from Gravity*, *JHEP* **02** (2009) 018 [[0806.0006](#)].
- [17] S. Bhattacharyya, R. Loganayagam, I. Mandal, S. Minwalla and A. Sharma, *Conformal Nonlinear Fluid Dynamics from Gravity in Arbitrary Dimensions*, *JHEP* **12** (2008) 116 [[0809.4272](#)].
- [18] S. Bhattacharyya, V.E. Hubeny, R. Loganayagam, G. Mandal, S. Minwalla, T. Morita et al., *Local Fluid Dynamical Entropy from Gravity*, *JHEP* **06** (2008) 055 [[0803.2526](#)].
- [19] S. Bhattacharyya, S. Lahiri, R. Loganayagam and S. Minwalla, *Large rotating ads black holes from fluid mechanics*, *Journal of High Energy Physics* **2008** (2008) 054–054.

- [20] R. Emparan and R.C. Myers, *Instability of ultra-spinning black holes*, *Journal of High Energy Physics* **2003** (2003) 025–025.
- [21] O.J.C. Dias, P. Figueras, R. Monteiro and J.E. Santos, *Ultraspinning instability of anti-de Sitter black holes*, *JHEP* **12** (2010) 067 [[1011.0996](#)].
- [22] M.M. Caldarelli, R. Emparan and M.J. Rodríguez, *Black rings in (anti)-de sitter space*, *Journal of High Energy Physics* **2008** (2008) 011–011.
- [23] R. Emparan and H.S. Reall, *Black holes in higher dimensions*, *Living Reviews in Relativity* **11** (2008) .
- [24] S.W. Hawking, C.J. Hunter and M. Taylor, *Rotation and the AdS / CFT correspondence*, *Phys. Rev. D* **59** (1999) 064005 [[hep-th/9811056](#)].
- [25] M.M. Caldarelli, G. Cognola and D. Klemm, *Thermodynamics of Kerr-Newman-AdS black holes and conformal field theories*, *Class. Quant. Grav.* **17** (2000) 399 [[hep-th/9908022](#)].
- [26] G.W. Gibbons, M.J. Perry and C.N. Pope, *The First law of thermodynamics for Kerr-anti-de Sitter black holes*, *Class. Quant. Grav.* **22** (2005) 1503 [[hep-th/0408217](#)].
- [27] S. de Haro, S.N. Solodukhin and K. Skenderis, *Holographic reconstruction of space-time and renormalization in the AdS / CFT correspondence*, *Commun. Math. Phys.* **217** (2001) 595 [[hep-th/0002230](#)].
- [28] O.J.C. Dias, J.E. Santos and B. Way, *Lumpy AdS₅ × S⁵ black holes and black belts*, *JHEP* **04** (2015) 060 [[1501.06574](#)].
- [29] R. Emparan and H.S. Reall, *Black rings*, *Classical and Quantum Gravity* **23** (2006) R169–R197.
- [30] J. Kinney, J.M. Maldacena, S. Minwalla and S. Raju, *An Index for 4 dimensional super conformal theories*, *Commun. Math. Phys.* **275** (2007) 209 [[hep-th/0510251](#)].
- [31] M. Gunaydin and N. Marcus, *The Spectrum of the s**5 Compactification of the Chiral N=2, D=10 Supergravity and the Unitary Supermultiplets of U(2, 2/4)*, *Class. Quant. Grav.* **2** (1985) L11.
- [32] G. Mack, *All unitary ray representations of the conformal group SU(2,2) with positive energy*, *Commun. Math. Phys.* **55** (1977) 1.
- [33] F.A. Dolan, *Character formulae and partition functions in higher dimensional conformal field theory*, *J. Math. Phys.* **47** (2006) 062303 [[hep-th/0508031](#)].
- [34] L.F. Alday, M. Kologlu and A. Zhiboedov, *Holographic correlators at finite temperature*, *JHEP* **06** (2021) 082 [[2009.10062](#)].
- [35] M. Abramowitz and I. Stegun, *Handbook of Mathematical Functions with Formulas, Graphs, and Mathematical Tables*, Dover Publications (1964).
- [36] N.D. Birrell and P.C.W. Davies, *Quantum Fields in Curved Space*, Cambridge Monographs on Mathematical Physics, Cambridge University Press, Cambridge, UK (1982), [10.1017/CBO9780511622632](#).
- [37] M.S. Costa, V. Gonçalves and J.a. Penedones, *Spinning AdS Propagators*, *JHEP* **09** (2014) 064 [[1404.5625](#)].